Republic of Iraq
Ministry of Higher Education
and Scientific Research
University of Babylon
College of Engineering
Civil Engineering Department

The Nonlinear Behavior of Prestressed Concrete Girders under Moving Loads by Finite Element Method

A Thesis
Submitted to the College of Engineering of the University of Babylon
in Partial Fulfillment of the Requirements for the Degree
of Master of Science in Structural Engineering

By
Alaa Mehdi Abbas

Supervised by
Ass. Prof. Dr. Haitham H. AlDaami
Ass. Prof. Mr. Abdul Ridah Saleh

August, 2009 **Sha'ban, 1430**

جمهورية العراق
وزارة التعليم العالي والبحث العلمي
جامعة بابل- كلية الهندسة
قسم الهندسة المدنية

السلوك اللاخطي للروافد الكونكريتية المسبقة الإجهاد تحت تأثير الأحمال المتحركة باستخدام طريقة العناصر المحددة

رسالة مقدمة إلى

قسم الهندسة المدنية في كلية الهندسة في جامعة بابل كجزء من متطلبات نيل شهادة الماجستير في هندسة الإنشاءات

من قبل

علاء مهدي عباس

إشراف

أ.م.د. هيثم حسن ألدعمي

أ.م.السيد عبد الرضا صالح هادي

آب ,2009 م

شعبان ,1430هـ

Abstract

In the present work the nonlinear finite element analysis has been used to investigate the behavior of prestressed concrete girders under moving loads. Solution is done by using ANSYS (V.9) computer program.

Eight-node brick element with embedded steel (ordinary and prestressed) reinforcement model has been used to model reinforced concrete. The ANSYS introduces this element in the code (SOLID65), which used the full Newton-Raphson method for the nonlinear solution algorithm. The material nonlinearity sources, namely cracking, crushing of concrete, and yielding of steel structure are taken into consideration during the analysis.

This study is divided into three parts represented by checking the model of moving load alone, and then checking the prestressed concrete model, finally the two cases are considered together to represent the prestressed concrete girder under dynamic moving load. This is due to the absence of experimental data that merge the two effects.

The simulation of the moving load is presented by using a transient analysis in ANSYS to move the force from one end to another at a constant velocity; while the prestressing force is modeled as an equivalent external force (equivalent pressure) acts on the brick elements.

Many cases are considered herein, the first one is used to check the modeling of moving load and the others are used to check the adopted model of prestressed concrete girders. The results are compared with experimental data to ensure the accuracy of the finite element modeling.

A parametric study of some factors is presented in this thesis, to investigate the effects of many parameters of the structural behavior

prestressing girders, such as mesh size, vehicle speed, number of vehicle axles, number of vehicle passing over the bridge, and effect of cross section of the girders.

From this investigation it is found that the natural frequency of the rectangular section is less than the (I shape) having the same stiffness. This is due to the increase in the weight of the girder. The prestressing force magnitude, strands arrangement, span length and vehicle velocity also play important roles on value of the natural frequency and the period of prestressed concrete girder.

الخلاصة

في الدراسة الحالية, تم استخدام التحليل اللاخطي بطريقة العناصر المحددة للتحري ودراسة سلوك الروافد الكونكريتية المسبقة الإجهاد تحت تأثير الأحمال المتحركة وتمت هذه الدراسة باستخدام برنامج ANSYS (V.9).

تم استخدام العنصر الطابوقي ذو ثمان عقد لتمثيل خرسانة الكونكريت المسلحة حيث تم تمثيل حديد التسليح الاعتيادي و حديد الشد كعنصر مطمور داخل العنصر الطابوقي (ضمنا). إن برنامج ANSYS يوفر العنصر الطابوقي ويقدمه باسم (Solid65). لقد تم حل معادلات التوازن اللاخطية باستخدام طريقة (Full Newton-Raphson) وكذلك عند تحليل المسألة تم الأخذ بنظر الاعتبار تصرف المواد اللاخطي والمتمثل بالتشقق والتهشم بالنسبة للخرسانة والخضوع بالنسبة لحديد التسليح.

لقد تم تقسيم الدراسة الحالية إلى ثلاثة أقسام لغرض مقارنة النتائج متمثلة بتدقيق النموذج والطريقة المستخدمة لتمثيل الحمل المتحرك مع الأخذ بنظر الاعتبار التأثير الديناميكي للحمل المتحرك, وكذلك تدقيق طريقة تمثيل الخرسانة المسبقة الشد وأخيرا تم دمج الحالتين المذكورتين في أعلاه لتمثيل التأثير الديناميكي للأحمال المتحركة على الروافد الخرسانية المسبقة الإجهاد. يعود سبب التقسيم أعلاه لغياب النتائج العملية حول الموضوع المتبنى.

تم تمثيل الحمل المتحرك كحمل عابر للأخذ بنظر الاعتبار التأثير الديناميكي للمركبة حيث تم استخدام برنامج ANSYS لنقل الحمل من طرف إلى الطرف الأخر للعتبة بسرعة ثابتة. وكذلك تم تمثيل قوة الشد كقوة خارجية مكافئة تؤثر على الرافدة من الأطراف.

لقد تم دراسة عدة حالات في المسألة الحالية تمثلت بتدقيق النتائج التي تم الحصول عليها باستخدام طريقة العناصر المحددة لطريقة تمثيل الحمل المتحرك وطريقة تمثيل الخرسانة المسبقة الإجهاد مع نتائج عملية لبيان ملائمة طريقة التمثيل.

عدة دراسات مقارنة لعوامل مؤثرة معينة على سلوك الروافد الخرسانية المسبقة الإجهاد تمت دراستها متمثلة بدراسة طريقة اختيار عدد العناصر الأمثل لتمثيل الرافدة المسبقة الإجهاد, وتأثير تغيير سرعة المركبة, وطريقة تمثيل المركبة (عدد المحاور الحقيقية مرة ومحصلة تلك المحاور مرة أخرى), وكذلك تأثير تغير عدد المركبات العابرة على الرافدة وتأثير شكل مقطع الرافدة.

من الدراسة المتبناة تم الحصول على إن تردد الرافدة للمقطع المربع أقل من المقطع ذو شكل (I) بالرغم من تساوي الصلادة للمقطعين يعود ذلك إلى زيادة وزن المقطع المربع على المقطع (I) وكذلك تم التوصل إلى إن مقدار قوة الشد, طريقة ترتيب وتوزيع حديد الشد, طول الرافدة وسرعة المركبة تلعب دور أساسي في تذبذب الرافدة المسبقة الشد وزمن الذبذبة.

Acknowledgments

In the name of Allah, the most gracious, the most merciful

All thanks and praise be to Allah my God who helped and enabled me to complete this research.

I wish to express my deep gratitude and thanks to my supervisors ***Ass.Prof. Dr. Haitham H. AlDaami*** and ***Ass.Prof. Mr. Abdul Ridah Saleh*** for their valuable guidance, advice, encouragement and assistance throughout the preparation of this research.

A special thank and gratitude to ***my mother***, ***my wife***, ***my brother (Salah)*** and ***my sisters*** for their care, patience and encouragement throughout the research period.

Finally, I would like to express my deepest gratitude to all who gave me a helpful hand throughout this study especially my friend (***Majid)***.

A.M. Abbas / 2009

Certificate of The Examining Committee

We certify as an Examining Committee that we have read this thesis titled "***The Nonlinear Behavior of Prestressed Concrete Girders under Moving Loads by Finite Element Method***" and examined the student "***Alaa Mehdi Abbas***" in its content and what related to it, and found it meets the standard of thesis for the degree of Master of science in Civil Engineering (Structural Engineering).

Signature:
Name: ***Ass.Prof. Dr. Haitham H. AlDaami***
(Supervisor)
Date: / /2009

Signature:
Name: ***Ass.Prof. Mr. Abdul Ridah Saleh***
(Supervisor)
Date: / /2009

Signature:
Name: ***Ass.Prof. Dr. Mustafa B. Dawood***
(Member)
Date: / /2009

Signature:
Name: ***Ass.Prof. Dr. Raad K. Shukur***
(Member)
Date: / /2009

Signature:
Name: ***Prof. Dr. Bayan S. Obaid***
(Chairman)
Date: / /2009

Approved by the Head of the Civil Engineering Department

Signature:
Name: ***Prof. Dr. Ammar Y. Ali***
(The Head of the Civil Engineering Department)
Date: / / 2009

Approved by the Dean of the College of Engineering

Signature:
Name: ***Ass.Prof. Dr. Salah Tawfeek Al-Bazzaz***
(The Dean of the College of Engineering)
Date: / / 2009

Certification

We certify that the preparation of this thesis titled "***The Nonlinear Behavior of Prestressed Concrete Girders under Moving Loads by Finite Element Method***" presented by "***Alaa Mehdi Abbas***" was made under our supervision at the Department of Civil Engineering / College of Engineering / University of Babylon, as a partial fulfillment of the requirements for the degree of Master of Science in Civil Engineering (Structural Engineering).

Signature:
Name: ***Ass.Prof. Dr. Haitham H. AlDaami***
Date: / / 2009

Signature:
Name: ***Ass.Prof. Mr. Abdul Ridah Saleh***
Date: / / 2009

References

1. ***Nilson, A.H.***, "Design of Prestressed Concrete", Wiley and Sons, 1987.
2. ***Hurst, M.K.***, "Prestressed Concrete Design", Chaman and Hall, 1988.
3. ***Canfield, S.R.***, "Full Scale Testing of Prestressed, High Performance Concrete, Composite Bridge Girders", M.Sc. Thesis, Georgia Institute of Technology, August 2005.
4. ***ACI318-08***, "Building Code Requirements for Reinforced Concrete (ACI 318M-08) and Commentary (ACI 318R M-08)", American Concrete Institute, Detroit, 2008.
5. ***Barnes R. W., Burns N. H. and Kreger M. E.***, "Development Length of 0.6-Inch Prestressing Strand in Standard I-Shaped Pretensioned Concrete Beams" Center for Transportation Research Research Report 1388-1, December 1999.
6. ***Kahn, L. F., Lai, J. S., Reutlinger, C., Dill, J. and Shams, M.***, "Direct Pull-Out Capacity and Transfer Length of 0.6-inch Diameter Prestressing Strand in High-Performance Concrete," Task 5 Report, Georgia Department of Transportation Project No. 9510, Georgia Institute of Technology, Atlanta, GA, April 2000, Cited by Ref. (3).
7. ***Lane, S. N.***, "Development Length of Prestressing Strand," Public Roads – A Journal of Highway Research and Development, Federal Highway Administration, Vol. 54, No.2, September 1990, pp. 200-205.
8. ***Tadros, M.K., Al-Omaishi, N., Seguirant, S.J. and Gallt, J.G.***, "Prestress Losses in Pretensioned High-Strength Concrete Bridge Girders", NCHRP Report 496, Transportation Research Board, Washington, 2003.
9. ***Ngo, D. and Scordelis, A.***, "Finite Element Analysis of Reinforced Concrete Beams", ACI J, Vol.64, No.3, March 1967.

10. ***Nilson, A.H.***, "Nonlinear Analysis of Reinforced Concrete by the Finite Element Method", ACI Journal, Vol.65, No.9, September 1968.

11. ***Scordelis, A.C., Ngo, D. and Franklin, H.A.***, "Finite Element Study of Reinforced Concrete Beams with Diagonal Tension Cracks", Proceedings of Symposium on Shear in Reinforced Concrete, ACI Publ. SP-42, 1974, Cited by Ref. (33).

12. ***Franklin, H.A.***, "Nonlinear Analysis of Reinforced Concrete Frames and Panels", PH.D. Dissertation, Division of Structural Engineering and Structural Mechanics, University of California, Berkeley, SEM 70-4, March 1970.

13. ***Cervenka, V. and Gerstel K.H.***, "Inelastic analysis of reinforced concrete panels: Theory (1), and experimental verification and application (2)", Publications, International Association for Bridges and Structural Engineering, Zurich, Vol.31, 1971.

14. ***Nam, C.H. and Salmon, C.G.***, "Finite Element Analysis of Concrete beams", Journal of Structural Division, ASCE, Vol.100. No. ST12, December 1974, pp. 2419-2432.

15. ***Buyukozturk, O.***, "Nonlinear Analysis of Reinforced Concrete Structures", Journal of Computer and Structures, Vol.7, February 1977, pp. 149-156.

16. ***Damijanic F. and Owin D.R.J.***, "Practical Considerations for Modeling of Post-Cracking concrete Behavior for Finite Element Analysis of Reinforced Concrete Structures", Invited Paprer, International Confernce, Computer-Aided Analysis, Cited by Ref. (33).

17. ***Al-Shaarbaf, I.A.S.***, "Three-Dimentional Non-Linear Finite Element Analysis of Reinforced Concrete Beams in Torsion", PH.D. Thesis, University of Bradford, 1990.

18. ***Al-Bahadly, H.M.A.***, "Nonlinear Analysis of Elasto-Plastic Steel and Reinforced Concrete Beams in Torsion using Three-Dimensional Finite Element Model", M.Sc. Thesis, University of Technology, Baghdad, 1995.

19. ***Al-Mousely, B.S.T***., "Three Dimensional Nonlinear Finite Element Analysis for Steel Fiber Reinforced Concrete Beams Subjected to Combined Bending and Torsion", M.Sc. Thesis, University of Technology, Baghdad, 1998.

20. ***Al-Taei, A.T.T.***, "Three Dimensional Nonlinear Finite Element Analysis of High Strength Reinforced Concrete Beams under Torsion and Bending", M.Sc. Thesis, University of Technology, Baghdad, 2000.

21. ***Janney, J.R., Hognestad E. and McHenry D.***, "Ultimate Flexural Strength of Prestressed and Conventionally Reinforced Concrete Beams", ACI Journal, Feb.1956.

22. ***Zienkiewicz, O.C., Owen, D.R.J., Phillips, D.V., and Nayak, G.C.***, "Finite Element Methods in the Analysis of Reactor Vessels", Nuclear Engineering and Design, Vol.20, No.2, 1972, pp. 507-541.

23. ***Argyris J.H., Faust, G., Szimmat J., Warnke E.P., and William K.J.***, "Recent Developments in the Finite Element Analysis of Prestressed Concrete Reactor Vessels", Nuclear Engineering and Design, Vol.28, 1974.

24. ***Connor J.J., and Sarne Y.***, "Nonlinear Analysis of Prestressed Concrete Reactor Pressure Vessels", Paper H2/2,3rd International Conference on Structural Mechanics in Reactor Technology, London, September 1975, Cited by Ref. (33).

25. ***Goodpasture D.W., Burdette E.G. and Callahan J.P.***, "Design and Analysis of Multicavity Prestressed Concrete Reactor Vessles", Nuclear Engineering and Design, Vol.46, 1978, Cited by Ref. (33).

26. ***Kang Y.J. and Scordelis A.C.***, "Nonlinear Analysis of Prestressed Concrete Frames", Journal of Structural Division, ASCE, Vol.106, No.ST2, Feb.1980.

27. ***Geunen J.V. and Scordelis A.C***., "Nonlinear Analysis of Prestressed Concrete Slabs", Journal of Structural Division, ASCE, Vol.106, No.ST2., Feb.1980.

28. ***Abdul-Rahman H.H. and Hinton E.***, "Nonlinear Finite Element Analysis of Reinforced Concrete Stiffened and Cellular Slabs", Computers and Structures, Vol.23, No.3, 1986.

29. ***Ghalib, A.M.***, "Interface Finite Element Analysis of Prestressed Concrete Multi-Planar Systems", M.Sc. Thesis, University of Baghdad, 1990.

30. ***Cruz, P.J.S, Mari, A.R. and Roca, P.***, "Nonlinear Time-Dependent Analysis of Segmentally Constructed Structures", Journal of Structural Engineering, March 1998, pp. 278-287.

31. ***Tawfieq, A.M.***, "Nonlinear Finite Element Analysis of Prestressed Concrete Beams", M.Sc. Thesis, University of Al-Nahreen, 2002.

32. ***Haines, R.A.***, "Shear Testing of Prestressed High Performance Concrete Bridge Girders", M.Sc. Thesis, Georgia Institute of Technology, August 2005.

33. ***Muhammed, H.S.***, "Nonlinear Analysis of Composite Prestressed Concrete Girders with Cast-in-Place Deck", PH.D. Thesis, University of Baghdad, August 2006.

34. ***Yousuf, F.K.***, "Non-linear Finite Element Analysis of Trapezoidal Concrete Box Girder Bridges", M.Sc. Thesis, University of Baghdad, 2008.

35. ***Hawk, H. and Ghali, A.***, "Dynamic Response of Bridges to Multiple Truck Loading", National Research Council of Canada, 1981, pp. 392-402.

36. ***Lee, P.K.K., Ho, D. and Chung, H.W.***, "Static and Dynamic Tests of Concrete Bridge", Journal of Structural Division, ASCE, Vol.113. No.1, January 1987, pp. 61-73.

37. ***Jawad, A.A.***, "Dynamic Response of Plate Girder Bridges to Moving Vehicles", M.Sc. Thesis, University of Baghdad, 1992.

38. ***Chen, H.L., Spyrakos, C.C. and Venkatesh, G.***, "Evaluating Structural Deterioration by Dynamic Response", Journal of Structural Division, ASCE, Vol.121. No.8, August 1995, pp. 1197-1204.

39. ***Karoumi, R.***, "Response of Cable-Stayed and Suspension Bridges to Moving Vehicles Analysis Methods and Practical Modeling Techniques", PH.D Thesis, Royal Institute of Technology, S-100 44, Stockholm, Sweden, 1999.

40. ***Thabet, A. and Haldane, D.***, "Three-Dimensional Simulation of Nonlinear Response of Reinforced Concrete Members Subjected to Impact Loading", ACI Journal, Vol.97, No.5, September 2000.

41. ***Martin, T.M., Baton, F.W., McKeel, W.T., Gomez, J.P. and Massarelli, P.J***., "Effect of Design Parameters on The Dynamic Response of Bridges", Virginia Transportation Research Council, Report VTRC 00-R23, June 2000.

42. ***Michaltsos, G.T., Sarantithou, E. and Sophianopoulos, D.S.***, "Flexural-Torsional Vibration of a Simply Supported Open Cross-

Section Steel Beams under Moving Loads", Journal of Sound and Vibration 280, 2005, pp.479-494.

43. ***Kavipurapu, P.K.***, "Forced Vibration and Hygrothermal Analysis of Composite Laminated Beams under the Action of Moving Loads", M.Sc. Thesis, University of West Virginia, 2005.
44. ***Harris, N.K., Obrien, E.J. and Gonzalez, A.***, "Reduction of Bridge Dynamic Amplification through Adjustment of Vehicle Suspension Damping", Journal of Sound and Vibration 302, 2007, pp.471-485.
45. ***Yu, L. and Chan, T.H.T.***, "Recent research on Identification of Moving Loads on Bridges", Journal of Sound and Vibration 305, 2007, pp.3-21.
46. ***Kato, M. and Shmada, S.***, "Vibration of PC Bridge during Failure Process", Journal of Structural Division, ASCE, Vol.112. No.7, July 1986, pp. 1692-1703.
47. ***Huang, D., Wang, T. and Shahawy, M.***, "Impact Studies of Multigirder Concrete Bridges", Journal of Structural Division, ASCE, Vol.119. No.8, August 1993, pp. 2387-2402.
48. ***Green, M.F., Cebon, D. and Cole, D.J.***, "Effects of Vehicle Suspension Design on Dynamics of Highway Bridges", Journal of Structural Division, ASCE, Vol.121. No.2, February 1995, pp. 272-282.
49. ***Abdalla, H. and Kennedy, J.B.***, "Dynamic Analysis of Prestressed Concrete Beams with Openings", Journal of Structural Division, ASCE, Vol.121. No.7, July 1995, pp. 1058-1068.
50. ***Chandolu, A.***, "Assessing The Needs for Intermediate Diaphragms in Prestressed Concrete Girder Bridges", M.Sc. Thesis, Louisiana State University, 2005.

51. ***Hamed, E. and Frostig, Y.***, "Natural Frequencies of Bonded and Unbounded Prestressed Beams-Prestress Force Effects", Journal of Sound and Vibration 295, 2006, pp.28-39.

52. ***Kwak, H.G. and Filippou, F.C.***, "Finite Element Analysis of Reinforced Concrete Structures under Monotonic Loads", California Department of Transportation, Report No. UCB/SEMM-90/14, University of California, Berkeley, November 1990.

53. ***Chen, W.F.***, "Plasticity in Reinforced Concrete", McGraw-Hill Book Co., New York, 1982.

54. ***Kupfer, H.B, Hilsdorf, H.K. and Rusch, H.***, "Behavior of Concrete under Biaxial Stresses", Journal of ACI, Vol.66, No.8, August, 1969, pp. 656-666.

55. ***Tasuji, M.E., Slate, F.O. and Nilson, A.H.***, "Stress-Strain Response and Fracture of Concrete in Biaxial Loading", Journal of ACI, Vol.75, No.7, July 1978, pp. 306-312.

56. ***Chen, W.F. and Saleeb, A.F.***, "Constitutive Equations for Engineering Materials: Elasticity and Modeling", Vol.1, John Wiley and Sons, New York, 1982.

57. ***Cook R.D.***, "Finite Element Modeling for Stress Analysis", John Wiley and Sons, New York, 1995.

58. ***ANSYS***, "ANSYS Help", Release 9.0, Copyright 2004.

59. ***Aparicio, J., Maia, I. and Salete, E.***, "ANSYS Customization for Bridges and Prestressed Concrete Structures Analysis and Design".

60. ***Yang, Y.B., Yau, J.D. and Wu, Y.S.***, "Vehicle-Bridge Interaction Dynamics with Applications to High-Speed Railway", World Scientific Publishing Co. Pte. Ltd., 2004.

61. American Association of state Highway and Transportation Officials (***AASHTO***), "Standard Specification for Highway Bridges", 2001.

62. ***Chaallal, O. and Shahawy, M.***, "Experimental Evaluation of Dynamic Amplification for Evaluation of Bridge Performance", Department of Construction Engineering, University of Quebec, Report No. ETS.DRSR.98.1, June 1998.

63. ***Wang, E. and Nelson, T.***, "Structural Dynamic Capabilities of ANSYS", Munich, Germany.

64. ***Bathe, K.J.***, "Finite Element Procedures", Prentice-Hall, Inc., The United States of America, 1996.

65. ***Bathe, K.J.***, "Finite Element Procedures in Engineering Analysis", Prentice-Hall, Englewood Cliffs (1982).

66. ***Zienkiewicz, O. C.***, "The Finite Element Method", McGraw-Hill Company, London, (1977).

67. ***Wolanski, A.J.***, "Flexural Behavior of Reinforced and Prestressed Concrete Beams Using Finite Element Analysis", M.Sc. Thesis, University of Maquette, Wisconsin, 2004.

68. ***Huyse, L., ,Hemmaty, Y., and Vandewalle, L.***, "Finite Element modeling of Fiber Reinforced Concrete beam", Proceeding of the ANSYS Conference ,vol.2. Pittsburgh, Pennsylvania, May 1994.

69. ***Xiong, D., and Zha, X.***, "A numerical Investigation on the Behavior of Concrete Filled Steel Tubular Columns under Initial Stresses", journal of Construction Steel Research, Vol63, 2007, pp599-611.

Chapter One

Introduction

1.1 General:

Prestressed concrete can be defined in general as the pre-loading of a structure before the application of the service load so as to improve its performance in specific ways [(1)].

This technique is successfully used in some applications such as multistory buildings, nuclear reactor vessels, long span bridge, offshore platforms, piles and other structures.

Although several patents were taken out in the last century for various prestressing schemes; they were unsuccessful because low-strength steel was used. It was only in the early part of the twentieth century that the French engineer Eugene Freyssinet approached the problem in a systematic way and using high-strength steel; he firstly applied the technique of prestressing concrete successfully. Since then the prestressed concrete has become a well established method of construction and the technology is available in most developed and in many developing countries [(2)].

1.2 Transfer Length:

Transfer length is the distance required to transfer the effective force from the prestressing strand to the concrete member [(3)] or it is the length of embedded pretensioned strand required to transfer the effective prestress to the concrete [(4)].

Figure (1.1) illustrates the idealized stress in a pretensioned strand during transfer. The plot is composed of two sections; the initial linearly varying portion and the constant effective stress plateau.

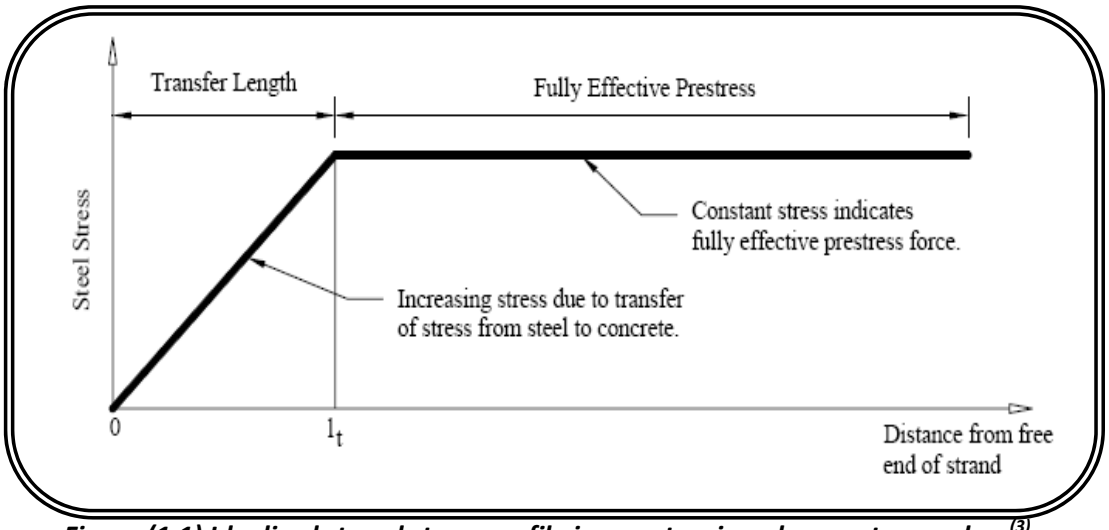

Figure (1.1) Idealized strand stress profile in a pretensioned concrete member [3]

The stress in the prestressing strand is transferred to the concrete member through bond stresses, which are developed by three methods: adhesion, Hoyer's effect and mechanical interlock [5]. The three mechanisms which create the bond between the prestressing strand and the concrete are discussed in Section (1.3), (Development Length). Several factors are believed to affect the transfer length [6], such as:

- ❖ Strand size and surface conditions.
- ❖ Concrete compressive strength at time of release.
- ❖ Modulus of elasticity at time of release.
- ❖ Method of release.
- ❖ Level of prestressing.
- ❖ Amount of confining steel.

1.3 Development Length:

Development length is comprised of two components, a transfer length and a flexural bond length; both are necessary to develop the maximum strand stress, f_{ps}, at nominal flexural strength of the member.

The transfer length is the length needed to transfer the effective prestressing force from the prestressing strand to the surrounding

concrete. Upon loading, the prestressing strand undergoes increased tensile stresses, thereby inducing greater bond stresses.

Flexural bond length is the additional length necessary to allow the development of the increased bond stresses, thereby allowing the strand to develop a stress, f_{ps}. An idealized stress profile is presented in ***Figure (1.2)***.

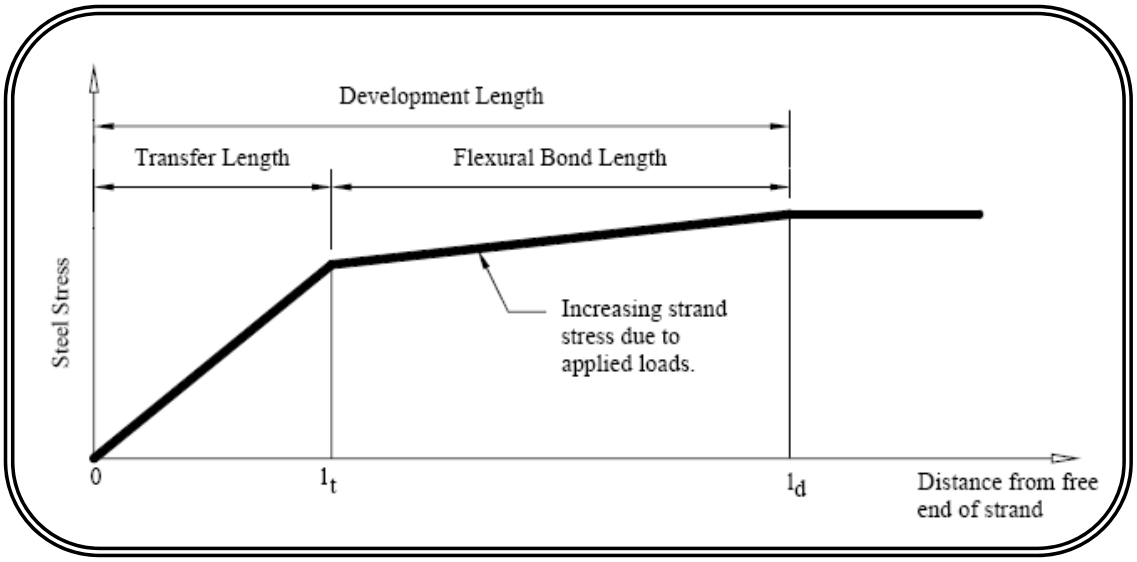

Figure (1.2) Idealized bilinear relationship between strand stress and distance from free end of strand [3]

The development of the strand stress, f_{ps}, is achieved through several mechanisms of bond: adhesion, Hoyer's Effect and mechanical interlock [7].

Adhesion is the chemical bond formed between the prestressing strand and the surrounding concrete, which acts to prevent slip between the strand and concrete. Once slip occurs, the chemical bond is lost. As such, adhesion occurs in the flexural bond length only, as small amounts of slip occur within the transfer length.

Hoyer's Effect, named after E. Hoyer who first investigated the mechanism, is a consequence of the tensioning process. As a prestressing strand is tensioned, the diameter decreases due to Poisson's effect, after which concrete is cast. Following casting, the strands are cut and the

strand is unstressed at the extreme end of the member but is stressed within the concrete member. The varying degree of stress within the strand causes a variation in the strand diameter; the strand diameter at the member end is greater than the diameter of the strand further in the member. The variation of strand diameter creates a wedge effect, helping to prevent strand slip.

Mechanical interlock is a function of the shape of a prestressing strand. A seven wire prestressing strand is manufactured with a single wire wrapped by six wires in a helical pattern. This pattern provides valleys on the strand perimeter which are filled with concrete during casting, ultimately creating an envelope around the strand. The strand is prevented from slipping as long as the strand does not twist, which is prevented by the Hoyer Effect within the transfer length.

1.4 Prestress Losses:

Use of high-strength concrete for pretensioned concrete bridge girders has become accepted practice by many state highway agencies because of its technical and economic benefits. High-strength concrete permits longer girders and increased girder spacing, thus reducing total bridge cost.

The design of pretensioned concrete girders requires accurate estimates of prestress losses. These losses are affected by factors such as mix design, curing, concrete strength, and service exposure conditions.

If one underestimates prestress losses, there is a risk of cracking the girder bottom fibers under full service loads. On the other hand, if prestress losses are overestimated, a higher prestress force must be provided, which will result in larger amounts of camber and shortening

than is necessary. It is, therefore, important to have a reasonably accurate estimate of prestress losses [8].

The primary purpose of calculating the effective prestress force acting on a prestressed concrete section is to evaluate concrete stresses and deformations under service conditions.

The most representative definition of prestress loss is the loss of compressive force acting on the concrete component of a prestressed concrete section. Creep and shrinkage cause member shortening and a loss of tension in the prestressing tendons as well as a compression force increment in non-prestressed reinforcement, if such reinforcement exists in a member. The sum of the reduction in tensile force in the tendons and compression force increment in the non-prestressed reinforcement is equal and opposite to the incremental loss of compression force in concrete. That force is the force needed for concrete stress analysis.

1.5 Components of Prestress Losses in Pretensioned Girders:

Components of prestress losses are illustrated in ***Figure (1.3)*** as described below [8].

(a) Loss is due to prestressing bed anchorage seating, relaxation between initial tensioning and transfer, and temperature change from that of the bare strand to temperature of the strand embedded in concrete.

(b) Instantaneous prestress loss at transfer is due to prestressing force and self weight.

(c) Prestress loss between transfer and deck placement is due to shrinkage and creep of girder concrete and relaxation of prestressing strands.

(d) Instantaneous prestress gain is due to deck weight on the non-composite section and superimposed dead loads (SIDL) on the composite section.

(e) Long-term prestress losses after deck placement are due to shrinkage and creep of girder concrete, relaxation of prestressing strands, and deck shrinkage.

Prestress losses in pretensioned high-strength concrete girders are influenced by material properties (internal factors) and environmental conditions (external factors). Accurate prediction of prestress losses requires accurate prediction of the long-term properties of concrete and prestressing strands, which is a very complex process because of the uncontrollable variables involved. The material properties that vary with time and affect prestress losses are compressive strength, modulus of elasticity, shrinkage (stress independent), and creep (stress dependent) of concrete, and relaxation of strands.

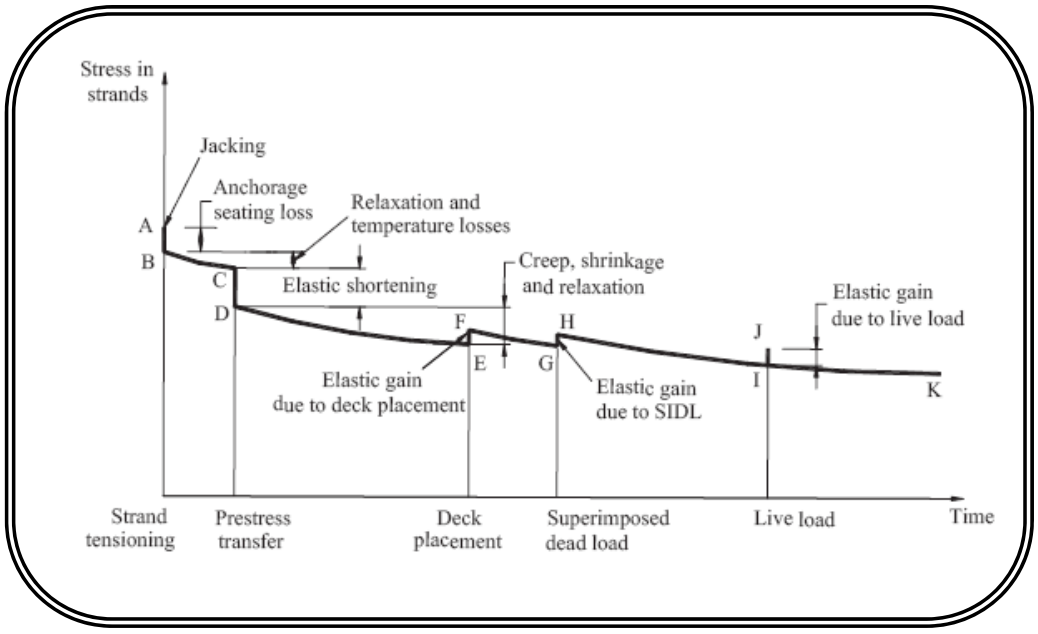

Figure (1.3) Stress versus time in the strands in a pretensioned concrete girder [8]

The rate at which concrete properties change with time depends on a number of factors, including type and strength of cement, type, quality,

and stiffness (i.e., modulus of elasticity) of aggregates, and quantity of coarse aggregates; type and amount of admixtures; water/cement ratio; size and shape of the girder; stress level; and environmental conditions (humidity and temperature). Relaxation of strands is a long-term reduction of stress when strands are subjected to an imposed strain, and can be estimated with good accuracy.

1.6 Advantages of Prestress Concrete:

Prestressing is a technique of inducing a state of pre-compression in a concrete section to increasing effective concrete section to resist service load. Concrete is inherently weak in tension although strong in compression. The fact of prestressed section is in compression means that under serviceability load conditions cracking will not tack place.

Prestressed concrete offers a number of distinct advantages over reinforced concrete. Perhaps the most important advantage is that the camber resulting from prestressing force will reduce or even eliminating the excessive down word deflection under full service load. Another advantage is that in prestressed concrete section the whole concrete area acts to resist bending, unlike the reinforced concrete where the concrete in tension zone is cracked and provides negligible contribution to the stiffness of the section. Hence for a given span and loading it is possible to design a beam or a slab of shallower depth if prestressed construction is used, this leads to aesthetic advantages, saving in materials and reduction in weight of the structure. In addition prestressing also minimizes the development of shear crack. Also prestressing has led to use high strength steel and concrete. This improves the carrying capacity of the concrete member and resulting in lighter structure. The use of high strength concrete helps to control the prestressing force losses due to

shrinkage and creep.

The prestressed concrete I-type girder is widely used in construction of bridge superstructures because they are relatively simple to design and construct and have less expensive maintenance and repair costs.

1.7 Moving Loads on the Girders Bridges:

Vehicle-induced dynamic response of bridges is one of the primary problems concerning bridge engineers. Moving vehicles usually produce larger bridge responses than static vehicles do. Bridge vibrations have become one of the causes of deterioration and reduction in long-term serviceability of bridges, although major bridge failures are not usually caused directly by moving vehicles. The effect of moving vehicles on the dynamic response of bridges is of primary importance in the design of these structures.

1.8 Objective and Scope:

The main objective of this research is to investigate the dynamic effects of a moving load on prestressed concrete girder, simply supported beam under various parameters such as various vehicle velocities, variable number of passing moving load on the girder, representation of moving load and various cross section of the prestressed girder.

For this purpose the computer program ANSYS (ANalysis SYStem) version 9.0 is developed using a three dimensional finite element analysis.

1.9 Layout of Thesis:

An introduction of prestress technique, transfer and development length of prestress force, prestress losses, and advantages of prestress concrete

are presented in ***Chapter One***, with the objective and scope of this investigation.

A literature review is presented in ***Chapter Two*** to give a brief historical review about analysis of reinforced and prestressed concrete members under static and moving load.

In ***Chapter Three***, the behavior of each concrete under compression load, and steel (ordinary and prestress) reinforcement under tension load and the nonlinear solution techniques are described. The model generation in ANSYS program represented by the used elements (BEAM3 and SOLID65) and the representation of the prestressed concrete girder in ANSYS are also described in this chapter.

The modeling and representation of vehicle in the dynamic analysis, methods of dynamic analysis in ANSYS, and the adopted model of moving load in ANSYS are presented in ***Chapter Four***.

Chapter Five contains the applications and results discussion where this chapter is divided into three parts represented by verification of the modeling of moving load, verification of the prestressed concrete model and finally the two verifications are considered together to represent the current problem and also a parametric study of some factors are considered by using ANSYS program.

The conclusions and the further studies are mentioned in the last section ***Chapter Six***.

Chapter Two

Literature Review

2.1 Introduction:

Because of the wide use of both prestressed and non-prestressed reinforced concrete structures, there will be an interest in understanding and using nonlinear analysis of reinforced concrete structures. In the mid sixties, the finite element method had started to use the nonlinear analysis of prestressed and reinforced concrete member such as beams, slabs and columns due to development of electronic digital computers.

In this chapter a historical review is given to show the work which was conducted on composite prestressed girders. The review includes the studies of nonlinear analysis of prestressed composite structures, and the estimation and modeling of live load on bridge.

2.2 Nonlinear FE Analysis of Reinforced and Prestressed Concrete Members:

To review the studies on nonlinear finite element analysis of reinforced and prestressed concrete members, it's of wisdom to start with the easiest one, i.e. (the reinforced concrete members), then to the more complicated subject which is the prestressed concrete members.

2.2.1 The Studies under Static Load

2.2.1.1 Reinforced Concrete Members

Ngo and Scordelis in 1967 [9] presented the earliest published applications of the finite element to reinforced concrete structures. In their study, several examples of simply supported concrete beams with

different idealized cracking patterns were considered. In their analysis, the beam subdivided into concrete and steel elements and bond linkage elements. The concrete and steel were represented by constant strain triangular elements. The bond stress and slip were simulated by using linkage elements having two degrees of freedom. The problem was carried out by using a linear solution. The linear solution required that concrete and steel be assumed as elastic materials. Various predefined cracking patterns were used in this study to investigate cracked concrete behavior.

By including cracking (discrete cracks), bond slip as well as nonlinear materials constitutive relationships, ***Nilson*** [10] was the first who introduced nonlinearity. The steel was represented by two dimensional triangular elements. The uncracked member was loaded incrementally until the principal tensile stress exceeds the modulus of rupture of concrete at one or more locations. Then cracking was allowed to take place along the edge between adjacent elements as used by Ngo and Scordelis to simulate the bond-slip. ***Scordelis, Ngo and Franklin*** [11] used the same approach to study shear in beams with diagonal tension cracks, considering the effect of stirrups, dowel shear, aggregate interlock, horizontal splitting along reinforcement near the supports.

Franklin [12] advanced the capability of the analytical method by developing a nonlinear analysis which accounted automatically within the finite elements and by redistribution of stress into the system, which made it possible to trace the response of two dimensional systems from initial loading to failure in one continuous computer analysis. Incremental loading, with iterations within each increment was used to account for cracking in the finite element and to account for the nonlinear properties of materials. He used special type elements, quadrilateral plane stress

elements, axial bar members, two-dimensional bond links and tie links to study reinforced concrete frames with and without reinforced concrete shear walls.

Two dimensional layered plane stress elements with composite concrete and steel properties were used to analyze planar reinforced concrete structures such as walls and spandrels beams by ***Cervenka and Gerstel*** [13]. Comparison with experimental results was found favorable. Quadrilateral isoparametric elements were used to represent the concrete, while the reinforcing bars were represented by linear bar elements, which were considered to be rigidly interconnected at the nodes of the concrete elements. It was assumed that yielding stress followed Von-Mises yield criterion to understand the behavior of concrete in compression. In tension if any principal stress exceeded the tensile strength of concrete, a crack was assumed to develop in a direction perpendicular to the principal stress. This nonlinear finite element model to analyze reinforced concrete beams was presented by ***Nam and Salmon*** in 1972 [14].

Buyukozturk [15] analyzed reinforced concrete deep beams by simulating them through the use of in-plane stress finite element model. The model was consisting of isoparametric triangular elements for concrete while the reinforcement was represented by equivalent steel layers within the concrete elements.

Damijanic and Owin [16] used 8-noded isoparametric quadrilateral elements to represent the concrete. Steel bars were represented by special elements embedded into the isoparametric elements. The presented finite element model covered the cracking and post-cracking behavior of reinforced concrete members. Tensile cracking was governed by a maximum tensile stress criterion. The cracking model was adjusted by

tension- stiffening and shear-retention parameters. Both the tensile stiffness (in the direction perpendicular to the cracked plane) and the shear stiffness were reduced to zero according to the linear descending stress-strain relations.

Al-Shaarbaf [17] described a nonlinear finite element model suitable for the analysis of reinforced concrete or steel members under general three- dimensional states of loading. The 20-Noded isoparametric brick elements were used to model the concrete and reinforcing bars were idealized as axial members embedded within the concrete elements. The behavior of concrete in compression was simulated by an elasto-plastic work hardening model followed by a perfectly plastic response, which is terminated at the onset of crushing. In tension a smeared crack model with fixed orthogonal cracks was used with inclusion of models for the retained post-cracking stress and reduced shear modulus. The nonlinear equations of equilibrium were solved using on incremental-iterative technique operating under load control.

Al-Bahadly [18], in 1995, adopted Al-Shaarbaf model to investigate the behavior of hallow reinforced concrete beams subjected to torsion. Good agreement between experimental and numerical results was obtained.

In 1998, ***Al-Mousely*** [19] used a three-dimensional non-linear finite element model to analyze steel fiber reinforced concrete beams subjected to combined bending and torsion. The 20-noded isoparametric brick elements have been used to model the concrete. The steel bars were idealized as axial members embedded within the concrete elements. Perfect bond between the concrete and reinforcement has been assumed. The compressive behavior of the steel fiber reinforced concrete was

simulated by an elasto-plastic work hardening model followed by a perfectly plastic plateau, which was terminated at the onset of the crushing. Good agreement between experimental and numerical curves is observed throughout the entire range of behavior.

In 2000, a three dimensional non-linear finite element model were used to analyze high strength reinforced concrete beams under torsion and bending adopted by ***Al-Taei*** [20]. The 20-noded isoparametric brick elements have been used to model the concrete. The steel bars were idealized as axial members embedded within the concrete elements. Perfect bond between the concrete and reinforcement has been assumed. The softening of concrete due to transverse straining of reinforcement was introduced. Good agreement has been observed throughout the entire range of behavior.

2.2.1.2 Prestressed Concrete Members

Structural concrete in buildings and bridges usually requires some kind of tension reinforcement to resist flexural loads. Intermediate-grade deformed bars constitute a major percentage of the reinforcing steel used in the United States [21], although an increasing amount of high-strength steel (usually wire or strand) is being used in conjunction with various applications of prestressed concrete. A prestressed concrete structure has many advantages, as mentioned in chapter one, several nonlinear models for prestressed concrete structures have been proposed during the past decades in order to analyze these sophisticated and complex prestressed concrete structures accurately and efficiently.

Comprehensive papers on the analysis of concrete vessels have been presented at the conferences by ***Zienkiewicsz et al*** [22], by ***Argyris et al***

[23], by ***Connor and Sarne*** [24] and by ***Goodpasture*** [25]. Finite element method was used for the analysis prestressed concrete nuclear reactor vessels using axisymmetric or three-dimensional solid elements.

Kang and Scordelis [26] presented a nonlinear method for the analysis of prestressed concrete frames which is based on the finite element method with included effect of time dependent variation due to load history, temperature history, creep, shrinkage and aging concrete. To simulate material properties a nonlinear model was used, which was capable of capturing the dominant flexural behavior of prestressed concrete frames in various load ranges and up to failure. The prestressed steel was incorporated as integral part of the structure. Thus the variation of prestress was traced automatically during various stages of prestressing and loading in a unified.

An efficient numerical model for the material and geometric nonlinear analysis of reinforced and prestressed concrete slabs and panels had been developed by ***Geunen and Scordelies*** [27]. The effect of time dependent variable due to load history, shrinkage, aging of concrete and relaxation of stress in prestressing steel had been included in this study. A flat triangular shell finite element used which consists of six degrees of freedom at each node. The reinforced concrete section was modeled as layered system of concrete and "equivalent smeared" steel layers.

Abdel-Rehman and Hinton [28] used a nonlinear finite element model to analyze ten prestressed concrete cellular slabs with different geometric and different loading conditions. The analysis is based on a slab-beam model and two dimensional finite element representations were used to model the concrete. The prestressing strands were replaced by ordinary reinforcement which has been represented as smeared steel

layer equivalent in area to the cross sectional area of one strand. The prestressing force was represented by axial forces acting at the center of reinforcement. Comparison of cracking loads, deflections and collapse loads were presented.

Reinforced and prestressed concrete structures were represented by an assemblage of a set of isoparametric, layered, 8-noded flat shell elements with a total of six degrees of freedom per node has been developed by ***Ghalib*** [29]. The concrete model was an elastic-plastic material with a work-hardening zone in compression and treated as elastic-brittle fracture material in tension. Reinforcement was represented by either a smeared, fully bonded steel layer of orthotropic properties to represent equally spaced reinforcement arrangements, or as a discrete, generally curved steel strand element to model special heavy reinforcement consideration. Prestressing tendons were considered as an integral part of the structure. An iterative-incremental technique was adapted to the analysis of several available experimental specimens.

In 1992, ***Cruz et al.*** [30] presented a general step-by-step model for the nonlinear and time-dependent analysis of reinforced concrete, prestressed concrete and composite steel concrete planner frame structures. The model dealt with pre-tensioned bonded and unbounded tendons. Based on the displacement formulation of the finite element method, the model can trace structural response during the construction of the structure and throughout its service life. Consideration of the geometric and material nonlinearities allows the structural response to be traced through the elastic, cracked and ultimate load levels.

A three-dimensional non-linear finite element model was used to analyze rectangular, I and T sections prestressed concrete members

subjected to bending has been adopted by ***Tawfiq*** [31]. A 20-noded isoparametric brick element has been used to model the concrete and prestressing steel bars have been idealized as axial member embedded within the brick elements. Perfect bond between concrete and prestressing steel reinforcement has been assumed to occur. In general good agreements between the finite element solutions and the experimental results have been obtained.

In 2005, ***Canfield*** [3] studied, experimentally, the flexural behavior of two large bridge girders with deck cast in place. The specimens were an AASHTO type IV and a modified PCI BT-56 girder. Two flexural tests were performed on each girder, the first flexural test was an evaluation of the cracking resistance compared to provisions in AASHTO Standard Specification 2002, and the final flexural test was intended to be an evaluation of the ultimate capacity provisions in AASHTO Specification 2002. Effect of transfer lengths of prestress force, prestress losses, thermal and shrinkage are calculated and compared with the Specifications.

The same bridge girders with deck cast in place that used in Canfield search were studied by ***Haines*** [32], to investigate resisting of girders under shearing effects. The AASHTO Standard, 1998 AASHTO LRFD, and 2004 AASHTO LRFD results were compared to results obtained from shearing test of the girders.

In 2006, ***Mohammed*** [33] presented a three-dimensional nonlinear finite element computer program developed for the analysis of composite prestressed concrete girders with cast-in-place deck. The 20-noded isoparametric brick element has been used to represent the concrete in the slab and prestressed concrete girder. The prestressed and ordinary

reinforced steel bars are idealized as an axial member embedded within the concrete elements. He studied two effects; the first was the interface behavior in transferring shear forces from slab to the girder and the second was the transmission of stresses from prestressed strands to the concrete.

In 2008, ***Yousuf*** [34] used ANSYS and FORTRAN Programs to investigate the behavior of prestressed concrete box-girder bridge under short-term loading by using a three-dimensional nonlinear finite element model, A 8-noded brick element has been used to model of the concrete and prestressing steel bars have been idealized as axial member embedded within the brick element, and prestressing forces are modeled by using the equivalent nodal forces concept. In general good agreement between the finite element solutions and the experimental results have been obtained.

2.2.2 The Studies under Moving Load

2.2.2.1 Reinforced Concrete Members

Hawk and Ghali [35], in 1981, investigated successfully the dynamic response of bridges (was a three-span continuous steel plate-girder structure with a concrete deck slab that was longitudinally prestressed for full composite action of the Conestogo River) to multiple truck loading by used analytical procedure called the Iterative Dynamic Substructuring Method (IDSM) was described for determining the response of a beam-slab bridge system traversed by multi-axle trucks. The trucks were idealized as systems of beams mounted on springs and the bridges as a grid. The IDSM applied mode superposition analysis to the bridge and truck as separate structures connected only at the time-dependent contact

points. The bridge was subjected to forces equal to the time-dependent forces on the truck springs, while the truck was subjected to "ground" motion displacements. In that investigation a comparison has been adopted between single and multiple vehicle loadings under various conditions of truck speeds and positions.

In 1987, both static and dynamic tests were carried out on an old reinforced concrete bridge prior to its demolition by ***Lee et al.*** [36]; they used the static test to calibrate the mathematical model that will be used in the structural analysis. This revised a mathematical model that was used to calculate the natural frequencies of the bridge deck and the results compared reasonably well with the measured frequencies from the dynamic tests. The structure under test was a three-span, two-lane, Reinforced Concrete Bridge. The decks were treated as two separate structures and the vibration of the bridge was excited as the following ways:

1. A cylindrical steel hammer weighing 840 kg was dropped from different heights onto the middle of the central and the two end spans where the hummer was dropped from a hoist fitted on the truck that was positioned on the adjacent lane.

2. A light truck weighing 2,200 kg was driven along the bridge at a varying speed.

Jawad [37], in 1992, developed a computer program BDDAP "Bridge Deck Dynamic Analysis Program" in FORTRAN language to study the dynamic response of plate girder bridges to moving vehicle. The vehicle was modeled as either a constant moving force or a moving mass along the bridge deck. The bridge deck was idealized as a grillage of smooth surface with or without a bump at its approach. Bridge damping, vehicle

model, vehicle speed and roughness of bridge deck were considered in the studied.

The dynamic response of two channel steel beams was evaluated in terms of the reduction in load-carrying capacity of the damaged state versus the undamaged stage by ***Chen et al.*** [38]. The beam specimens were sized and configured to have similar frequency response observed in actual bridges. A finite-element model was used to calculate the dynamic response of the simulated damaged structures. The experimental and analytical results were scrutinized to correlate increasing deterioration and changes in the dynamic response. Good correlations were found between the experimental and the analysis.

In 1998, two different approaches were adopted to solve the moving load problem of cable-stayed and suspension bridges by ***Karoumi*** [39] where the first used approach was a simplified analysis method to study the dynamic response of simple cable-stayed bridge model. The bridge was idealized as a Bernoulli-Euler beam on elastic supports with varying support stiffness and to solve the equation of motion of bridge, the finite difference method and the mode superposition technique were used. The second approach was based on the nonlinear finite element method and was used to study the response of more realistic cable-stayed and suspension bridge models considering exact cable behavior and nonlinear geometric effects and two methods for evaluating the dynamic response were presented. The first was used for evaluating the linear traffic load response using the mode superposition technique and the deformed dead load tangent stiffness matrix, and the second was used for the nonlinear traffic load response using the Newton-Newmark algorithm.

A triaxial failure criterion was applied with the theory of plasticity to model the behavior of reinforced concrete structures subjected to impact loading. This investigation was adopted by ***Thabet and Haldane*** [40]. The concrete nonlinearity, the cracking in the concrete elements, and the loading and unloading were simulated using an elastic-plastic fracture model. In tension, a smeared crack model was used with a tension-softening model for the retained postcracking stresses. The reinforcing bars were represented by tensile stiffeners that were smeared in the appropriate direction over the element cross section.

In 2000, ***Tracy et al.*** [41] developed a procedure for representing moving loads on a bridge model within the context of a commercially available computer code. The relative effects of various parameters that have a substantial effect on dynamic response were adopted in this study. Finite element models of typical bridge structures were developed using ANSYS software. The algorithm developed to represent transient loads in the finite element beam model solution provided results essentially identical with those determined from theory.

Investigation of linearized model analysis of the combined flexural-torsional vibration of simply supported steel beams with open monosymmetric cross-section, acted upon by a load of constant magnitude, traversing its span eccentrically with constant velocity was adopted by ***Michaltsos et al.*** [42].

In 2005, ***Kavipurapu*** [43] studied the dynamic response of simply supported composite beams subjected to moving loads in a hygrothermal environment was carried out using the general purpose finite element program ANSYS. A two-dimensional element was used to model the

isotropic beam (BEAM3) where the beam was modeled with 20 elements. The full transient analysis was adopted to solve this problem.

Reduction of bridge dynamic amplification through adjustment of vehicle suspension damping was adopted in 2006 by ***Harris et al.*** [44]. In their study bridge response was defined in term of the dynamic amplification factor (DAF), which was a measure of the maximum total response resulting from the interaction of moving loads and the bridge structure, as a proportion of the maximum static response. The vehicle model was used for simulation of dynamic tire forces imparted to the bridge was a 5-axles multiple degree of freedom articulated truck, as shown in ***Figure (2.1)*** below;

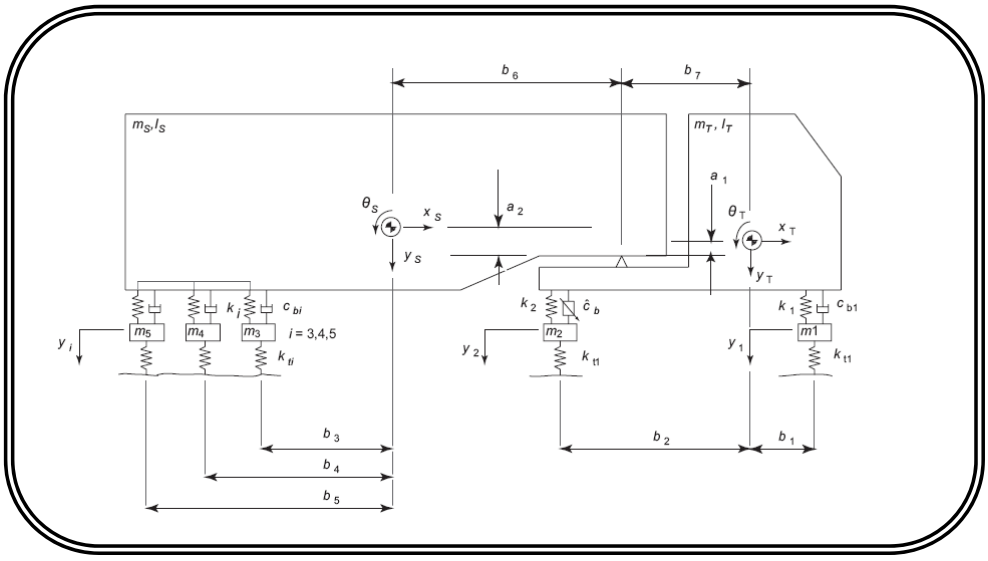

Figure (2.1) Tractor semi-trailer vehicle model [44]

While the bridge model was a simply supported beam (Euler-Bernoulli beam) subjected to five time-varying forces corresponding to the vehicle axle loads, was used to obtain bridge response to the vehicle crossing event.

A review on advances of identification of moving loads on bridges was adopted by ***Yu and Chan*** [45]. Where Numerical simulations, illustrative examples and comparative studies on the effects of different

parameters, such as vehicle-bridge parameters, measurement parameters and algorithm parameters have been carried out and critically investigated.

2.2.2.2 Prestressed Concrete Members

A vibration measurement was carried out on an existing prestressed concrete bridge during its failure test by ***Kato and Shimada*** in 1986 [46], where the change of vibrational characteristics during the failure process of prestressed-concrete-frame bridge (π shape) was discussed by experiment and numerical analysis. The vibration test was carried out at each step of the static loading process until the bridge collapsed.

In 1993, the impact behavior of multiple vehicles moving across rough bridge decks on seven multigirder concrete with different span length was studied by ***Huang et al.*** [47] where the bridge was modeled as a grillage beam systems, and the vehicle was simulated as a nonlinear vehicle model with 12 degrees of freedom according to the HS20-44 truck design loaning in American Association of State Highway and Transportation Officials (AASHTO) specifications. The parametric analysis shows that the impact of exterior girders of short-span bridges is highly sensitive to such factors as lateral loading position, vehicle weight, road roughness, number of loading lanes, and lateral stiffness.

Green et al. [48] investigated the effects of heavy vehicles with leaf-spring and air-spring suspensions on the dynamic response of short-span highway bridges where the dynamic bridge responses were calculated by modeling the bridge and vehicle separately and combining the models with an iterative procedure. Two typical highway bridges were tested. The first was a four-span, prestressed concrete, box-girder bridge, and the

second was a three-span, slab-on-girder, prestressed concrete bridge. They find that the air-sprung vehicle generated significantly smaller theoretical dynamic responses than the leaf-sprung vehicle on all two bridges.

The dynamic analysis and design of simply supported and continuous prestressed concrete beams with rectangular openings were presented by ***Abdalla et al.*** in 1995 [49]. Several design parameters were varied such as opening width and depth, horizontal and vertical locations of the opening, type of cross section, and presence of more than one opening was studied and a good agreement was shown between the theoretical and the experimental results.

Chandolu [50] was adopted assessing the need of reinforced concrete intermediate diaphragms in prestressed concrete girder bridges and the determine of their effectiveness and also to search for an alternative steel diaphragm configuration which would be as effective as reinforced concrete intermediate diaphragms to can replace them if necessary. Systematic parametric studies for various bridge configurations, which were representative of an entire range of bridge geometries with different parameters, were analyzed through simplified and solid finite element models, which were already calibrated under live loads. The study was carried out on right and skewed bridges which were simply supported and continuous. A reduction factor which could be multiplied by a load distribution factor to account for the influence of the diaphragm in load distribution was developed. To assess the effectiveness of various diaphragms in protecting the girders against the lateral impact and to determine the design forces in the steel bracing members during construction of deck, a finite element analysis was carried out by using 3-D solid models.

In 2006, the effect of the magnitude of the prestress force on the natural frequencies of prestressed beams with bonded and unbonded tendons was studied by ***Hamed and Frostig*** [51] where a nonlinear analytical model was formulated for the dynamic behavior of prestressed beams, in order to achieve this goal. The equations of motion for a prestressed beam and its associated boundary and continuity conditions were rigorously derived using the variational principle of virtual work following Hamilton's principle. The kinematic relations for the concrete were those of large displacements and moderate rotations, in order to take into account the compressive force effect caused by the prestress force. For the tendons, the same kinematic relation has been used including the cable profile as an imperfection. The effect of the magnitude of the prestress force on the natural frequencies was mathematically examined. Numerical examples were presented to illustrate the difference between natural frequencies determined by the proposed model and other models mentioned in the literature.

2.3 Summary

From the historical review, it found that there are no or a few papers about this project this is because of the difficulties representation of prestressed concrete girders under moving loads so that it is very important to investigate the behavior of these girders under moving loads.

Chapter Three

Finite Element Modeling

3.1 Introduction:

Reinforced concrete structures are made up of two materials with different characteristics, concrete and steel. Steel can be considered a homogeneous material and its material properties are generally well defined. Concrete is, on the other hand, a heterogeneous material made up of cement, mortar and aggregates. Its mechanical properties scatter more widely and cannot be defined easily. For the convenience of analysis and design, however, concrete is often considered a homogeneous material in the macroscopic sense.

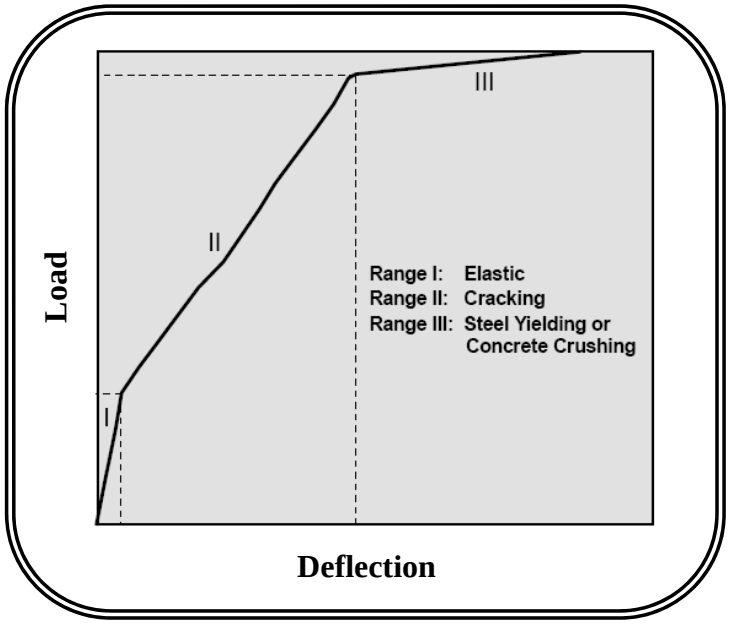

Figure (3.1) Typical Load-Displacements Response of RC Element [52]

The typical stages in the load-deformation behavior of a reinforced concrete simply supported beam are illustrated in ***Figure (3.1)***. Similar relations are obtained for other types of reinforced concrete structural elements. This highly nonlinear response can be roughly divided into

three ranges of behavior: the uncracked elastic stage, the crack propagation and the plastic (yielding or crushing) stage.

The nonlinear response is caused by two major effects, cracking of concrete in tension, and yielding of the reinforcement or crushing of concrete in compression. Nonlinearities also arise from the interaction of the constituents of reinforced concrete, such as bond-slip between reinforcing steel and surrounding concrete, aggregate interlock at a crack and dowel action of the reinforcing steel crossing a crack. The time-dependent effects of creep, shrinkage and temperature variation also contribute to the nonlinear behavior. Furthermore, the stress-strain relation of concrete is not only nonlinear, but is different in tension than in compression and the mechanical properties are dependent on concrete age at loading and on environmental conditions, such as ambient temperature and humidity. The material properties of concrete and steel are also strain-rate dependent to a different extent.

Because of these differences in short- and long-term behavior of the constituent materials, a general purpose model of the short- and long-term response of reinforced concrete members and structures should be based on separate material models for reinforcing steel and concrete, which are then combined along with models of the interaction between the two constituents to describe the behavior of the composite reinforced concrete material [52].

3.2 Modeling of Materials

The basic information required in any three-dimensional nonlinear finite element analysis of reinforced concrete structures is the material constitutive relationships, which describe the multi-dimensional stress-strain relations that govern the behavior of the materials of the structures,

Since prestressed concrete is a complicated composite material, its behavior cannot be obtained without considering the constitutive relations of its constituents (concrete and prestressing steel) independently.

3.2.1 Behavior of Concrete

Depending on the nature and the level of the applied stresses, concrete may behave either as a linear or nonlinear material. Under a low level of stresses, linear elastic behavior is observed, while concrete exhibits a highly nonlinear response at higher stress levels. Strength and stiffness properties of concrete subjected to multiaxial loading conditions differ from those displayed under uniaxial loading. Under ordinary experience, concrete is brittle in tension and has a limited deformation in compression.

3.2.1.1 Uniaxial Behavior of Concrete

3.2.1.1.1 Behavior under Compression Load

A typical stress-strain relationship for concrete subjected to uniaxial compression is shown in ***Figure (3.2)***. The stress-strain curve has a nearly linear-elastic behavior up to about 30 percent of its maximum compressive strength f'_c. For stresses above this point, microcracks form at the mortar-coarse aggregate interfaces and propagate through the mortar upon further loading. At a stress level of about 0.75 f'_c , the rate of crack propagation increases rapidly and the stress-strain curve bend sharply until the peak stress level is reached. Beyond the peak stress level, concrete shows a softening response, which is presented by the descending portion of the stress-strain curve [53].

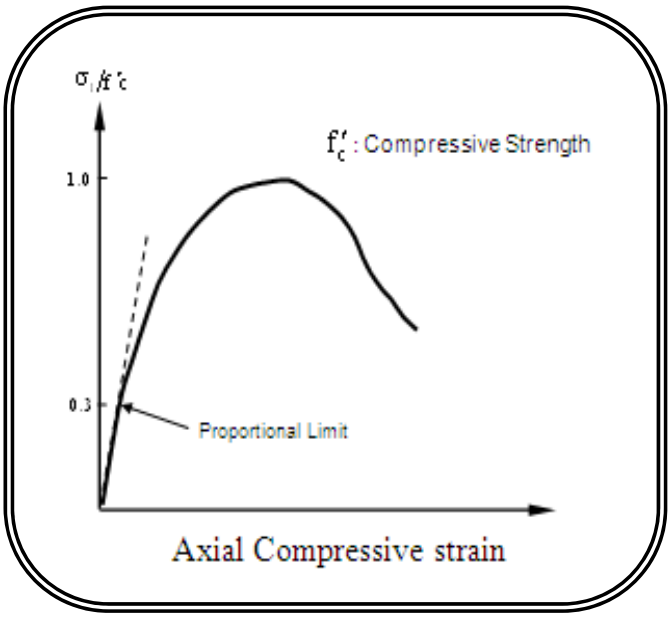

Figure (3.2) Typical uniaxial stress-strain curve for concrete in compression [53]

The shape of the stress-strain curve is similar for concrete of low, normal and high strength, as shown in ***Figure (3.3)***. A high-strength concrete behaves in a linear fashion to a relatively higher stress level than the low-strength concrete, but all peak points are located close to the strain value of (0.002) [53].

As shown in ***Figure (3.3)***, the initial modulus of elasticity of concrete is highly dependent on the compressive strength. In lieu of actual test data, the initial modulus of elasticity E_c can be calculated with reasonable accuracy from empirical formula [4]:

$$E_c = 0.043\ (w_c)^{1.5}\ (f_c')^{0.5} \quad \ldots\ldots\ldots\ldots\ldots\ldots\ldots\ldots\ (3.1)$$

In which, w_c is the air-dry unit weight of concrete in (kg/m³), f_c' is the cylinder compressive strength of concrete in (MPa) and E_c is the modulus of elasticity of concrete in (MPa).

For the normal weight concrete based on a dry unit weight (2200-2500) kg/m^3, E_c can be permitted to be taken as [4]:

$$E_c = 4730\ \sqrt{f_c'} \quad \ldots\ldots\ldots\ldots\ldots\ldots\ldots\ldots\ (3.2)$$

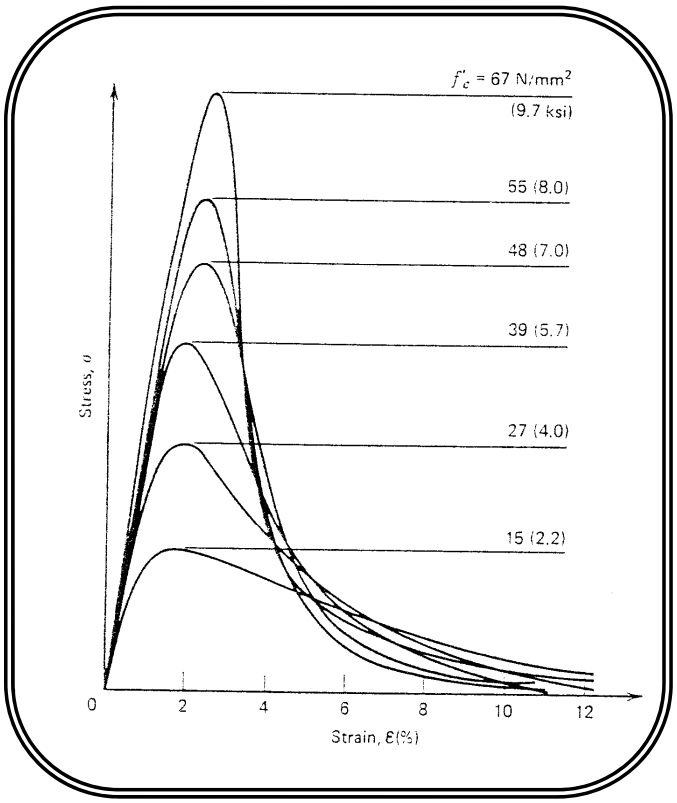

Figure (3.3) Uniaxial compressive stress-strain curves for concrete with different strengths [53].

3.2.1.1.2 Behavior under Tensile Load

Figure (3.4) shows the stress-strain curve for concrete in uniaxial tension. All curves linear up to a relatively high stress level. The shape of the curves shows many similarities to the uniaxial-compression curves. For stress less than about 60 percent of the uniaxial tensile strength, f_t, the creation of new microcracks is negligible. Thus, this stress level will correspond to a limit of elasticity; above this level, the bond microcracks start to grow [53].

The direction of crack propagation for uniaxial tension is transverse (normal) to the stress direction. The growth of every new crack will reduce the available load-stress capacity and this reduction causes an increase in the stresses at critical crack tips. The failure in tension is caused by a few connected cracks rather than by numerous cracks, as it is for compressive states of stress.

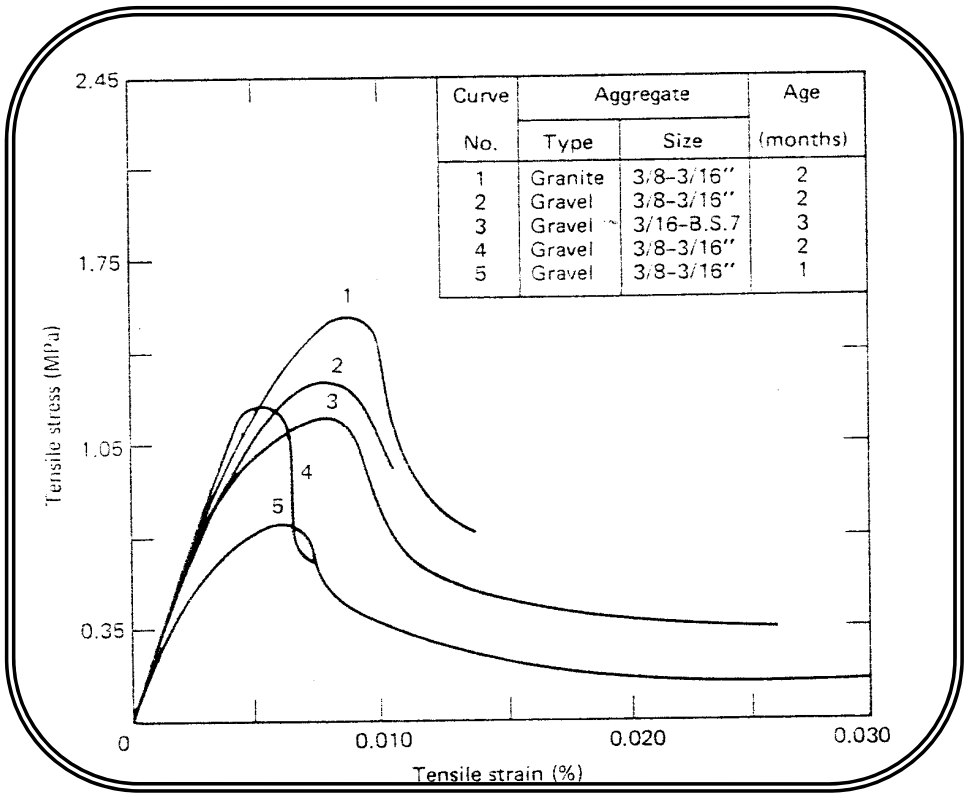

Figure (3.4) Typical uniaxial stress-strain curve for concrete in tension [53]

The ratio between uniaxial tensile strength (f_t) and compressive strength f'_c may vary considerably but usually ranges from 0.05 to 0.1. The modulus of elasticity under uniaxial tension is somewhat higher and Poisson's ratio somewhat lower than in uniaxial compression [53].

The direct tensile strength of concrete is difficult to measure and is normally taken as 0.3 to $0.4\sqrt{f_c'}$. Many times, either the modulus of rupture, f_r, or the split cylinder strength (f_t) is used to approximate the tensile strength of concrete. The value of the modulus of rupture of concrete varies quite widely but is normally as in ***equation (3.3)***. The split cylinder tensile strength is usually somewhat lower, at approximately 0.45 to $0.55\sqrt{f_c'}$ in N/mm^2, $f_r$can be permitted to be taken as [4]:

$$f_r = 0.62\,\gamma\,\sqrt{f_c'} \qquad \text{..... (3.3)}$$

Where:

γ =1 for normal weight concrete.

γ =0.85 for sand-lightweight concrete.

γ =0.75 for all-lightweight concrete.

3.2.1.2 Multiaxial Behavior of Concrete

Under biaxial and triaxial states of stress, the strength and stress-strain envelope of concrete is different from that of uniaxial state. ***Figure (3.5)*** shows a typical biaxial failure envelope for concrete [54]. The maximum compressive strength increases for the biaxial compressive state of stress. A maximum increase in compressive strength of approximately 25% is achieved at a stress ratio of lateral stress / axial stress of 0.5. For equal biaxial compressive stresses, the increase in the compressive strength is about 16%. Under biaxial compression-tension state of stress, the compressive strength decreases almost linearly as the applied tensile stress is increased. Under biaxial tensile stresses, the tensile strength is almost the same as that of uniaxial tensile strength [55].

Under triaxial compressive stresses, concrete exhibits strength, which increases with the increase of confining pressures. Under very high confining stresses, extremely high strengths have been recorded. Experimental studies indicate that the three-dimensional failure envelope is a function of the three principal stresses. ***Figure (3.6)*** shows a schematic failure surface of concrete in three-dimensional stress space [**56**].

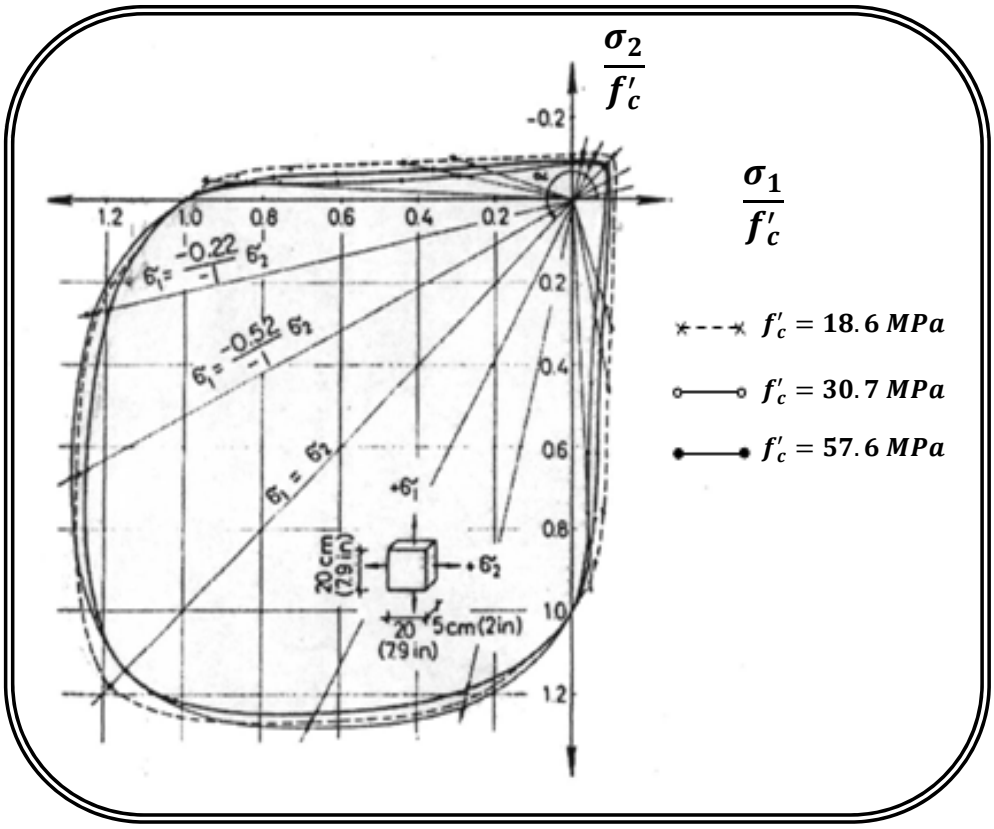

Figure (3.5) Failure envelope of concrete in biaxial stress space [54]

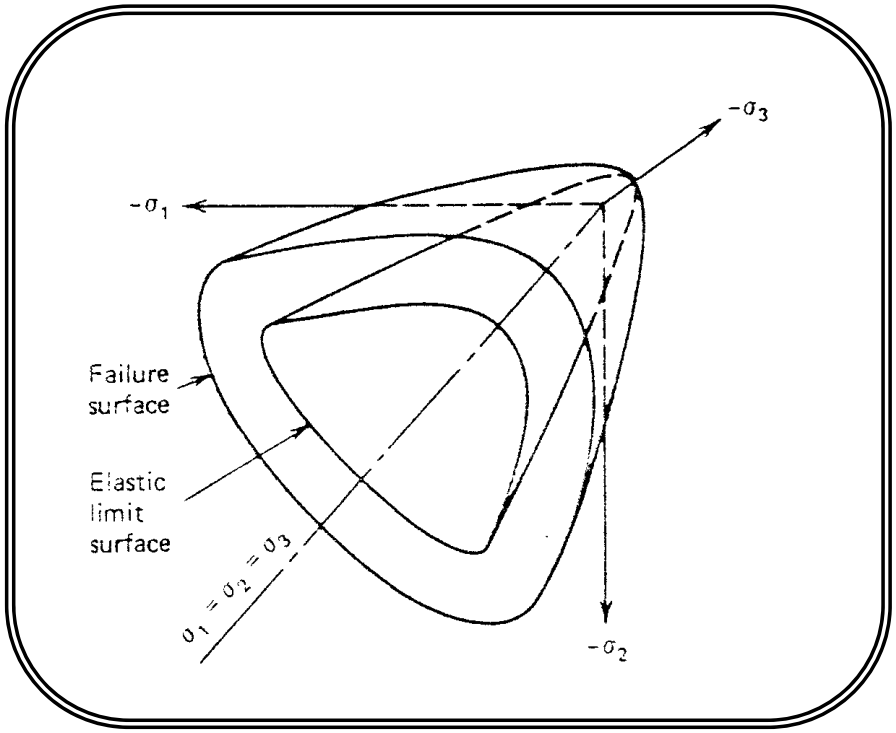

Figure (3.6) Typical triaxial failure envelope of concrete [56]

3.2.2 Behavior of Steel Reinforcement

Modeling of ordinary and prestressing steel in connection with the finite element analysis of pre-stressed concrete beams is much simpler than the modeling of concrete. The ordinary and prestressing steel bars are usually long and slender and therefore can be generally assumed to be capable of transmitting axial forces only.

The stress-strain curve for a typical prestressing steel bar differs from the ordinary steel bar reinforcement. The main differences are the much higher proportional elastic limit and strength available in the round wire and alloy bars used for prestressing, and the substantially lower ductility. ***Figure (3.7)*** shows a typical stress-strain diagram for prestressing steel in comparison with a mild steel bar reinforcement [(1)].

There are three different idealizations of stress-strain curve for steel, as shown in ***Figure (3.8)***, they have been known to be used, depending on the accuracy required, and it can use these models to represent the behavior of prestressing reinforcement.

3.3 Nonlinear Solution Techniques

The main objective of the finite element analysis for the reinforced and prestressed concrete structures is to determine the response of the structure under the applied loading. The typical load-deformation curve for a monotonically loaded member is shown in ***Figure (3.9)***, the response from the starting till point "a" is linear beyond this point a nonlinear response occurs, such response is due to either material or geometric nonlinearity or a combination of both.

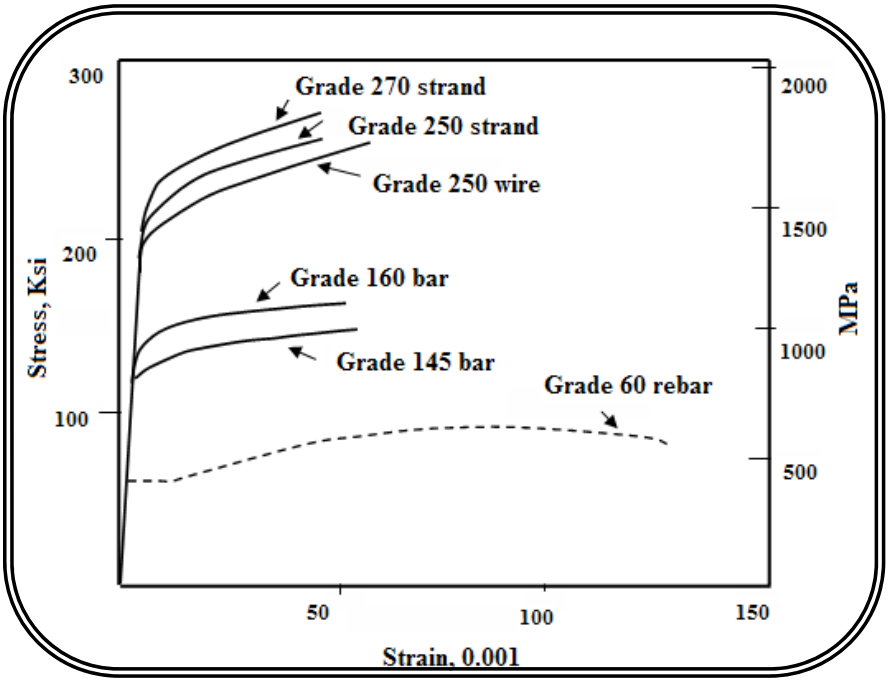

Figure (3.7) Stress-strain diagram for pre-stressing steel in comparison with mild steel bar reinforcement [1]

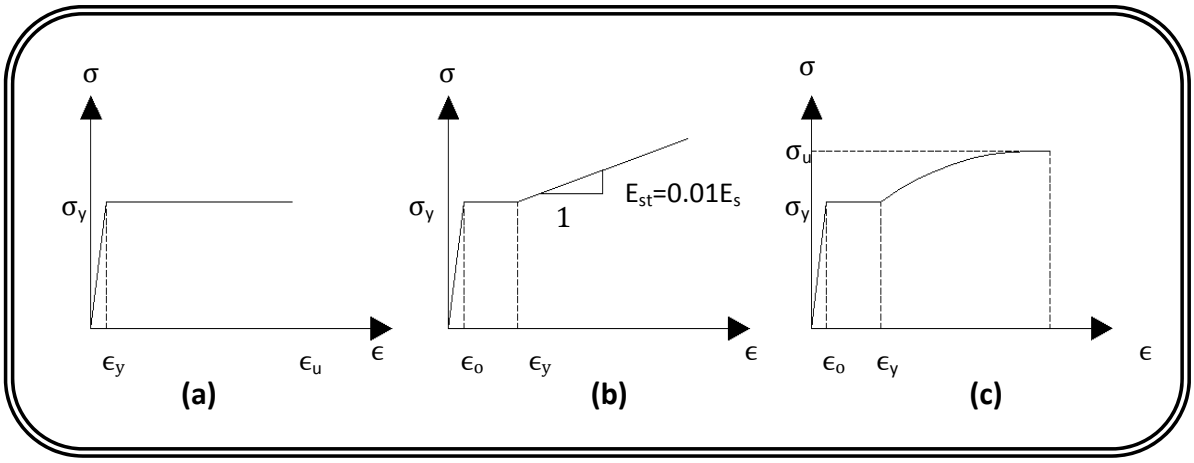

Figure (3.8) Idealizations for the stress-strain curve for steel in tension:

(a) elastic perfectly plastic (b) trilinear (c) complete curve [53]

The material nonlinear behavior includes sudden changes in the element stiffness due to cracking, crushing of concrete, and yielding of the reinforcement, while the geometric nonlinearity is related to the large deformations. In the present study, material nonlinearity due to material nonlinear behavior is considered.

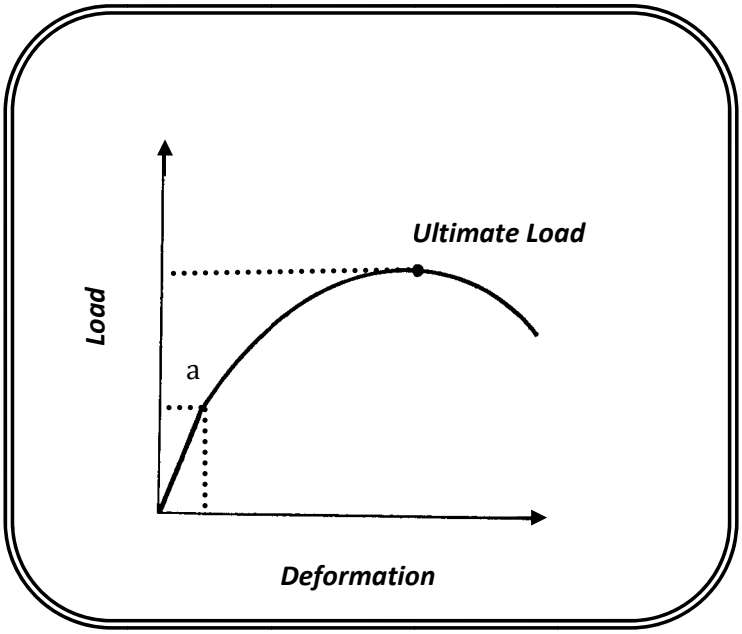

Figure (3.9) Typical structure response

3.4 General Nonlinear Solution Procedure

Applying the finite element method for any problem leads in general to a set of algebraic equations (linear or nonlinear) having the following form:

$$[K].\{a\} = \{P\} \quad \text{……..…..... (3.4)}$$

In a simple linear elastic problem the solution for these equations can be obtained directly. While, this direct solution cannot be achieved when the nonlinearity is present in the stiffness matrix[K], which will depend on the displacement level, therefore, the solution cannot be exactly obtained before the determination of the unknown nodal displacements{a}. The solution of the nonlinear problem may be obtained by using one of the following techniques:

3.4.1 Incremental Technique

In this technique the load is applied on the structure as a series of equal or unequal increments and if such increments are sufficiently small, then the

behavior within each increment can be assumed to be linear. ***Equation (3.4)*** can be rewritten in the following incremental form:

$$[K].\delta\{a\} = \delta\{P\} \quad \text{..... (3.5)}$$

Where [K] is the stiffness matrix at the beginning of the increment, $\delta\{a\}$ and $\delta\{P\}$ represent increments of displacements and loads respectively.

The error resulting from this piecewise linearization process mainly depends on the increment size of the load, the accumulation of this error over several increments result an incorrect solution, the incremental procedure is repeated until the failure load has been reached. ***Figure (3.10.a)*** shows such a solution can be deviated from the true one.

3.4.2 Iterative Technique

Two different techniques are usually used with the purely iterative techniques.

3.4.2.1 Direct Iterative Technique

Full load is applied once at the first iteration and then a new stiffness matrix has to be formed each iteration. Then full system of ***equation (3.4)*** solved in each iteration to evaluate the displacement vector$\{a\}$, initially, some values for $\{a\} = \{a_\circ\}$ is assumed, then an improved approximation is obtained as:

$$\{a\} = -[K]^{-1}\{P\} \quad \text{..... (3.6)}$$

For n-times repetition ***equation (3.6)*** can be written as:

$$\{a_n\} = -[K_{n-1}]^{-1}\{P\} \quad \text{..... (3.7)}$$

This is terminated when the error (e) becomes sufficiently small or within acceptable value ($e = a_n - a_{n-1}$), ***Figure (3.10.b)***.

3.4.2.2 Newton-Raphson Technique

Full load is applied once at the first iteration, then the portion of the total loading that is not balanced is calculated and used in the next step to compute an additional increment of displacements (Δa_i) using the relation:

$$\{\Delta a_i\} = -[K_T(a_i)]^{-1}\{r(a_i)\} \quad \text{.....} \quad (3.8)$$

Where $[K_T(a_i)]$ is the tangent stiffness matrix at iteration "i " and $\{r(a_i)\}$ is the unbalanced nodal forces vector at iteration "i " given by:

$$\{r_i\} = \{P\} - \{f_i\} = \{p\} - \sum \int_{vol.} [B]^T \{\sigma_i\} dV \quad \text{.....} \quad (3.9)$$

Where $\{P\}$ is the external applied load vector, $\{f_i\}$ is the internal nodal load vector at iteration "i ", and $\{\sigma_i\}$ is the current stresses at iteration "i ", The procedure is repeated until the increments of displacement or the unbalanced forces become sufficiently close to a preselected criterion, ***Figure (3.10.c)***.

The iterative technique is not suitable for tracing the nonlinear equilibrium path because it fails to produce information about intermediate stages of loading.

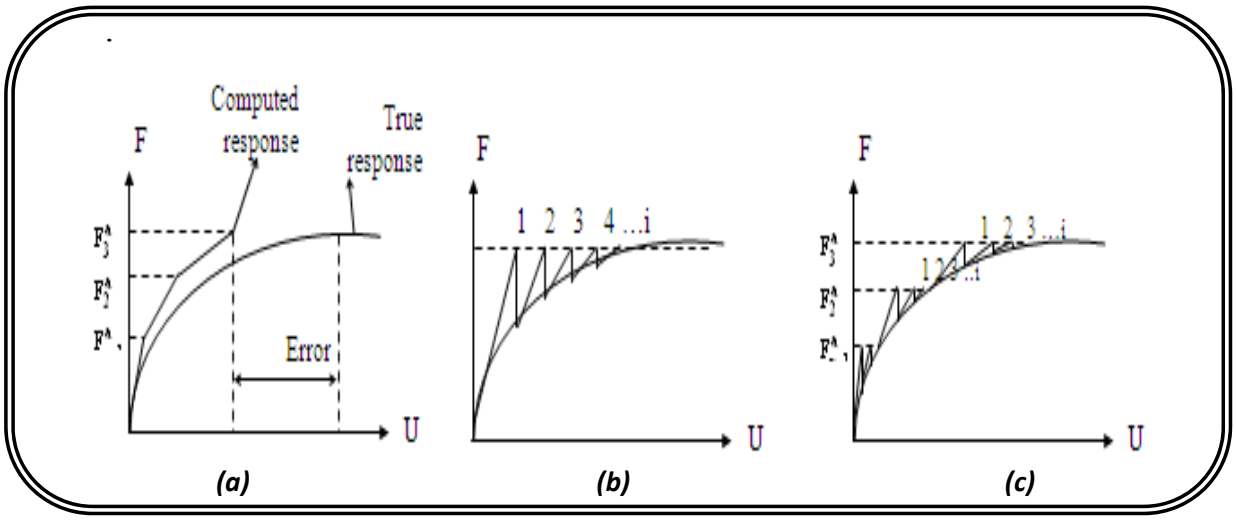

Figure (3.10) Basic technique for solving the nonlinear equation:

(a) Incremental (b) Iterative (c) Incremental-iterative

3.4.3 Combined Incremental-Iterative Technique

This technique utilizes a combination of the incremental and iterative techniques, ***Figure (3.11)***. The load is applied incrementally, and within each increment of loading iterative cycles is performed in order to obtain a converged solution for that increment.

This technique has been widely used in nonlinear analysis of reinforced and prestressed concrete structures. This is due to its ability to trace the response history of the structure and provide information about cracking of concrete that occurs at different load levels, yield of the reinforcement, crushing of concrete and load-deflection curve. For these reasons this study will adopt this technique, two methods used in connection with the incremental-iterative technique, the standard and modified Newton-Raphson method.

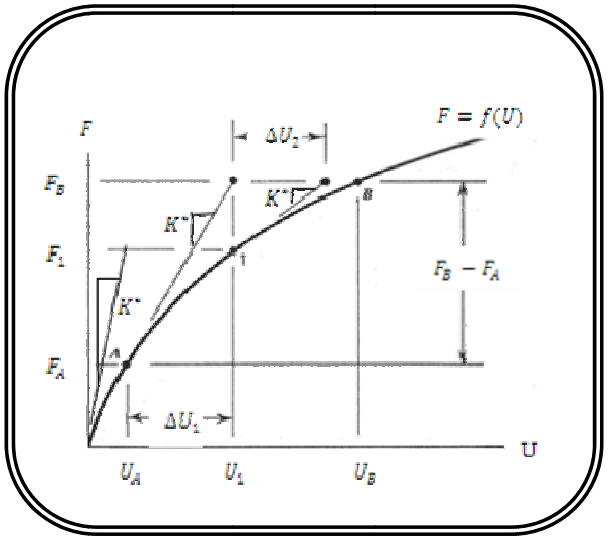

Figure (3.11) Incremental-iterative procedures, full Newton-Raphson procedure

3.4.3.1 Standard Newton-Raphson Method

It is also known as full Newton-Raphson method , ***Figure(3.11)*** the external load is incrementally applied, a series of iterations are performed within each increment of load in order to bring the amount of unbalanced

forces to an acceptable limit. The tangential stiffness matrix is updated and new systems of equations are solved for each iterations. This is an expensive computation procedure practically if the size of the load increment is small. To overcome this, the algorithm can be modified by only updating the stiffness matrix occasionally [57].

3.4.3.2 Modified Newton-Raphson Method

The most commonly used technique; it is a modified form from the standard Newton-Raphson method where the stiffness matrix is updated only once, for each load increment. ***Figure (3.12)***, shows that the stiffness matrix is updated at the beginning of the first iteration of each load increment, other method start updating the stiffness matrix at the beginning of the second iteration , so that the nonlinear effects are more accurately represented in the stiffness matrix [57].

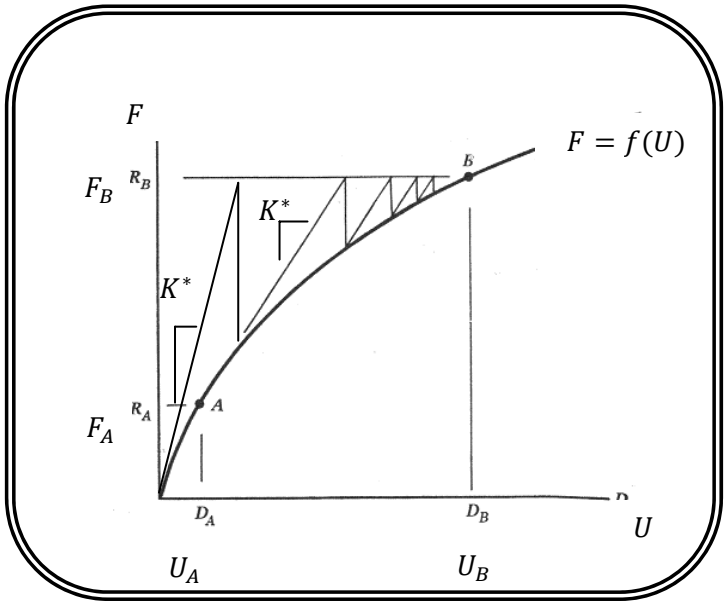

Figure (3.12) Incremental-iterative procedures, Modified Newton-Raphson procedure

These methods are generally more powerful than the standard (conventional) Newton-Raphson method since they involve fewer

stiffness matrix reformation and inversion. The convergence is slower and a large number of iterations are required to a converged solution, this is practically true for an increment of loading at which a sudden softening may occur due to cracking. In order to make the modified methods more effective at loading stages in which slow convergence occurs, stiffness matrix may be updated more than once within such an increment the developed program incorporates a modified Newton-Raphson method in which the stiffness matrix updated at the $2^{nd}, 12^{th}, 22^{th}, \ldots\ldots$ etc. iterations of each increment loading.

3.5 Model Generation in ANSYS Program

3.5.1 Overview of ANSYS

The ANSYS is a versatile finite element package which can be used to analyze structural, thermal, electrical, and contact problems. The ANSYS Graphical User Interface (GUI) is divided into three modules, namely, preprocessor (/PREP7), solution (/SOLU) and post processor (/POST1). The preprocessor step consists of selecting the proper elements, providing real constants, material properties, and meshing the model; loads and displacement boundary conditions can also be applied in this module. Alternatively, the boundary conditions may be applied in the solution module, whose primary role is to solve for the desired quantities. The results of the solution are displayed using the general post processor. Contour plots of stresses, deformations, nodal solution, and element solution can be carried out in this module.

The ANSYS solution module provides for a number of options such as static, transient, harmonic, modal, buckling and sub structuring analyses. In this thesis, only static and transient analyses are carried out.

3.5.2 Model Generation

In the following, 2 elements are described to be used in the adopted model in the present thesis: the first element (BEAM3) is for steel which is used in represent the example (1), and the second element (SOILD65) is for reinforced concrete which is used in examples (2,3 and 4), as showed in chapter five.

3.5.2.1 BEAM3 [58]

3.5.2.1.1 Element Description

BEAM3 is a uniaxial element with tension, compression, and bending capabilities. The element has three degrees of freedom at each node: translations in the nodal x and y directions and rotation about the nodal z-axis, see ***Figure (3.13)***.

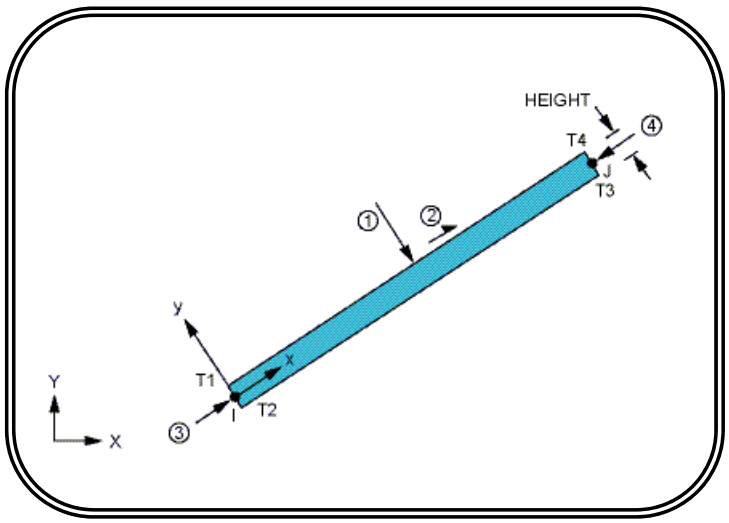

Figure (3.13) BEAM3 Geometry [58]

3.5.2.1.2 Assumptions and Restrictions

- The beam element must lie in an X-Y plane and must not have a zero length or area.
- The beam element can have any cross-sectional shape for which the moment of inertia can be computed. However, the stresses are determined as if the distance from the neutral axis to the extreme fiber is one-half of the height.
- The element height is used only in the bending and thermal stress calculations.
- The applied thermal gradient is assumed linear across the height and along the length.
- The moment of inertia may be zero if large deflections are not used.

3.5.2.2 SOLID65 [58]

3.5.2.2.1 Element Description

SOLID65 is used for the 3-D modeling of solids with or without reinforcing bars (rebar). The solid is capable of cracking in tension and crushing in compression. In concrete applications, for example, the solid capability of the element may be used to model the concrete while the rebar capability is available for modeling reinforcement behavior. Other cases for which the element is also applicable would be reinforced composites (such as fiberglass), and geological materials (such as rock). The element is defined by eight nodes having three degrees of freedom at each node: translations in the nodal x, y, and z directions. Up to three different rebar specifications may be defined.

The most important aspect of this element is the treatment of nonlinear material properties. Concrete is capable of cracking (in three orthogonal directions), crushing, plastic deformation, and creep. The rebar are capable of tension and compression, but not shear. They are also capable of plastic deformation and creep, see ***Figure (3.14)***

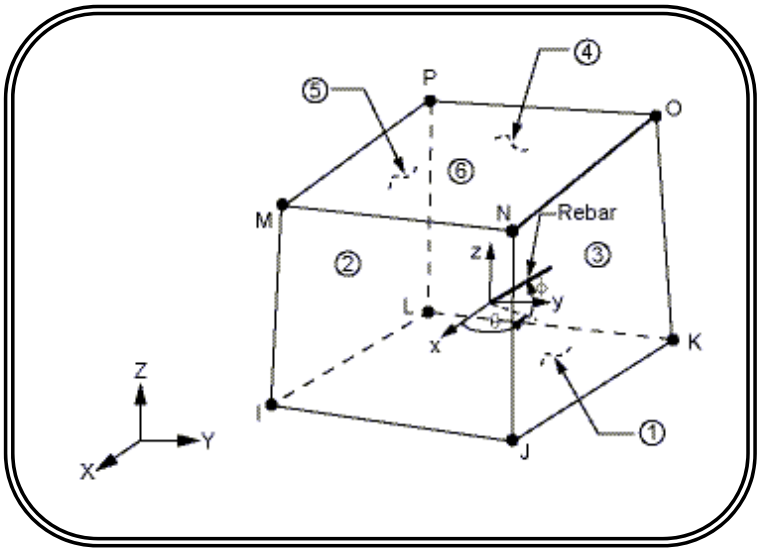

Figure (3.14) SOLID65 Geometry [58]

3.5.2.2.2 Assumptions and Restrictions

- ❖ Zero volume elements are not allowed.
- ❖ Elements may be numbered either as shown in ***Figure (3.14)*** or may have the planes IJKL and MNOP interchanged. Also, the element may not be twisted such that the element has two separate volumes. This occurs most frequently when the elements are not numbered properly.
- ❖ All elements must have eight nodes.
- ❖ A prism-shaped element may be formed by defining duplicate K and L and duplicate O and P node numbers. A tetrahedron shape is also

available. The extra shapes are automatically deleted for tetrahedron elements.

- Whenever the rebar capability of the element is used, the rebar are assumed to be "smeared" throughout the element. The sum of the volume ratios for all rebar must not be greater than 1.0.
- The element is nonlinear and requires an iterative solution.
- When both cracking and crushing are used together, care must be taken to apply the load slowly to prevent possible fictitious crushing of the concrete before proper load transfer can occur through a closed crack. This usually happens when excessive cracking strains are coupled to the orthogonal uncracked directions through Poisson's effect. Also, at those integration points where crushing has occurred, the output plastic and creep strains are from the previous converged substep. Furthermore, when cracking has occurred, the elastic strain output includes the cracking strain. The lost shear resistance of cracked and/or crushed elements cannot be transferred to the rebar, which have no shear stiffness.
- The following two options are not recommended if cracking or crushing nonlinearities are present:
  - Stress-stiffening effects.
  - Large strain and large deflection. Results may not converge or may be incorrect, especially if significantly large rotation is involved.

3.5.3 Prestressed Concrete Girder Representations

As noted earlier, the preprocessor is used to define suitable elements, real constants for those elements, material properties and to model the

geometry. In the present analysis, SOLID65, review a three-dimensional brick element is used to model the concrete of girder and deck and the reinforcement is modeled as an embedded bar in the brick element.

There are two possible ways of taking into account prestress actions in finite element models. The first one is to model the prestressing tendons, using beam or link elements with an initial strain, inside the model we have already created. To do this model, the mesh must be adapted the original finite elements mesh, to locate the nodes where the tendons will be, to be able to connect the link elements to the solid elements. Also putting together in the same model elements with such a different nature (solids and links), with different degrees of freedom, etc. can easily lead to errors in the results, meshing problems, peaks of stresses on certain nodes, etc. and therefore results should be checked very carefully [59].

The second way of considering prestress actions is to create a group of loads equivalent to the action the prestressing tendon will create on the model. These loads will be put directly in the model's faces, without having to change its geometry or mesh.

This method, which is the one implemented by ANSYS and CivilFEM, has the advantage that it can be used on any kind of model, or mesh. It can also be applied on a model made up of beam elements [59].

For above reasons, embedded representation model is used to represent ordinary and prestress reinforcement, and also prestressing forces are made equivalent to lateral pressure acted on the face of brick element. A good agreement is obtained by using this model, as it is shown in chapter five.

3.5.4 Adopted Materials Model and Solution Technique

The ANSYS computer program requires the uniaxial stress-strain relationship for concrete and steel (ordinary and prestress) reinforcement. A Multilinear Isotropic Hardening stress-strain curve is used in the present analysis for concrete both girder and deck which are given by a results test of each experimental girders are used in the present study, see ***Figure (3.15a)***. While an isotropic work hardening (biaxial stress-strain curve) model is adopted to simulate the uniaxial stress-strain behavior of the reinforcing and prestressing steel bars, see ***Figure (3.15b)***.

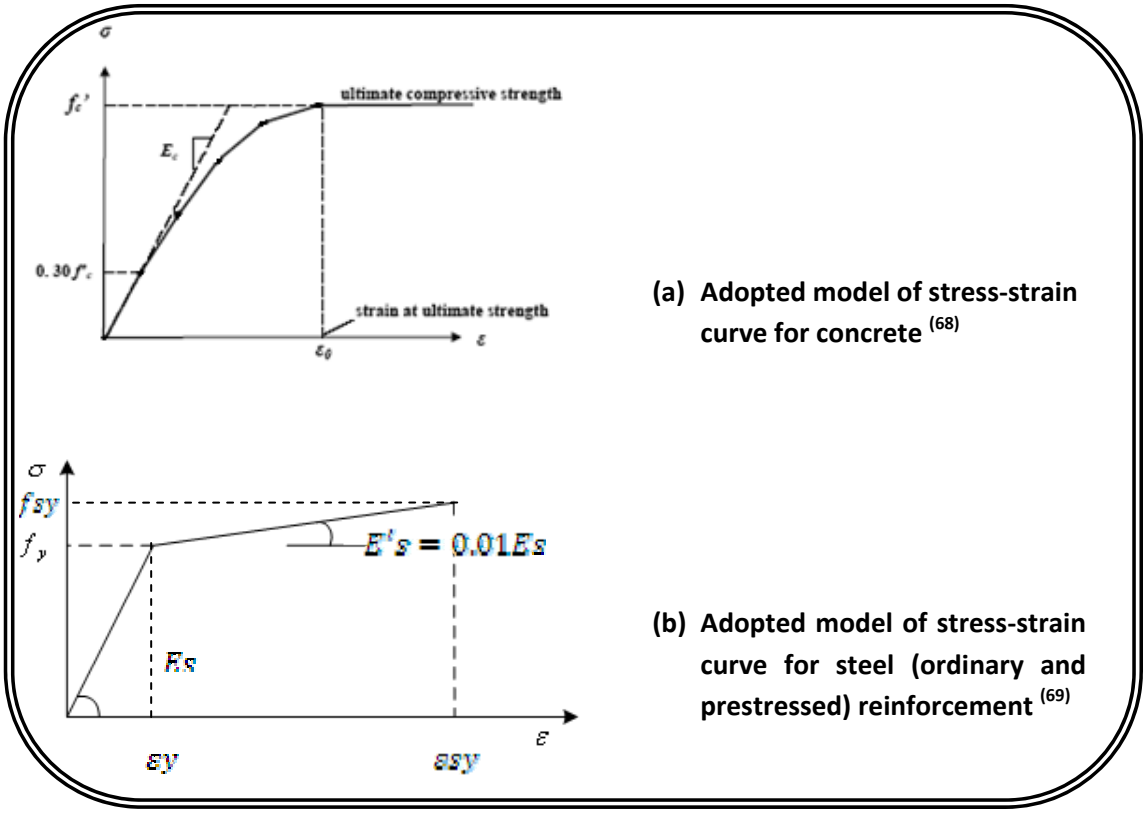

Figure (3.15) Adopted model of stress-strain curve for material in analysis

In ANSYS, there are three nonlinear analysis techniques provided to solve the problems which are represented by:

1. Incremental procedure.
2. The iterative or Newton-procedure.

3. Incremental-iterative procedure (full Newton-Raphson).

As viewed in ***Figure (3.10)*** above and in the present study, the full Newton-Raphson method is used in the analysis.

3.5.5 Analysis Termination Criterion

In the physical test under load control, collapse of a structure takes place when no further loading can be sustained. This is usually indicated in the numerical tests by successively increasing iterative displacements and a continuous growth in the dissipated energy. Hence, the convergence of the iterative process cannot be achieved. A maximum number of iterations for each increment are specified to stop the nonlinear solution if the convergence limit has not been achieved for this study. It has been observed that a maximum number is about 25 iterations. it's generally sufficient to predict the solution divergence or failure. This maximum number of iterations depends on the type of the problem, extent of nonlinearities, and on the specified tolerance. In the present study a maximum number of iteration equals 20 is adopted for load control problems.

Chapter Four

Vehicle Modeling and Dynamic Analysis

4.1 Introduction:

The dynamic response of beams subjected to moving loads has been of interest from the early 1900's. The aim of these studies has always been to design and build safe, economical, and durable bridges. In general the stresses and deflections produced due to moving loads are higher than that of stationary loads. Therefore, proper estimate of the dynamic effect of moving loads is very important to evaluate the load- carrying capacity of a girder.

The dynamic response of bridges subjected to moving vehicles is complicated. This is because the dynamic effects induced by moving vehicles on the bridge are greatly influenced by the interaction between vehicles and the bridge structure. The important parameters that influence on the dynamic response are [39]:

- Vehicle speed
- Road surface roughness
- Characteristics of the vehicle, such as the number of axles, axle spacing, axle load, natural frequencies, and damping and stiffness of the vehicle suspension system
- The number of vehicles and their travel paths
- Characteristics of the bridge structure, such as the bridge geometry, support conditions, bridge mass and stiffness, and natural frequencies.

4.2 Dynamic Amplification Factors (DAF):

For design purpose, structural engineers worldwide rely on dynamic amplification factors (DAF), which are usually related to the first vibration frequency of the bridge or to its span length. The DAF states how many times the static effects must be magnified in order to cover additional dynamic loads resulting from the moving traffic (Impact Factor is the ratio of the maximum dynamic to the maximum static response of the bridge under the same load minus one) [60].

One typical definition for the impact factor (I) is:

$$I = \frac{R_{dyn} - R_{Stat}}{R_{stat}} \quad \text{..... (4.1)}$$

where R_{dyn} and R_{stat} are the maximum dynamic and static response of the bridge, respectively; therefore:

$$R_{dyn} = DAF \times R_{stat} \quad \text{..... (4.2)}$$

where *DAF* is the dynamic amplification factor given by:

$$DAF = 1 + I \quad \text{..... (4.3)}$$

Care must be taken to distinguish the maximum impact factor from the maximum total response calculated for a beam. Occasionally, unreasonably large impact factors may be computed for a beam at some points due to the fact that the static responses, i.e., the denominator of ***equation (4.1)***, are very small. For this reason, the impact factor computed or measured for a bridge should not be regarded as the only criterion in the design of bridges [60].

It is well known that a number of factors may affect the impact factor of a bridge under the excitation of moving vehicular loads, for instance, the dynamic properties of the vehicle, the dynamic properties of the bridge, the vehicle speed, and the pavement roughness. Many bridge codes, including the American Association of State Highway and Transportation Officials (AASHTO) Specifications (Standard, 2001) [61]

have related the impact factor to a single parameter of the bridge, such as the span length or frequency of vibration, and have applied the same impact factor to all responses of the bridge including the deflection, shear force, and bending moment. According to the AASHTO Specifications, the impact factor (I) is related to the loaded length (L) of the bridge as:

$$I = \frac{15.24}{38.1+L} \leq 0.3 \quad \text{..... (4.4)}$$

where (L) expressed in (m).

In the other hand the ***Figure (4.1)*** shows the variation of the DAF with respect to the fundamental frequency of the bridge, recommended by different standards [39] [62]. For cases where the DAF was related to the span length, the fundamental frequency was approximated from the span length. It is apparent from ***Figure (4.1)*** that the national design codes disagree on the evaluation of the dynamic amplification factors, and although the specified traffic loads vary in these codes, this does not explain such a wide range of variation for the DAF. In the Swedish design code for new bridges [39], the Swedish National Road Administration includes the additional dynamic loads, due to moving vehicles, in the traffic loads specified for the different types of vehicles. This gives a constant DAF that is totally independent on the characteristics of the bridge. For bridges like cable-stayed bridges that are more complex and behave differently compared to ordinary bridges, this approach can lead to incorrect traffic loads to be used for designing the bridge.

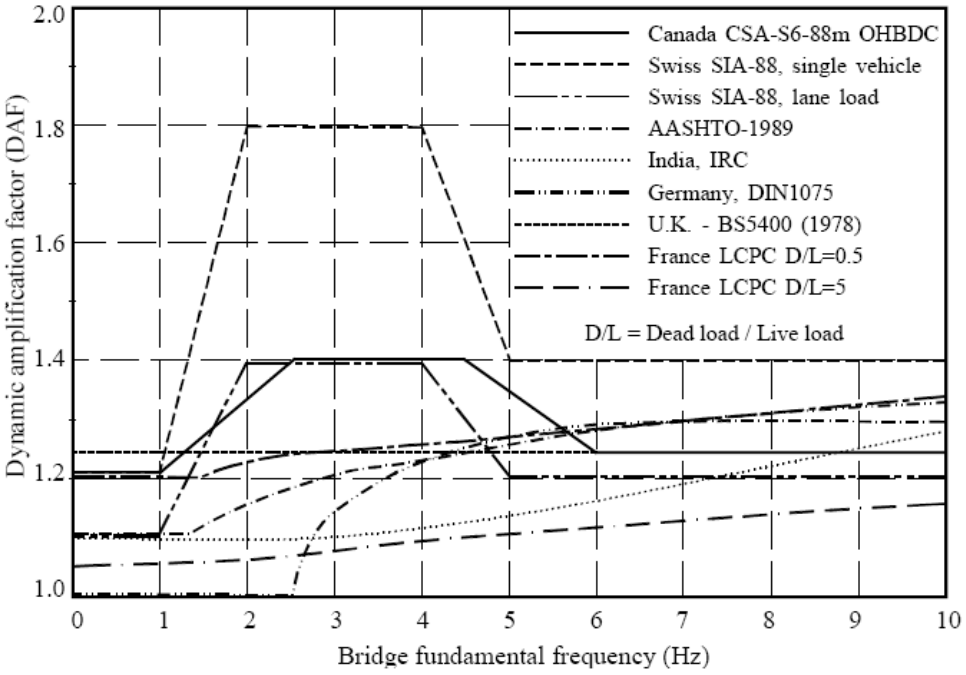

Figure (4.1) Dynamic Amplification Factors used in different national codes [39] [62]

4.3 Standard Live Loads for Highway Bridges:

AASHTO specifications provide two systems of standard vehicle loads, H loads and HS loads. Each system consists of individual truck loads and lane loads. Lane loads are intended to be equivalent in weight to a series of vehicles. The type of loading used for design, whether truck load or lane load, is that producing the highest stress. It should be noted that bridges are designed for the stresses and deflection produced by a standard highway loading, not necessarily the individual vehicles. The design loads are hypothetical and are intended to resemble a type of loading rather than a specific vehicle. Actual stresses produced by vehicles crossing the structure should not exceed those produced by the hypothetical design vehicles.

4.3.1 Truck Loads:

There are currently two classes of truck loads for each standard loading system ***Figure (4.2)***. The H system consists of loading H 15-44 and loading H 20-44. These loads represent a two-axle truck and are designated by the letter H followed by a number indicating the Gross Vehicle Weight (GVW) in tons.

The load designations also include a "-44" suffix to indicate the year that the load was adopted by AASHTO (1944). The weight of an H truck is assumed to be distributed two-tenths to the front axle and eight-tenths to the rear axle. Axle spacing is fixed at 14 feet and track width at 6 feet. Truck loads for the HS system consist of loadings HS 15-44 and HS 20-44.

These loads represent a two-axle tractor truck with a one-axle semitrailer and are designated by the letters HS, followed by a number indicating the gross weight in tons of the tractor truck. The configuration and weight of the HS tractor truck is identical to the corresponding H load. The additional semitrailer axle is equal in weight to the rear tractor truck axle and is spaced at a variable distance of 14 to 30 feet. The axle spacing used for design is that producing the maximum stress.

4.3.2 Lane Loads:

Lane loads were adopted by AASHTO in 1944 to provide a simpler method of calculating moments and shears. These loads are intended to represent a line of medium-weight traffic with a heavy truck positioned somewhere in the line. Lane loads consist of a uniform load per linear foot of lane combined with a single moving concentrated load, positioned to produce the maximum stress (for continuous spans, two concentrated

loads - one placed in each of two adjoining spans - are used to determine maximum negative moment). Both the uniform load and the concentrated loads are assumed to be transversely distributed over a 10-foot width.

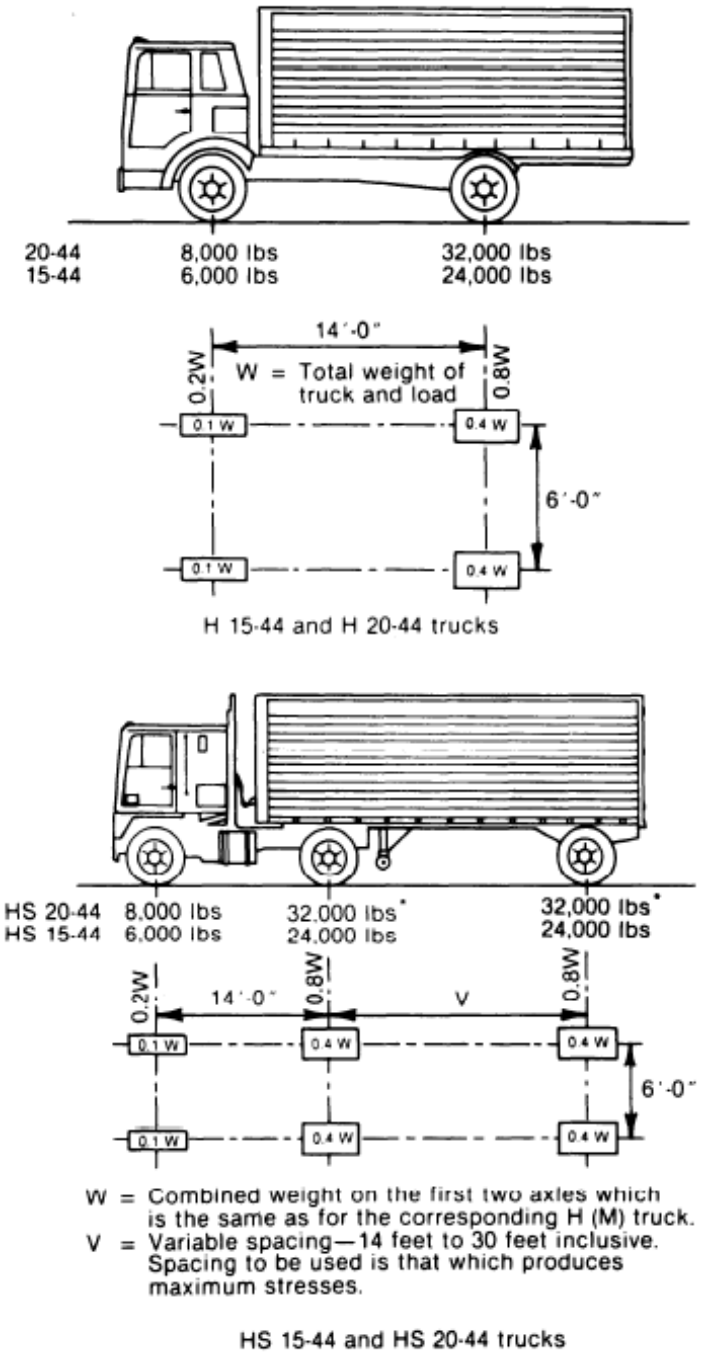

Figure (4.2) Standard AASHTO truck loads

AASHTO specifications currently include two classes of lane loads: one for H 20-44 and HS 20-44 loadings and one for H 15-44 and HS 15-

44 loadings, ***Figure (4.3)***. The uniform load per linear foot of lane is equal to 0.016 times the Gross Vehicle Weight (GVW) for H trucks or 0.016 times the weight of the tractor truck for HS trucks. The magnitude of the concentrated loads for shear and moment are 0.65 and 0.45 times those loads, respectively.

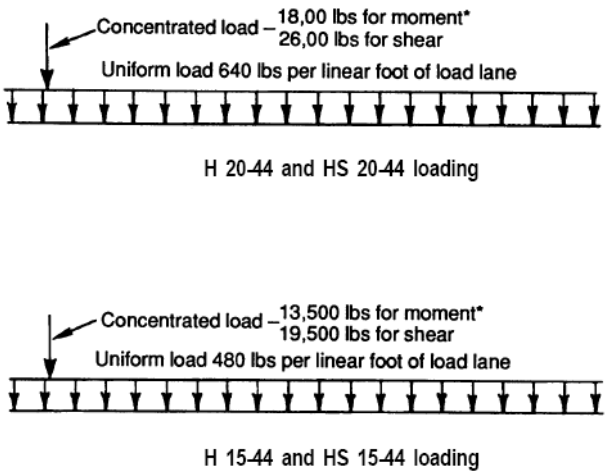

Figure (4.3) Standard AASHTO lane loads

4.4 Vehicle Modeling:

Heavy vehicles consist of several major components, such as tractors, trailers and suspension systems, and can be modeled by a set of lumped masses, springs and dampers. As illustrated in ***Figure (4.4)***.

The moving force model (constant force magnitude) is sufficient if the inertia forces of the vehicle are much smaller than the dead weight of the vehicle. For a vehicle moving along a straight path at a constant speed, these inertia effects are mainly caused by bridge deformations (bridge-vehicle interaction) and bridge surface irregularities. Hence factors that are believed to contribute in creating vehicle inertia effects include: high vehicle speed, flexible bridge structure, large vehicle mass,

small bridge mass, stiff vehicle suspension system and large surface irregularities.

The vehicle model can still be enhanced through consideration of the elastic and damping effects of the suspension systems. The simplest model in this case is a moving mass supported by a spring-dashpot unit, the so-called sprung mass model ***Figure (4.4)***. Biggs (1964) presented a semi-analytical solution to the problem of a simple beam traversed by a sprung mass. By using the series expansion technique, Pesterev et al. (2001) examined the response of an elastic continuum to multiple moving oscillations. Later, Pesterev et al. (2003) studied in depth the asymptotics of the solution of the moving oscillator problem and found that in the limiting case the moving oscillator problem and the moving mass problem for a simply supported beam are equivalent in terms of the beam displacements, but not in terms of the beam stresses. Also, it was shown that for small values of spring stiffness, the moving oscillator problem is equivalent to the moving load problem. In the book by Fr´yba (1972), a comprehensive treatment was given for the various vehicle models, i.e., the moving load, moving mass, and moving sprung mass, concerning primarily the dynamic response of the structure traveled by vehicles [39].

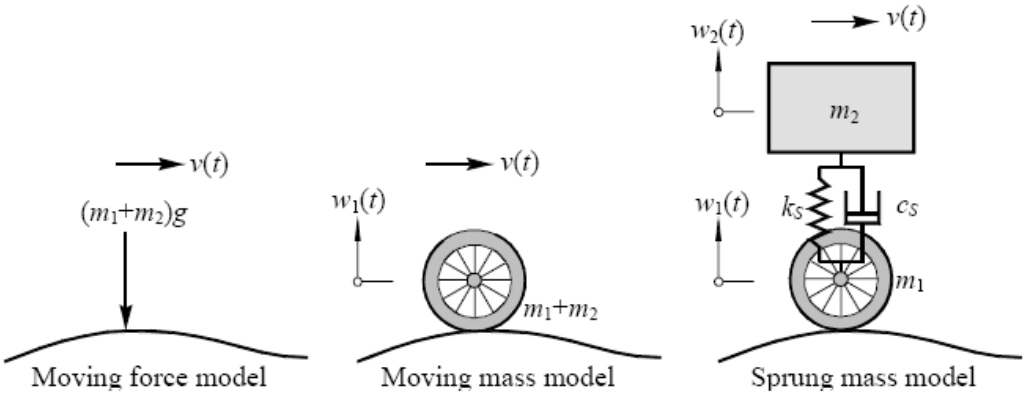

Figure (4.4) Vehicle modeling [39]

4.5 Dynamic Analysis (Numerical Methods in ANSYS)

Dynamic response analysis is the calculation of how a structure responds to arbitrary time-dependent loading [57]. All problems in structural dynamics can be formulated based on the equation of motion; where the equation of motion can be written as:

$$M\,.\,u'' + C\,.\,u' + K\,.\,u = f(t) \qquad \ldots\ldots\ldots\ldots\ldots\ldots\ldots\ldots\ldots (4.5)$$

In the above equation

M, C and K denote the structural mass, damping and stiffness matrices respectively.

u'', u' and u denote the vectors of nodal accelerations, velocities and displacements respectively.

$f(t)$ is the vector of applied forces and the dynamical equilibrium is obtained if equation (4.5) holds for all times (t).

Several types of structural dynamics analyses are listed according to the representation of the applied load, and it also discussed present solution algorithms of ANSYS and described practical applications for each type of dynamic analysis.

1. Modal Analysis
2. Harmonic Analysis
3. Spectrum Analysis
4. Transient Analysis

In the present study, a transient dynamic analysis is adopted to model the dynamic effects of moving load on the prestressed concrete girder so it's very important to understand the transient analysis. In the other hand it's very important to take a view on the other types of analyses.

4.5.1 Modal Analysis

A modal analysis is used to determine the vibration characteristics of a structure while it is being designed. Hence, the goal of a modal analysis is determining the natural frequencies and mode shapes. The right hand side of the equation of motion (4.5) is considered to be zero, i.e. $f(t) = 0$. A modal analysis can also be taken as a basis for other more detailed dynamic analyses such as a transient dynamic analysis, a harmonic analysis or even a spectrum analysis based on the modal superposition technique. The modal analysis is a linear analysis. Any nonlinearity which may have been specified by the user is ignored. However, prestress effects may be considered [63].

4.5.2 Harmonic Analysis

Any sustained cyclic load will produce a sustained cyclic response in a structure which is often called a harmonic response. The harmonic response analysis solves the equation of motion (4.5) for linear structures undergoing steady-state vibrations. All loads and displacements vary sinusoidal with the same known frequency although not necessarily in phase. The use of a complex notation allows a compact and efficient description of the problem. For the function of applied force on the right hand side of the equation of motion (4.5), the following expression is used, i.e.

$$f(t) = f_{max} \cdot e^{i(\Omega t + \Psi)} \quad \text{..... (4.6)}$$

where f_{max} represents the amplitude of the force.

Ω denotes the imposed circular frequency measured in (radians/time).

Ψ stands for the force phase shift which is measured in (radians).

4.5.3 Spectrum Analysis

A spectrum analysis is a dynamical calculation discipline in which the results of a modal analysis are used together with a well-known spectrum to calculate certain quantities in the structure like displacements and stresses for example. A spectrum is simply a graph of a spectral quantity like the acceleration versus frequency that captures the intensity and frequency content of time-history loads.

The spectrum analysis is often used instead of a transient dynamic analysis to determine the response of structures due to random or time-dependent loading conditions such as earthquakes, wind loads, ocean wave loads, jet engine thrusts, rocket motor vibrations and so on. Contrary to a transient analysis a spectrum analysis does not calculate the dynamic answer for the whole considered time range where the dynamic forces have been acting. Rather a conservative estimation for the maximum response of a certain quantity like the displacements or stresses is obtained from this type of analysis [63].

4.5.4 Transient Analysis

A transient dynamic analysis is a technique which is used to determine the time history dynamic response of a structure to arbitrary forces varying in time [63]. This type of analysis yields the displacement, strain, stress and force time history response of a structure to any combination of transient or harmonic loads. The transient dynamic equilibrium equation of interest is as follows for a linear structure:

$$[M]\{\ddot{u}\} + [C]\{\dot{u}\} + [K]\{u\} = \{F^a\} \quad \text{..... (4.7)}$$

There are two methods in the ANSYS program which can be employed for the solution of the linear equation (4.7):

- The forward difference time integration method

- The Newmark time integration method (including an improved algorithm called HHT).

They can be broadly classified into implicit and explicit methods. The forward difference method is used for explicit transient analyses while the Newmark method and HHT method are used for implicit transient analyses [58], as described below. Considering the stability of these two types of integration methods it notice that implicit methods are usually unconditionally stable which means that different time step sizes can be chosen without any limitations originating from the method itself.

Explicit methods on the other hand are only stable if the time step size is smaller than a critical one which typically depends on the largest natural frequency of the structure. Due to the small time step necessary for stability reasons explicit methods are typically used for short-duration transient problems in structural dynamics [63].

Since both types of time integration methods are available with the ANSYS product family it will discuss them below in more detail.

4.5.4.1 Implicit Time Integration

The implicit time integration algorithm in ANSYS is the Newmark method [64]. The stability of this method is controlled by two parameters that are set up by default so that the scheme is unconditionally stable and the effect of numerical damping is minimized. Applying the Newmark method to the equation of motion (4.7) results in a linear system of equation for each time step. Since the stiffness matrix appears on the left hand side it must be inverted in each time step in the incremental solution process. Since its inversion is computationally expensive especially for highly nonlinear problems the implicit solution technique in ANSYS is always a good choice to solve a transient analysis if the problem is not crucially dominated by nonlinearities [58].

❖ The Newmark method uses finite difference expansions in the time interval Δt, in which it is assumed that [65]:

$$\{\dot{u}_{n+1}\} = \{\dot{u}_n\} + [(1-\delta)\{\ddot{u}_n\} + \delta\{\ddot{u}_{n+1}\}]\Delta t \quad \ldots\ldots\ldots\ldots\ldots\ldots (4.8)$$

$$\{u_{n+1}\} = \{u_n\} + \{\dot{u}_n\}\Delta t + \left[\left(\frac{1}{2} - \propto\right)\{\ddot{u}_n\} + \propto \{\ddot{u}_{n+1}\}\right]\Delta t^2 \quad \ldots\ldots\ldots (4.9)$$

Where:

α, δ = Newmark integration parameters

$\Delta t = t_{n+1} - t_n$

$\{u_n\}$ = nodal displacement vector at time t_n

$\{\dot{u}_n\}$ = nodal velocity vector at time t_n

$\{\ddot{u}_n\}$ = nodal acceleration vector at time t_n

$\{u_{n+1}\}$ = nodal displacement vector at time t_{n+1}

$\{\dot{u}_{n+1}\}$ = nodal velocity vector at time t_{n+1}

$\{\ddot{u}_{n+1}\}$ = nodal acceleration vector at time t_{n+1}

Since the primary aim is the computation of displacements$\{u_{n+1}\}$, the governing equation (4.7) is evaluated at time (t_{n+1}) as:

$$[M]\{\ddot{u}_{n+1}\} + [C]\{\dot{u}_{n+1}\} + [K]\{u_{n+1}\} = \{F^a\} \quad \ldots\ldots\ldots\ldots\ldots\ldots (4.10)$$

The solution for the displacement at time (t_{n+1}) is obtained by first rearranging equations (4.8) and (4.9) such that:

$$\{\ddot{u}_{n+1}\} = a_0(\{u_{n+1}\} - \{u_n\}) - a_2\{\dot{u}_n\} - a_3\{\ddot{u}_n\} \quad \ldots\ldots\ldots\ldots\ldots\ldots (4.11)$$

$$\{\dot{u}_{n+1}\} = \{\dot{u}_n\} + a_6\{\ddot{u}_n\} + a_7\{\ddot{u}_{n+1}\} \quad \ldots\ldots\ldots\ldots\ldots\ldots (4.12)$$

Noting that $\{u_{n+1}\}$ in equation (4.11) can be substituted into equation (4.12), equations for $\{\ddot{u}_{n+1}\}$ and $\{\dot{u}_{n+1}\}$ can be expressed only in terms of the unknown$\{u_{n+1}\}$. The equations for $\{\ddot{u}_{n+1}\}$ and $\{\dot{u}_{n+1}\}$ are then combined with equation (4.10) to form:

$$a_0[M] + a_1[C] + [K]\{u_{n+1}\} = \{F^a\} + [M](a_0\{u_n\} + a_2\{\dot{u}_n\} + a_3\{\ddot{u}_n\}) + [C](a_1\{u_n\} + a_4\{\dot{u}_n\} + a_5\{\ddot{u}_n\}) \quad \ldots\ldots\ldots\ldots (4.13)$$

Where:

$$a_0 = \frac{1}{\alpha\Delta t^2} \qquad a_1 = \frac{\delta}{\alpha\Delta t} \qquad a_2 = \frac{1}{\alpha\Delta t}$$

$a_3 = \frac{1}{2\alpha} - 1$ $a_4 = \frac{\delta}{\alpha} - 1$ $a_5 = \frac{\Delta t}{2}\left(\frac{\delta}{\alpha} - 2\right)$

$a_6 = \Delta t(1-\delta)$ $a_7 = \delta \Delta t$

Once a solution is obtained for$\{u_{n+1}\}$, velocities and accelerations are updated as described in equations (4.11) and (4.12). The solution of these equations is unconditionally stable for [66]:

$\alpha \geq \frac{1}{4}\left(\frac{1}{2} + \delta\right)^2$, $\delta \geq \frac{1}{2}$, and $\frac{1}{2} + \delta + \alpha > 0$ …….. (4.14)

So that the Newmark parameters (α, and δ) are related to the input as follows:

$\alpha = \frac{1}{4}(1+\gamma)^2$, and $\delta = \frac{1}{2} + \gamma$ …… (4.15)

Where γ = amplitude decay factor, takes a small value (in ANSYS, the default is 0.005).

The Newmark method becomes the constant average acceleration method when γ = 0, which in turns means (α = 0.25, and δ = 0.5) [65].

- The basic form of the HHT method is given by:

$[M]\{\ddot{u}_{n+1-\alpha_m}\} + [C]\{\dot{u}_{n+1-\alpha_f}\} + [K]\{u_{n+1-\alpha_f}\} = \{F^a_{n+1-\alpha_f}\}$ …. (4.16)

Where:

$\{\ddot{u}_{n+1-\alpha_m}\} = (1-\alpha_m)\{\ddot{u}_{n+1}\} + \alpha_m\{\ddot{u}_n\}$

$\{\dot{u}_{n+1-\alpha_f}\} = (1-\alpha_f)\{\dot{u}_{n+1}\} + \alpha_f\{\dot{u}_n\}$

$\{u_{n+1-\alpha_f}\} = (1-\alpha_f)\{u_{n+1}\} + \alpha_f\{u_n\}$

$\{F^a_{n+1-\alpha_f}\} = (1-\alpha_f)\{F^a_{n+1}\} + \alpha_f\{F^a_n\}$

α_m, and α_f are two extra integration parameters for the interpolation of the acceleration and the displacement, velocity and loads.

Introducing the Newmark assumption as given in equations (4.11) and (4.12) into equation (4.17), the displacement $\{u_{n+1}\}$ at the time step $(n+1)$ can be obtained:

$$a_0[M] + a_1[C] + \left(1-\alpha_f\right)[K]\{u_{n+1}\} = \left(1-\alpha_f\right)\{F_{n+1}^{a}\} + \alpha_f\{F_n^{a}\} - \alpha_f\left\{F_n^{int}\right\} + [M](a_0\{u_n\} + a_2\{\dot{u}_n\} + a_3\{\ddot{u}_n\}) + [C](a_1\{u_n\} + a_4\{\dot{u}_n\} + a_5\{\ddot{u}_n\}) \quad \text{.. (4.17)}$$

Where:

$a_0 = \frac{1-\alpha_m}{\alpha \Delta t^2}$ $\quad a_1 = \frac{(1-\alpha_f)\delta}{\alpha \Delta t}$

$a_2 = \frac{1-\alpha_m}{\alpha \Delta t}$ $\quad a_3 = \frac{1-\alpha_m}{2\alpha} - 1$

$a_4 = \frac{(1-\alpha_m)\delta}{\alpha} - 1$ $\quad a_5 = \left(1-\alpha_f\right)\left(\frac{\delta}{2\alpha} - 1\right)\Delta t$

The four parameters (α, δ, α_f, and α_m) used in the HHT method are related to the input as follows [58].

$$\alpha = \frac{1}{4}(1+\gamma)^2$$
$$\delta = \frac{1}{2} + \gamma \quad \text{... (4.18)}$$
$$\alpha_f = \gamma$$
$$\alpha_m = 0$$

Alternatively, (α, δ, α_f, and α_m) can be input directly. But for the unconditional stability and the second order accuracy of the time integration, they should satisfy the following relationships:

$$\delta \geq \frac{1}{2}$$
$$\alpha \geq \frac{1}{2}\delta \quad \text{... (4.19)}$$
$$\delta = \frac{1}{2} - \alpha_m + \alpha_f$$
$$\alpha_m \leq \alpha_f \leq \frac{1}{2}$$

If both (α_f, and α_m) are zero when using this alternative, the HHT method is same as Newmark method.

4.5.4.1.1 Solution of Newmark Equation

ANSYS provides three methods of solution for the Newmark method equation (4.13) and each are described subsequently. Only the full solution method is available for HHT equation (4.16).

- Full Method
- Reduced Method
- Modal Superposition Method

The Full Method does not reduce the dimension of the considered problem since original matrices are used to compute the solution. As a consequence it is simple to use, all kinds of nonlinearities may be specified, automatic time stepping is available, all kinds of loads may be specified, masses are not assumed to be concentrated at the nodes and finally all results are computed in a single calculation. The main disadvantage of the Full Method is the fact that the required solution time will increase with the size of the considered model.

The Reduced Method originates from earlier years. Because of the reduced system matrices which are used to solve the transient problem, this method has an advantage when compared with the Full Method with respect to the required solution time. However, the user has to specify master degrees of freedom which represent the dynamic behavior as good as possible. The only nonlinearity which can be specified is node-to-node contact via a gap condition. However, automatic time stepping is not possible. Consequently, this method is not very popular any more since all its disadvantages do not really compensate the advantage of lower costs in solution time.

The Modal Superposition Method usually reduces the dimension of the original problem as well since the transient analysis is finally performed in the modal subspace which has the dimension of the number

of mode shapes used for the superposition. The main advantage is again the reduction of solution time. It turns out that this method is actually the most efficient one compared with the other two. The accuracy just depends on the number of mode shapes used for the modal superposition. Even if a few modes shapes are taken the requested solution time might still be less when compared with the Full and the Reduced Method. Contact can be applied using the gap condition it mentioned in the discussion of the Reduced Method. The time step has to be chosen as constant which means that automatic time stepping is not available for this method. It should also be noted that a modal analysis has to be performed before the transient problem can be solved with the modal superposition technique. Hence, the solution process consists basically of two analyses, the modal analysis and the transient analysis in the modal subspace. Since for most problems in structural dynamics the natural frequencies of a structure are of interest this is not really a disadvantage. Summing up, using the modal superposition technique for a transient analysis reduces not only solution time, but the user also obtains information about the natural frequencies and the undamped mode shapes, respectively [63].

Comparing the above solution options, the Modal Superposition Method is the most powerful method considering the required solution time. However, it cannot handle nonlinearities. The Full Method requires more time to finish the analysis but can handle nonlinearities, so that a transient analysis with full solution method is used in the present study.

4.5.4.2 Explicit Time Integration

ANSYS also provides the possibility to perform an explicit transient analysis. ANSYS/LS-DYNA as a product of the ANSYS family

combines the LS-DYNA explicit finite element solver with the powerful pre- and postprocessing capabilities of ANSYS.

As an explicit time integration algorithm, LS-DYNA uses a central difference scheme [64]. Similarly as the implicit Newmark method linear systems of equation have to be solved in each time step. However, the stiffness matrix will appear on the right hand side during the solution process and therefore does not need to be inverted in each step. For this reason ANSYS/LS-DNYA can handle highly nonlinear problems in transient dynamics very well. Fast solution capabilities are provided for short-time large deformation dynamics, quasi-static problems with large deformations and multiple nonlinearities and also for complex contact/impact problems. For highly nonlinear transient problems the product ANSYS/LS-DYNA might be the better choice compared with ANSYS in its implicit version.

Because of the small time step which has usually to be taken for stability reasons in ANSYS/LS-DYNA long-time transient problems might run inefficiently with this code and ANSYS in its implicit form could be a better choice [63].

4.6 Adopted Moving Load Representation:

A moving force model is adopted in the present study, where a resultant force (P) equivalent to the half weight of the AASHTO standard [61] truck (HS 15-44) or (HS 20-44) (as follow in chapter five) is moved on a simply supported prestressed concrete girder where a transient dynamic analysis (Full Method) is carried out in this study by using ANSYS program to move the load (P) from left end to the right end of the girder at a specific time (*t*) depending on the span length and vehicle velocity.

Figure (4.5) below shows the adopted time history model of the moving force (P) during the passing node (*i*) at a two time step (2Δ*t*) where the time step (Δ*t*) represent the required time to move (P) from one node to the next node at a specified velocity, as shown in ***Figure (4.5a)***.

From the above definition, and because of the analysis of the prestressed concrete girder in finite element, it must divide the required time (*t*) of the force (P) which passing the girder (from one end to the other end at a constant velocity) into a many time step size (Δ*t*) depending on the meshing girder in span direction (Z) to get a constant number of time stepping.

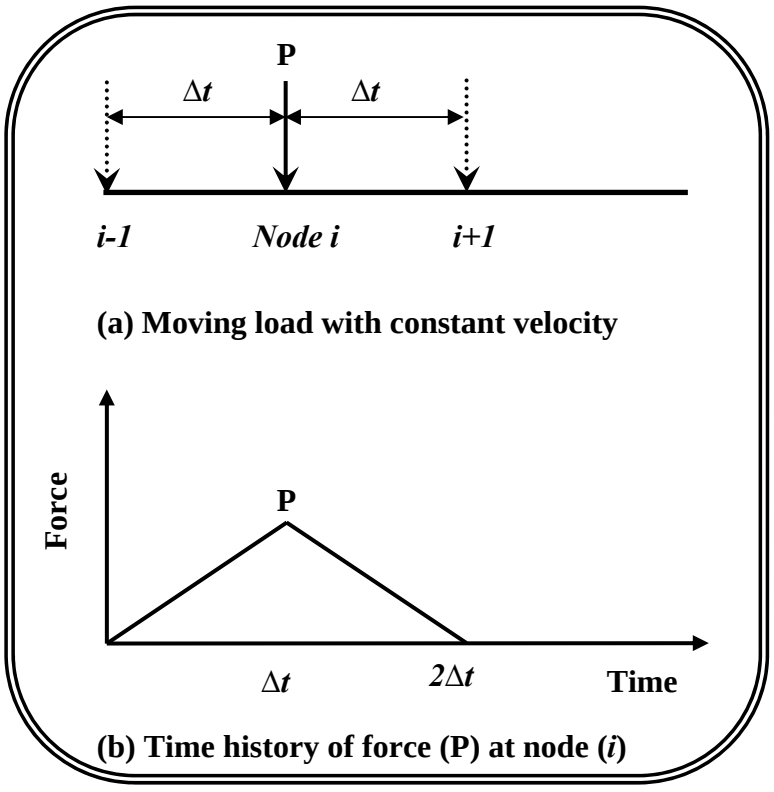

Figure (4.5) Adopted moving load in ANSYS

Chapter Five

Applications and Results Discussion

5.1 Introduction:

In this chapter, the prestressed concrete girder under dynamic moving load is analyzed by the finite element method, using ANSYS program.

Many examples are adopted in this chapter, and their results are discussed. Because of there are no experimental data about prestressed concrete girder under dynamic moving load, as reviewed, the comparison of the present problem is divided into ***three parts***, ***the first part*** is represented by checking the model of moving load that is used in the present problem with a simply-supported steel beam subjected to dynamic moving load was adopted by Kavipurapu [43].

The second part represented checking the model of prestressed concrete girder that is used to model the present problem. The verification is achieved by comparing the load – deflection curve with experimental data adopted by Wolanski [67], and Canfield [3].

From these comparisons, the prestressed concrete girder under moving loads can be represented, as shown in ***part three***.

A comprehensive study has been carried out to investigate the effect of some various parameters which are expected to control the design of prestressed concrete girder. The parameters include the following:

1. Vehicle speed.
2. Representation of vehicle, such as the number of axles.
3. Number of vehicles which are passing on the girder.

4. Characteristics of the bridge structure, such as the cross section of the girder.

Part One: Verification of Moving Load

5.2 Example (1):

Kavipurapu (2005) analyzed numerically (Finite Element Method) by using ANSYS program a simply supported steel beam under action of moving load where the same beam was tested in a laboratory by Tahri in 1987.

5.2.1 Geometrical Properties

The geometrical properties of the steel analyzed beam are illustrated in ***Figure (5.1)***, where the length, width, and thickness of the beam (steel bar) are 101.6 mm (4 in.), 6.35 mm (0.25 in.), and 6.35 mm (0.25 in.), respectively. The beam has a modulus of elasticity, E= 206841 MPa (30×10^6 psi), and a density, ρ= 7830 kg/m^3.

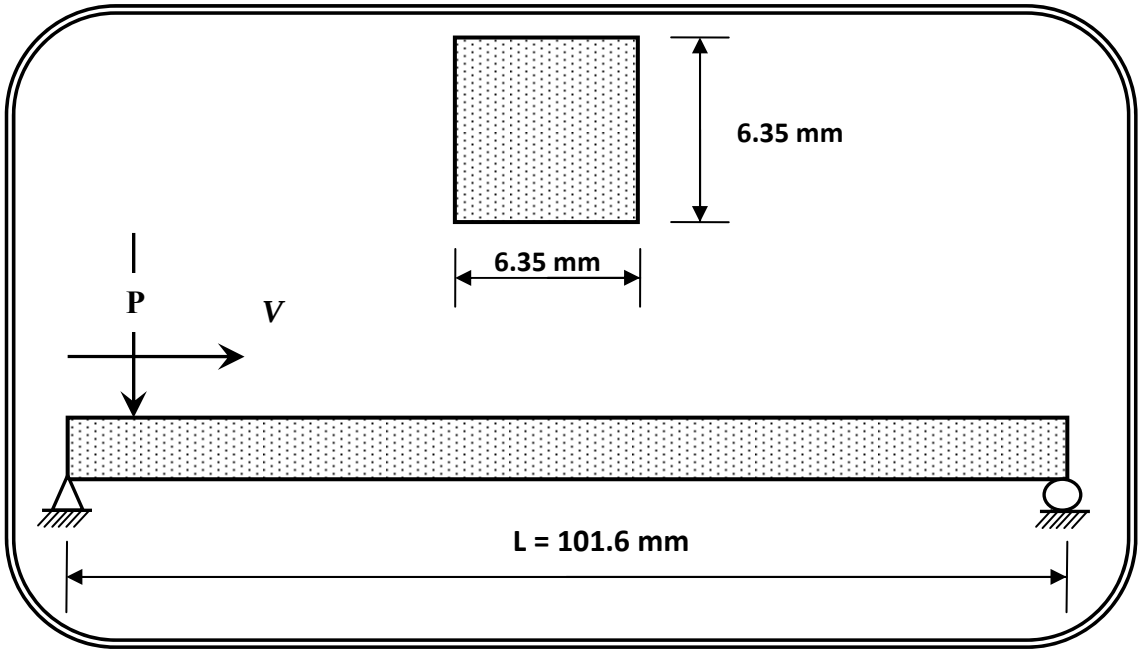

Figure (5.1) Geometrical properties of Kavipurapu beam

5.2.2 Finite Element Idealization

In this example, BEAM3, a two-dimensional beam element is used to model the isotropic beam in ANSYS program. At each node, this beam has three degrees of freedom (U_X, U_Y and ROT_Z). It is a uniaxial element which can account for axial and bending deformations. The beam is defined by two nodes, I and J, area of cross section, moment of inertia and beam height. In the present study, the beam is modeled with twenty elements, simply supported at the two ends, as adopted by Kavipurapu, and as shown in ***Figure (5.2)***. At one end, the beam is constrained in the global X and Y directions and at the other end it is restricted only in the global Y direction.

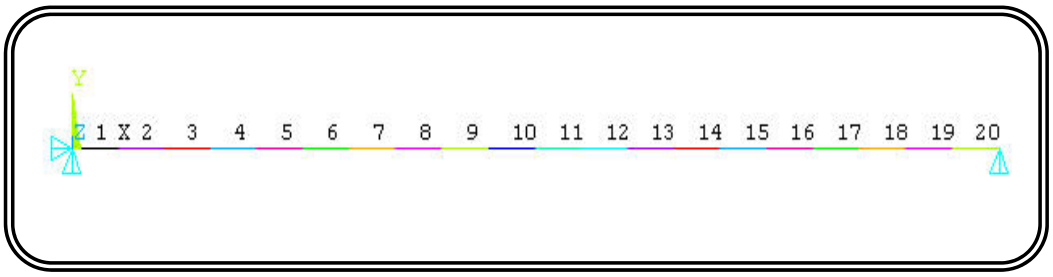

Figure (5.2) Finite element idealization of steel simply supported beam in ANSYS (V9.0)

5.2.3 Applied Moving Load

A moving force (P) of magnitude 4.448 N (1 lb) is moved on the simply supported steel beam with a constant velocity, (V) where the load (P) is applied at the left end of the beam and then the load moves toward the right end.

In this verification, two types of analysis are carried out in ANSYS represented by static and dynamic (transient) analysis. In static analysis, the force (P) is applied on the mid-span of the beam where the maximum deflection of the beam at the mid-span is compared with the analytical Kavipurapu results in ***Table (5.1)*** and they are in excellent agreement.

Table (5.1) Static mid-span deflection of the steel beam

Kavipurapu 2005	ANSYS Result (Present Analysis)	Difference Percent
3.4696654×10^{-3} mm	3.4678×10^{-3} mm	0.053

In the dynamic analysis, a transient analysis is used to simulate the moving load from the left end to the right end of the beam with twenty time steps by using ANSYS program. The load (P) is moved from one node to the next node at a time step (Δt) where the load (P) is applied on the first node (i) at the time (0) then moved to the next node ($i+1$) at a time (Δt) , ***review Figure (4.5) in the previous chapter***.

Where:-

$$\Delta t = \frac{L}{V * No.of\ time\ step} \qquad \ldots\ldots\ldots\ldots\ldots\ldots\ldots\ldots (5.1)$$

(Δt): represents the required time for the force (P) to move from one node to the next node at a constant velocity (V).

L = span length of the beam.

V = velocity of moving force.

Table (5.2) shows several velocities values for the moving load which are considered in this study, time step size for each velocity and the value of maximum deflection of the beam under various velocities. These results are compared with that of Kavipurapu (2005) and are in a very good agreement; see ***Figures (5.3), (5.4), (5.5)*** and ***(5.6)*** below. From this verification it can be seen that the adopted model of moving load can be used it in the current study.

Note: *upward deflection is positive for the dynamic analysis only.*

Table (5.2) Maximum central deflection for various moving load velocities

Moving Load Velocity km/h (ft/s)	Time Step (Δt) sec	Analytical Results (Kavipurapu 2005) mm	ANSYS Results (Present Analysis) mm	Difference Percent
56.134 (51.16)	3.257×10^{-4}	-3.60680×10^{-3}	-3.59733×10^{-3}	0.263
112.3 (102.33)	1.628×10^{-4}	-3.70840×10^{-3}	-3.79213×10^{-3}	2.208
224.57 (204.66)	0.814×10^{-4}	-4.11480×10^{-3}	-3.99771×10^{-3}	2.929
900 (820.16)	0.203×10^{-4}	-5.47116×10^{-3}	-5.62264×10^{-3}	2.694

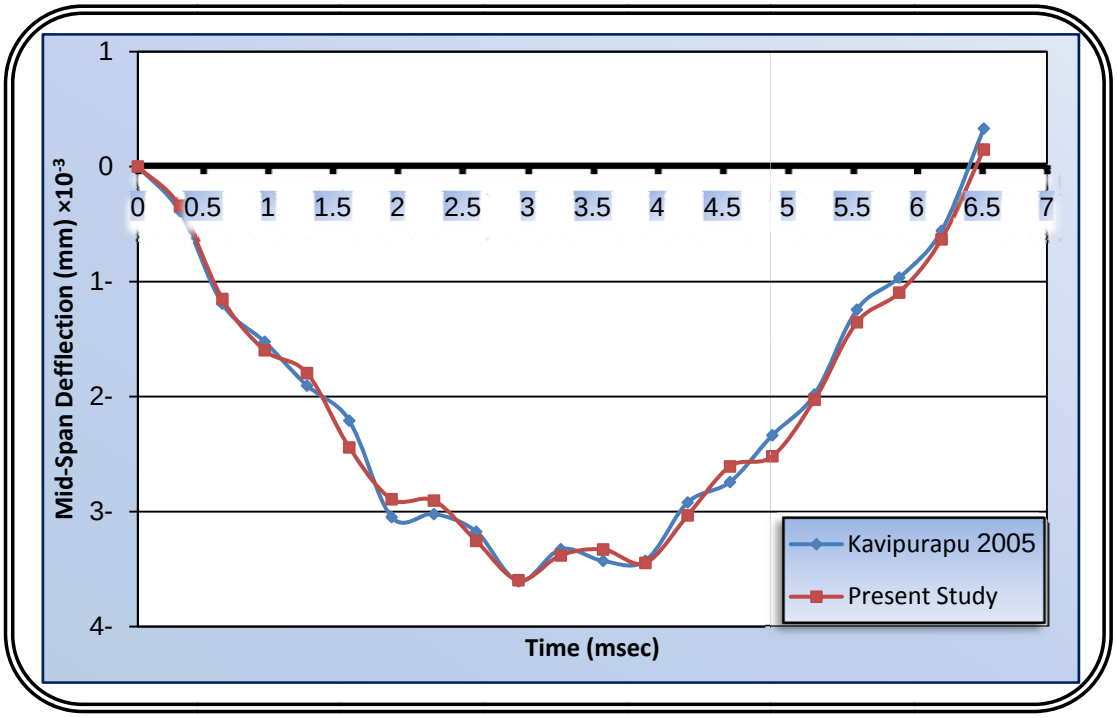

Figure (5.3) Time history of mid-span deflection for V = 56.134 km/h (51.16 ft/s)

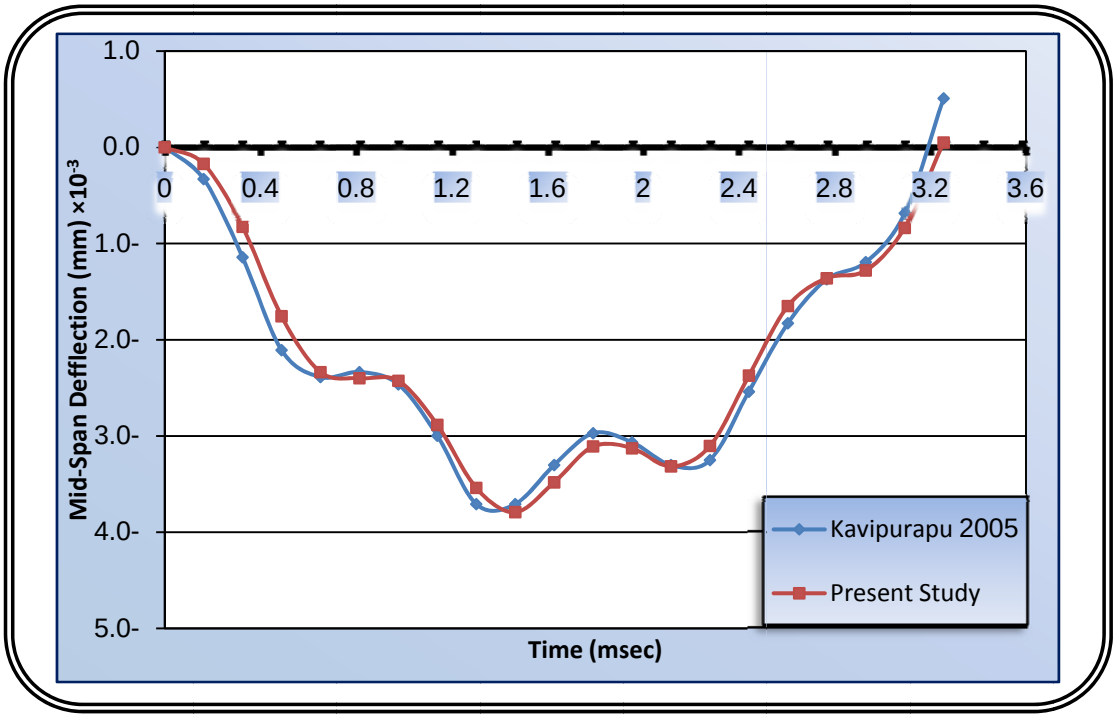

Figure (5.4) Time history of mid-span deflection for V = 112.3 km/h (102.33 ft/s)

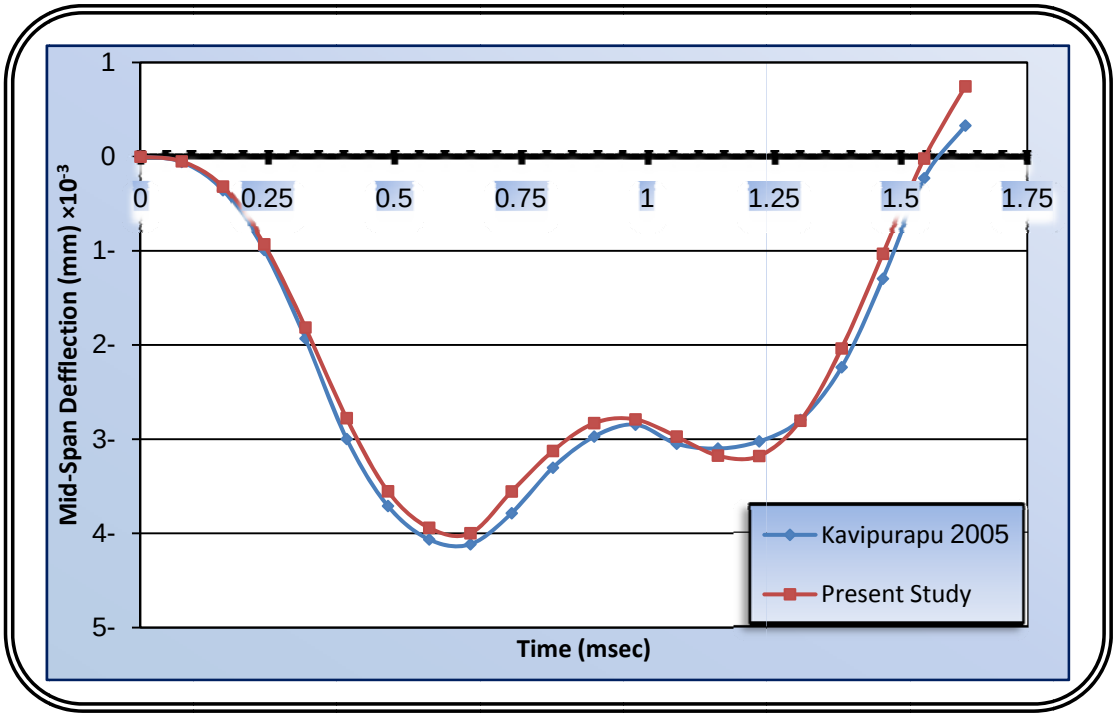

Figure (5.5) Time history of mid-span deflection for V = 224.57 km/h (204.66 ft/s)

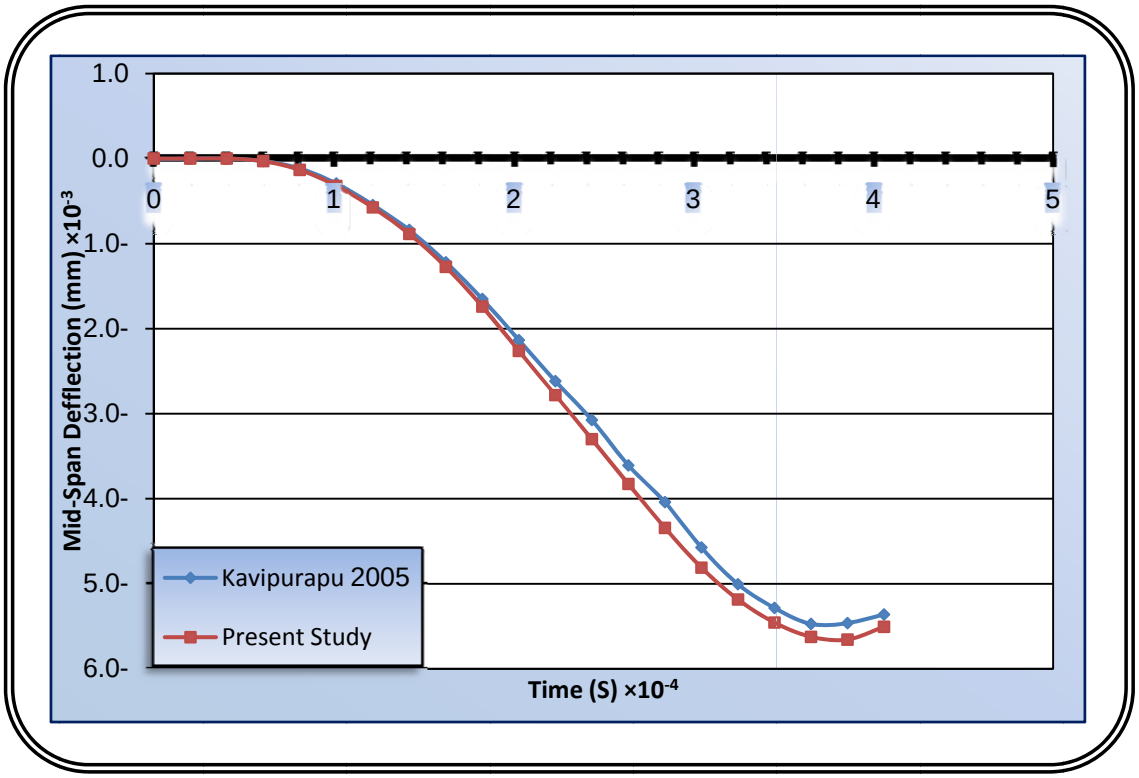

Figure (5.6) Time history of mid-span deflection for V = 900 km/h (820.16 ft/s)

Part two: Verification of Prestressed Concrete

In this part, three examples which are simply supported prestressed concrete girders under flexural load are used to check the adopted model of prestressed concrete by using ANSYS program.

The first example represented by a rectangular prestressed concrete beam was introduced by Wolanski, 2004, and the other examples represented by the two full scale bridge girders were presented by Canfield in 2005. Two types of specimens were used in his investigation, an ***AASHTO Type (IV) girder*** and a ***Modified PCI (BT-56) girder***, having lengths of 27.2 m and a 203 mm thick by 1524 mm wide composite deck cast atop of each girder.

5.3 Example (2):

In this example, a rectangular prestressed concrete beam under flexural load was tested by Wolanski in 2004.

5.3.1 Geometrical Properties

The geometrical property of Wolanski beam are illustrated in ***Figure (5.7)*** below, which is explains the cross section and reinforcement details with a length 4.725m. The material properties of the beam are given in ***Table (5.3)***, and the stress-strain model of concrete that given by Wolanski is shown in ***Table (5.4)***.

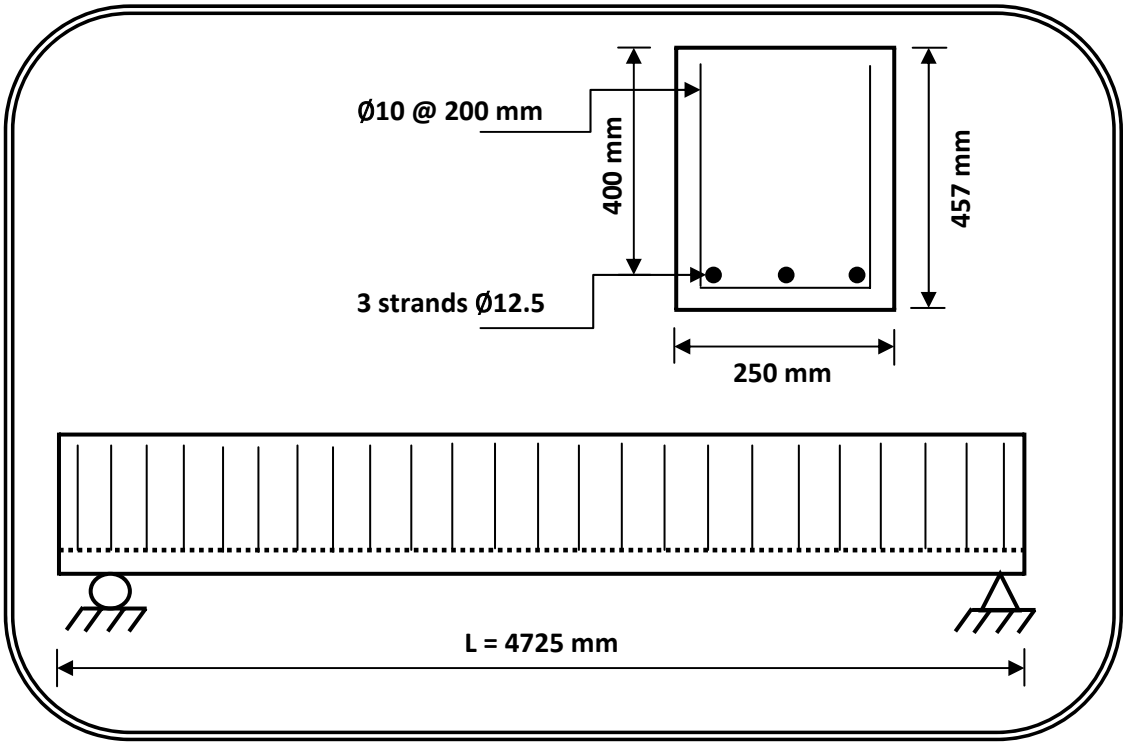

Figure (5.7) Geometrical properties of the prestressed Wolanski beam

5.3.2 Finite Element Idealization

In the present analysis, brick element 8-noded (SOLID65) is used to represent the concrete. Embedded model of steel (ordinary and prestress) reinforcement is used in this problem. The girder is a simply supported at

the two ends; see ***Figure (5.8)***, as considered by Wolanski. At one end, the beam is constrained in all directions and at the other end it is restricted only in the global Y direction. The prestressing force is model as a lateral equivalent pressure acts on the beam, review ***Figure (5.8)***.

Table (5.3) Materials properties of Wolanski beam

Properties of concrete beam		Properties of (12.5^{mm}) prestressing strands	
Modulus of elasticity, E (GPa)	27.228	Modulus of elasticity, E (GPa)	193.052
Compressive strength, f_c' (MPa)	33	Ultimate strength, f_{pu} (MPa)	1860
Tensile strength, f_t (MPa)	3.575	Tangent modulus, (MPa)	2739
Density, γ (kN\m^3)	24	Prestressing force (kN)	36.26
Poisson's ratio, v	0.2	Poisson's ratio, v	0.3
Properties of steel reinforcement			
Yield stress, f_y (MPa)	414	Modulus of elasticity, E (GPa)	200
Tangent modulus, (MPa)	20	Poisson's ratio, v	0.3

Table (5.4) A multilinear stress-strain model of concrete beam adopted by Wolanski

Strain	Stress (MPa)
0.00036	9.8023
0.0006	15.4
0.0013	27.5
0.0019	32.1
0.00243	33

In ANSYS, three cases of the mesh size are used to represent the present prestressed concrete beam, see ***Figure (5.9)***, to get the best agreement between the experimental data and the numerical model and to choose the best one to use it in the other analysis. These cases are represented as the following:

Mesh (a): total number of elements =324

Mesh (b): total number of elements =540

Mesh (c): total number of elements =1134

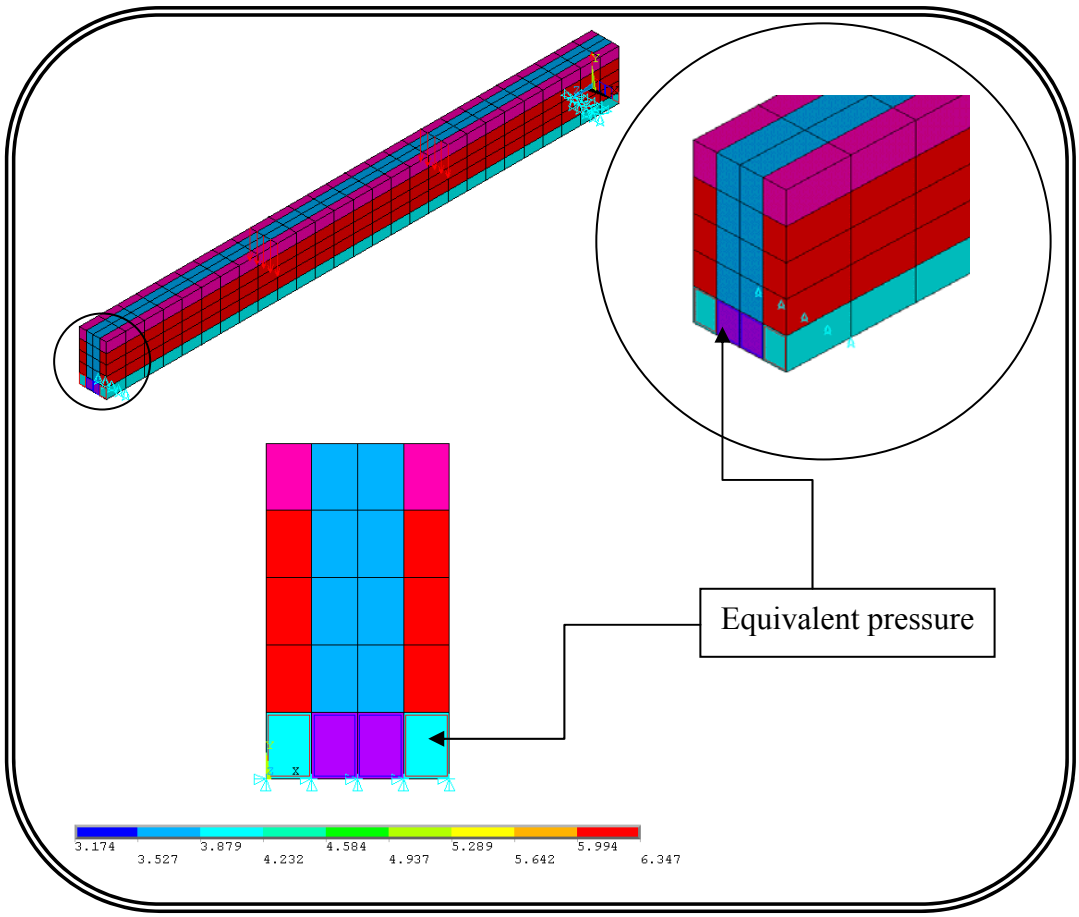

Figure (5.8) Finite element idealization of the prestressed Wolanski beam in ANSYS (V9.0)

5.3.3 Checking the Adopted Model

The three cases of mesh size that are considered in representation of the prestressed concrete beam in this investigation are checked with Wolanski data where the beam was tested under flexural load but at the first, the cambering of the beam before loading also is checked, see ***Table***

(5.5). A two 222.4 kN (50 kip) capacity load cells were placed at third points as shown in ***Figure (5.10)***. ***Figure (5.11)*** shows the comparison of the cases of the mesh size that considered for the present example and the used mesh (b).

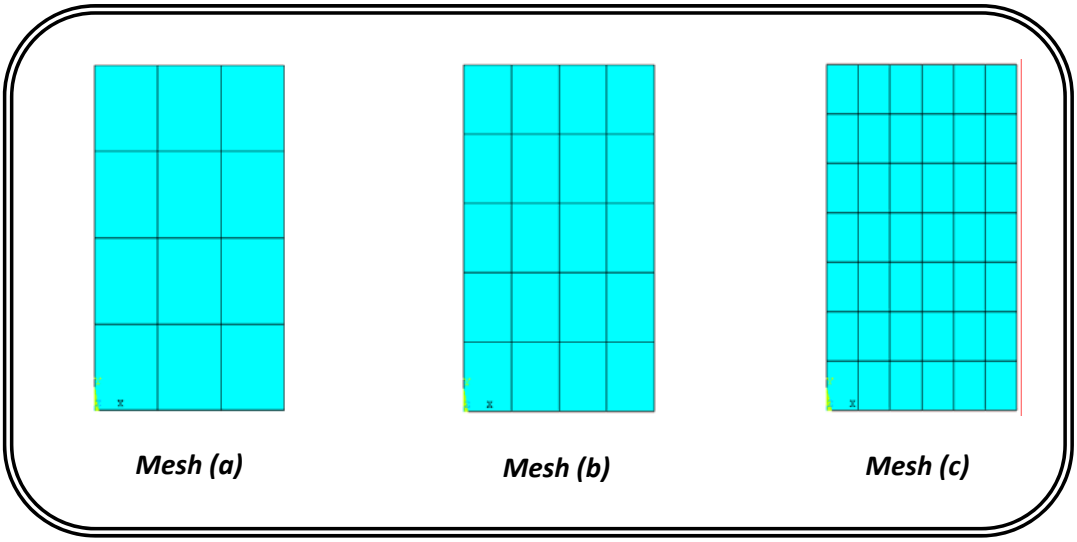

Figure (5.9) Mesh size details of the prestressed Wolanski beam

Table (5.5) Cambering of the prestressed Wolanski beam

Cases	Cambering due to prestressing force and self weight (mm)		Difference Percent
	Experimental	Present Study	
a	0.53594	0.6335	18.2
b	0.53594	0.60447	12.787
c	0.53594	0.5045	5.866

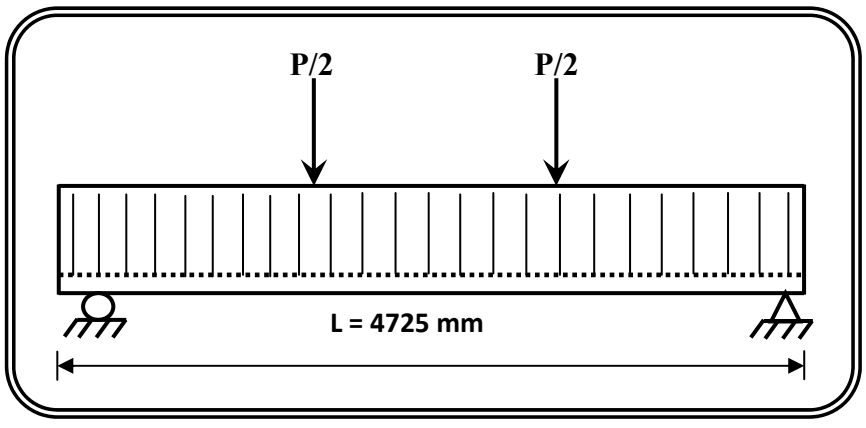

Figure (5.10) Flexural test setup of Wolanski beam

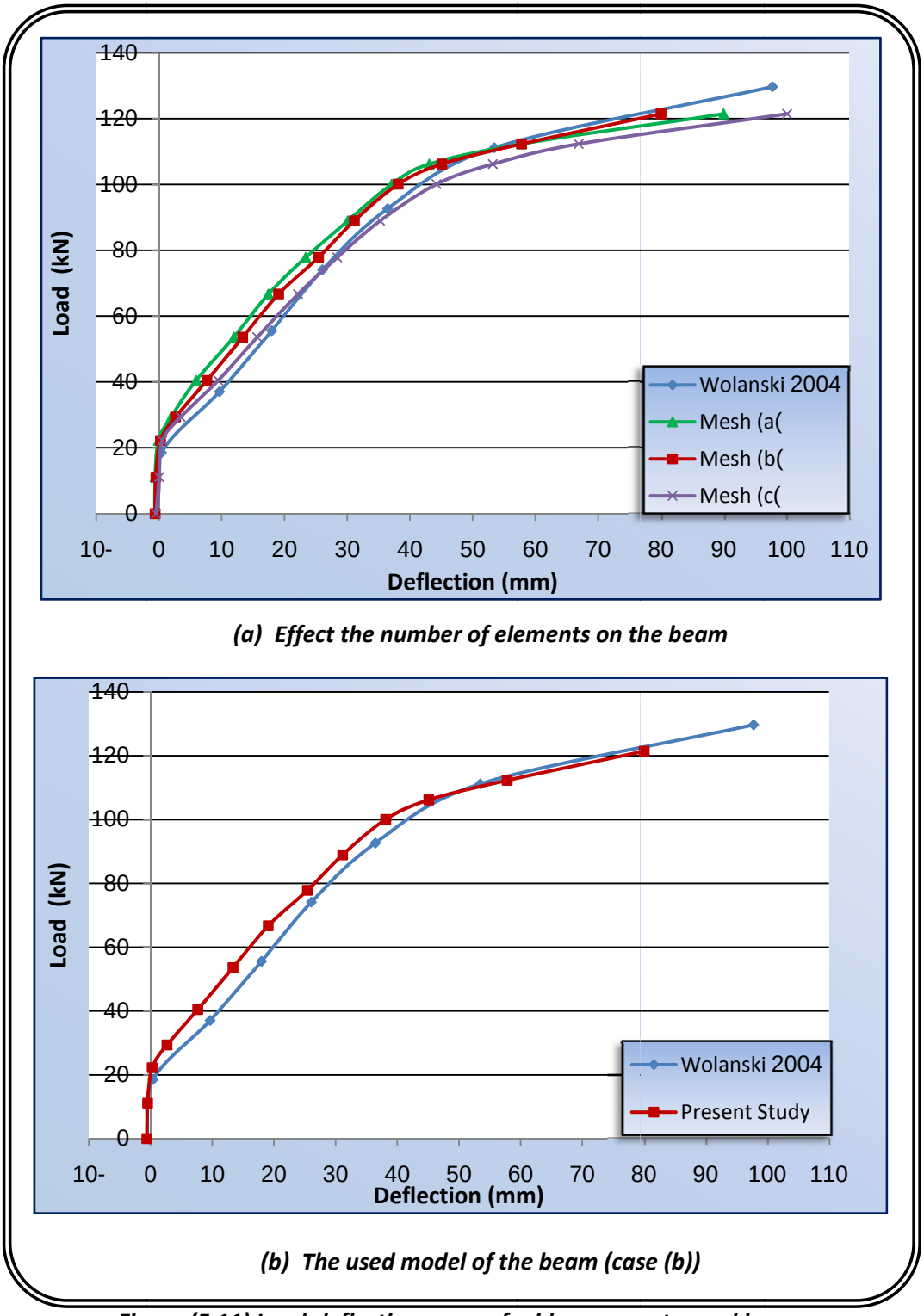

Figure (5.11) Load-deflection curve of mid-span prestressed beam

The mesh (b) gives a good convergence for experimental than the other cases (a and c) this is due to the location of prestressing strands which affects the eccentricity of prestressing force in the prestressed

concrete beam so that it has been used in the other analysis (dynamic analysis).

5.4 Example (3): AASHTO Type (IV) Girder:

5.4.1 Geometrical Properties

The cross section of girder type (IV) and reinforcement details are shown in ***Figure (5.12a)*** below which had a length 27.2m, and 52 strands (Grade 270). Girder had a composite decks (203×1524×27200) mm, see ***Figure (5.12b)***, that were cast after (66 days) from girder construction.

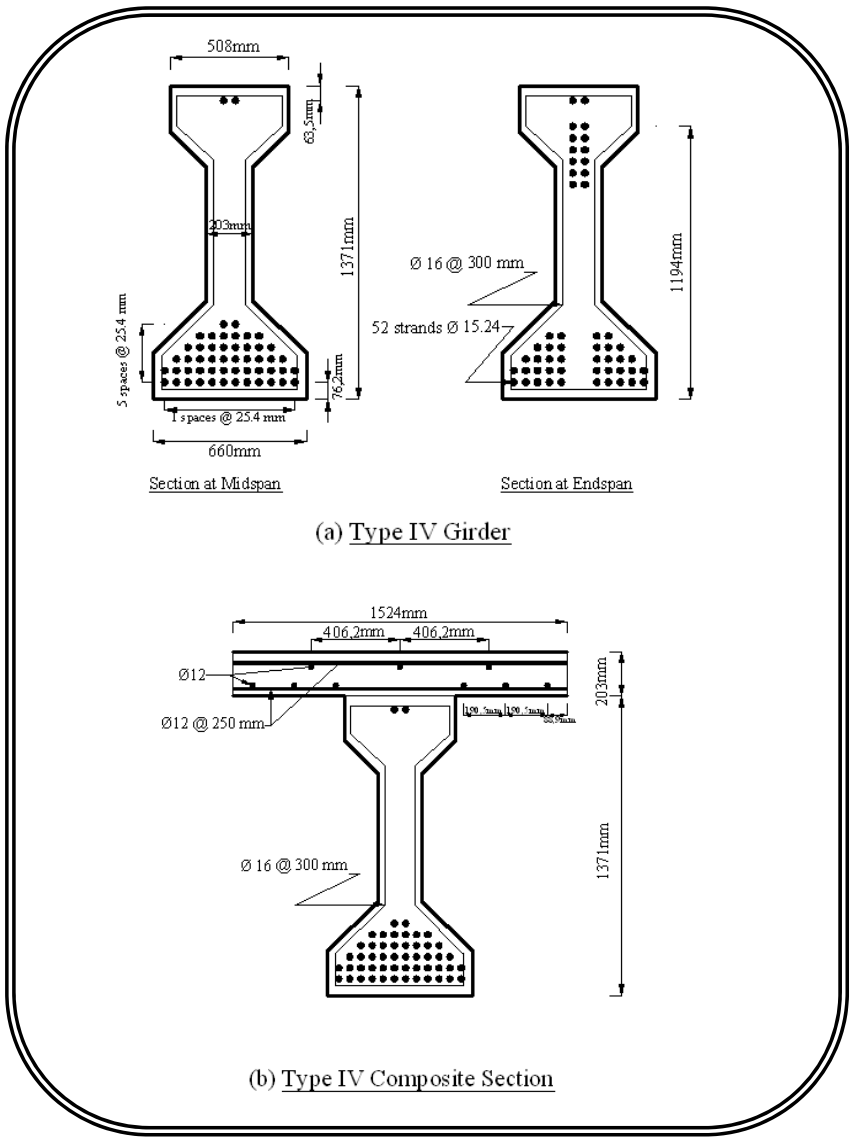

Figure (5.12) Cross section and reinforcement details of the prestressed girder type (IV)

The properties of each material used in this study are tested by Canfield in 2005 and as arranged in ***Table (5.6)***. The stress-strain model of concrete that considered in the analysis of the prestressed concrete girder type (IV) is shown in ***Table (5.7)***, which was given by Canfield.

Table (5.6) Materials properties of the prestressed girder type (IV)

Properties of concrete girder		Properties of (15.24^{mm}) prestressing strands	
Modulus of elasticity, E (GPa)	46.764	Modulus of elasticity, E (GPa)	204.65
Compressive strength, f_c' (MPa)	99	Yield stress, f_{py} (MPa)	1827.5
Tensile strength, f_t (MPa)	6.169	Tangent modulus, (MPa)	2743.8
Poisson's ratio, v	0.16	Poisson's ratio, v	0.3
Density, γ (kN\m^3)	24	Prestressing force (kN)	198.8256
		Total prestress losses (kN)	35.89
Properties of concrete deck		Properties of steel reinforcement	
Modulus of Elasticity, E (GPa)	24.624	Modulus of elasticity, E (GPa)	200
Compressive strength, f_c' (MPa)	50	Yield stress, f_y (MPa)	510.59
Tensile strength, f_t	4.384	Tangent modulus, (MPa)	2541.3
Poisson's ratio, v	0.18	Poisson's ratio, v	0.3
Density, γ (kN\m^3)	24		

Table (5.7) A multilinear stress-strain that used in analysis of the girder (IV)

Concrete Girder		Concrete Deck	
Strain	Stress (MPa)	Strain	Stress (MPa)
0.001769	83.736	0.00112	27.579
0.002	91.04	0.0021	41.368
0.00223	96.526	0.00325	48.263
0.00234	98.824	0.0038	50
0.00246	99		
0.00278	68.947		
0.0045	29.111		

5.4.2 Finite Element Idealization

The same model used in example (2) is adopted in this example where the concrete modeled by using brick element (SOLID65) with embedded steel reinforcement representation (ordinary and prestress). The girder is modeled as a simply supported at the two ends, as adopted by Canfield, see ***Figure (5.13)*** with equivalent lateral pressure acts on the girder to model of prestressing force as explained in ***Figure (5.13)***.

To choose the best mesh size in finite element method for this example and to get a good convergence for the experimental data, three cases of the mesh size are used to represent the prestressed concrete girder type (IV) by using ANSYS, see ***Figure (5.14)***. These cases are represented as the following:

Mesh (a): total number of elements =2720

Mesh (b): total number of elements =4216

Mesh (c): total number of elements =12512

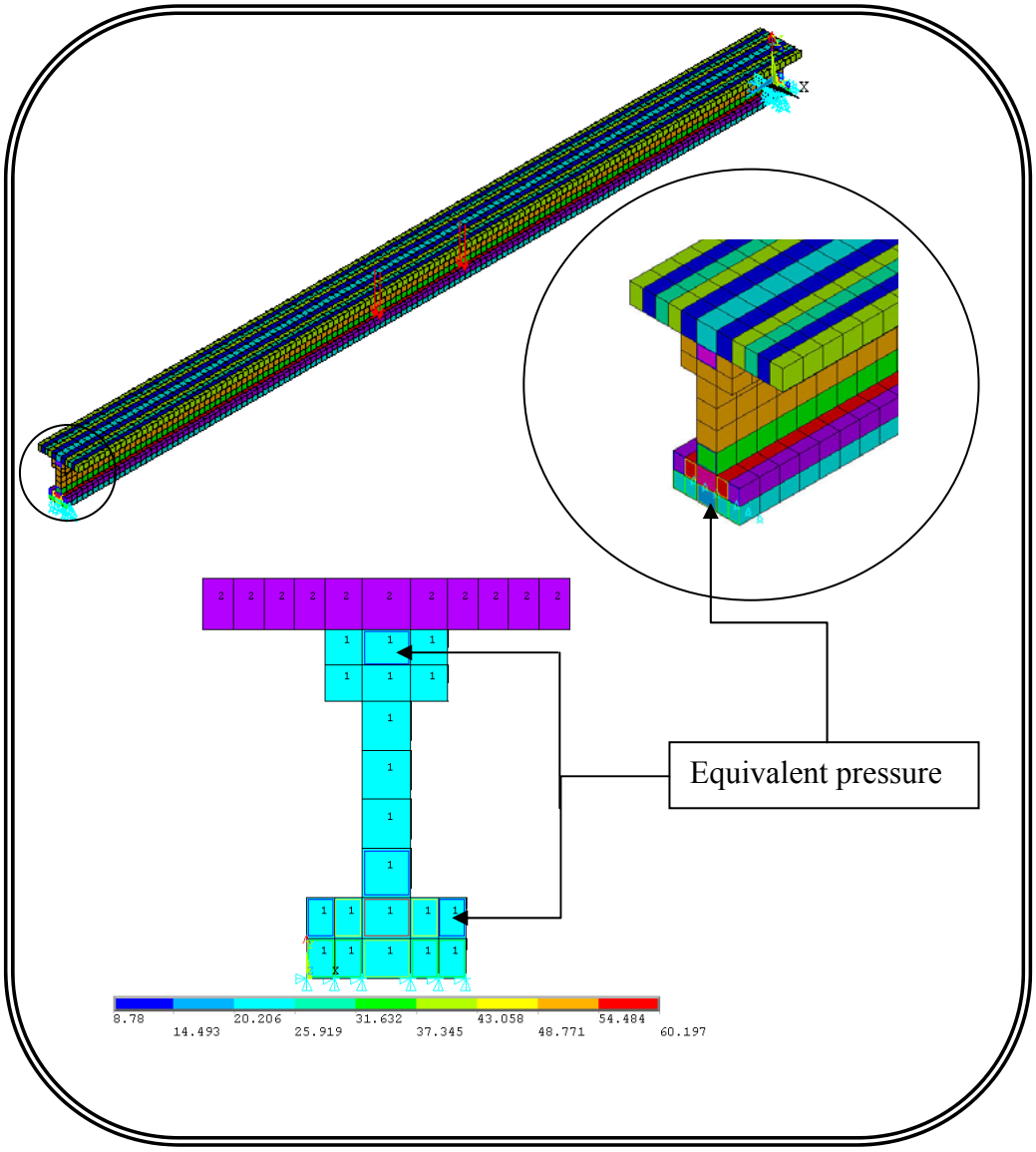

Figure (5.13) Finite element idealization of the prestressed girder type (IV) in ANSYS (V9.0)

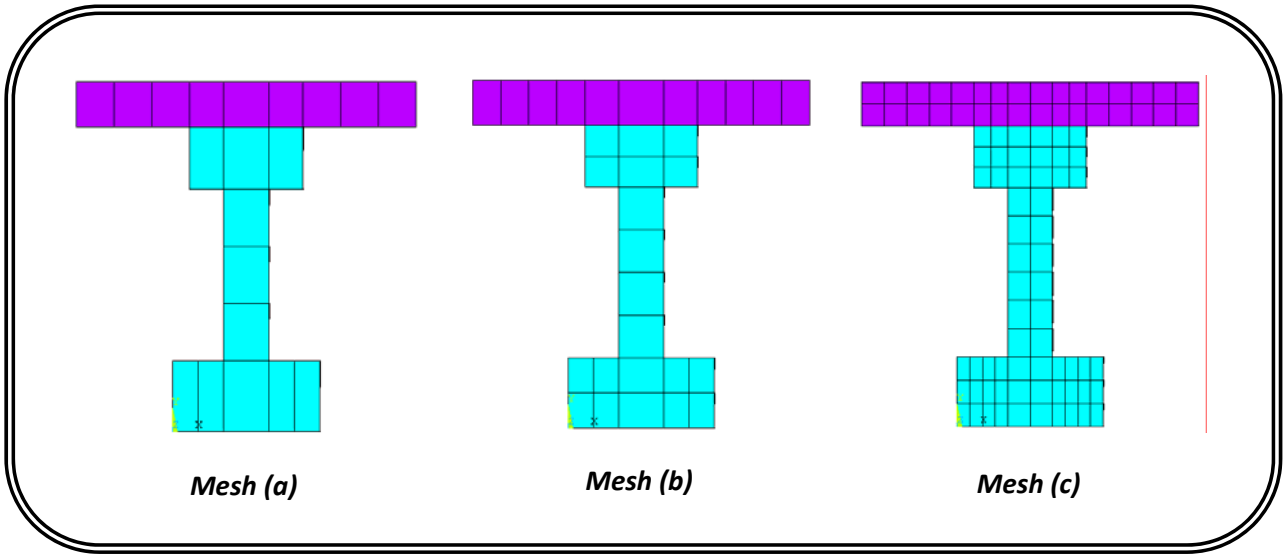

Figure (5.14) Mesh size details of the prestressed girder type (IV)

5.4.3 Checking The Adopted Model

The cases of mesh size of this example are considered to choose the best case by using ANSYS. In this verification, every mesh size of the girder is checked with experimental data at various stages of construction represented by:-

1- Cambering of girder without deck (girder under self weight only with 20% of total losses in prestressing force).

2- Initial cambering of girder with deck (2days after casting deck with 40% of total losses in prestressing force).

3- Final cambering of girder with deck (77 days after casting deck with total losses of prestressing force).

Where the cambering of mid-span of girder (IV) for above stages is found and compared with experimental results in ***Table (5.8)***.

Table (5.8) Cambering of mid-span prestressed girder (IV) in various stages

Stages	Experimental (mm)	Mesh a (mm)	Mesh b (mm)	Mesh c (mm)
Girder without deck	64.8	51.53	64.675	66.162
Girder with deck Initial	55.4	47.106	52.204	55.231
Girder with deck Final	46.8	39.341	45.982	48.921

Finally, Canfield tested the girder (IV) under flexural load by using a hydraulic jack, see ***Figure (5.15)***, and the load-deflection curve of the test is compared with the adopted model in ANSYS program for the various mesh size, see ***Figure (5.16a)***. It can be seen that the mesh size case (c) is the best one and gives a very good convergence with experimental data than the other cases this is due a good representation of the location's strands in the girder in the other wards a good representation of the eccentricity of prestressing force in the girder type (IV). Case (b) also give a good agreement and it has been used in the present study, see ***Figure (5.16b)***, because of the running time and the

convergence of the problem are the main factors in choice the mesh size where the number of elements in case (c) can say three times the number of elements in case (b), so that the case (b) in the present example has been used in the other analysis.

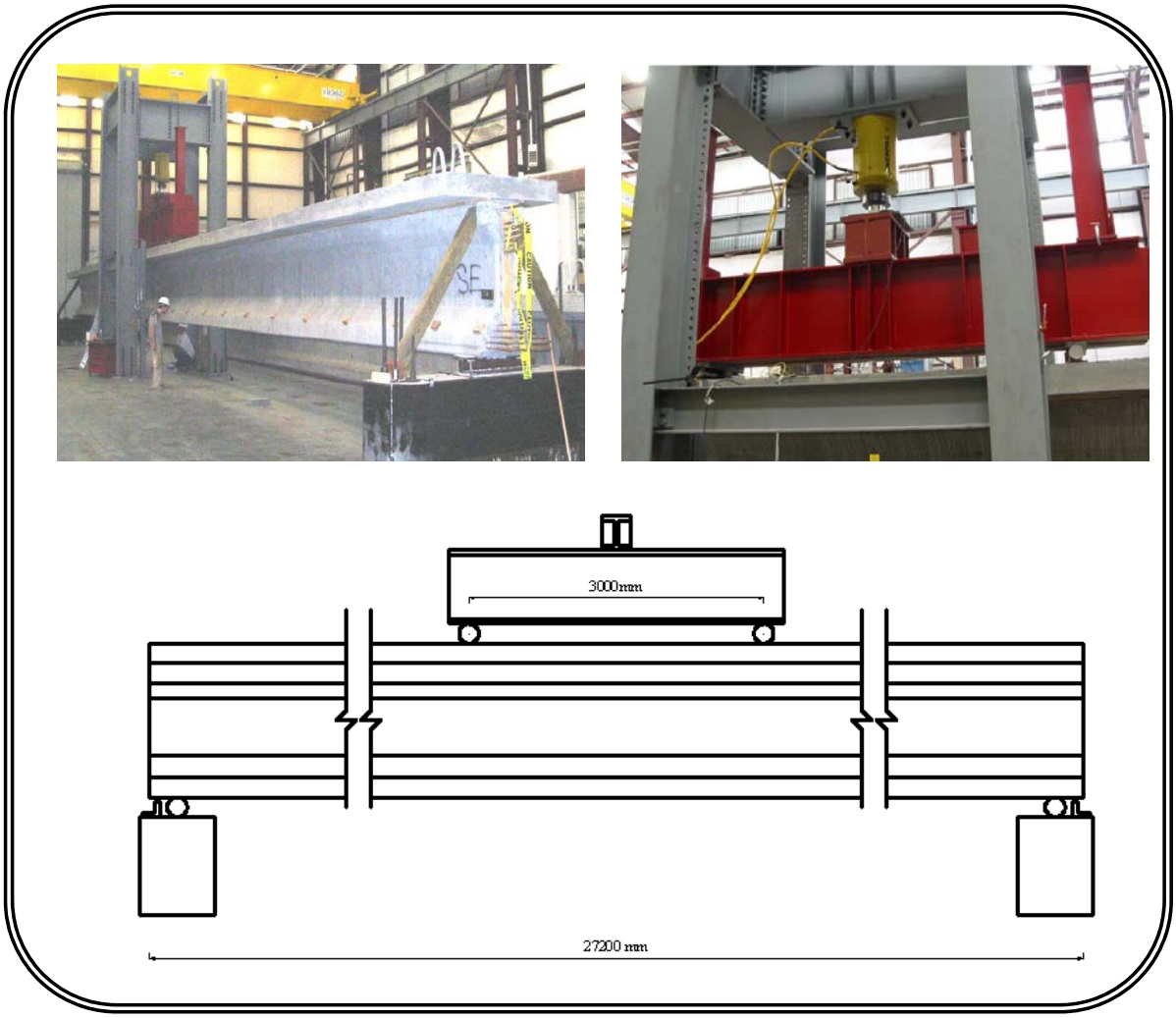

Figure (5.15) Pictures and drawing of girder (IV) in the flexural test setup [3]

5.5 Example (4): Modified PCI (BT-56) Girder:

The second girder (specimen) that adopted by Canfield [3] was type (BT-56) and the same procedure that done in girder type (IV) was used on type (BT-56) to investigate the behavior of prestressed concrete girder under flexural load. This investigation also is used to verify the adopted model of prestressed concrete girder in the present study.

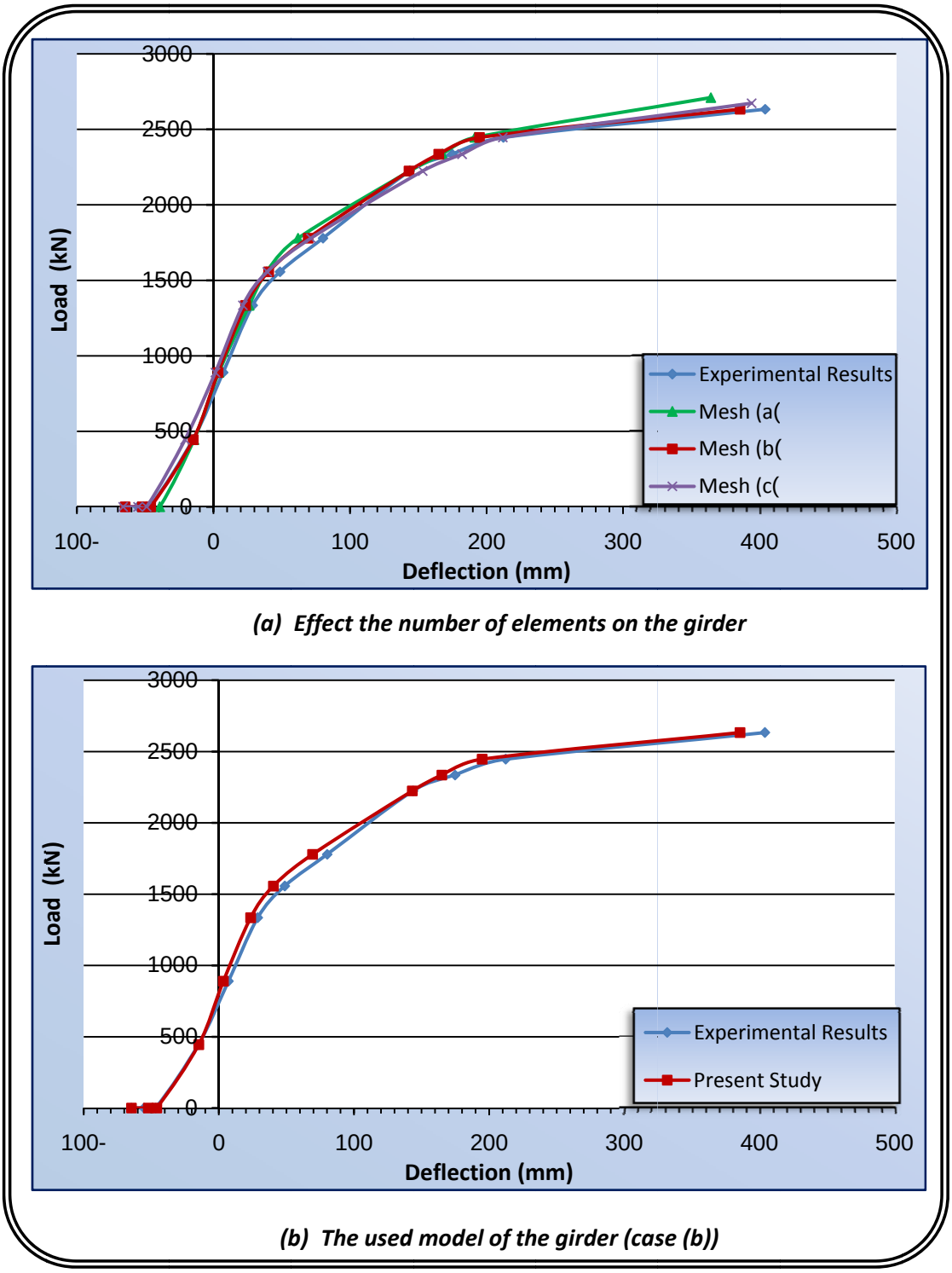

Figure (5.16) Load-deflection curve of mid-span prestressed girder type (IV)

5.5.1 Geometrical Properties

Figure (5.17) shows the cross section and details of prestressed concrete girder type (BT-56), which had length 27.2m, and 44 strands (Grade 270). A composite deck (203×1524×27200) mm was cast on a top of

girder after (129 days) from casting girder. The materials properties are given in ***Table (5.9)***. In this analysis, a multilinear stress-strain model of concrete is used as shown in ***Table (5.10)***, which is adopted by Canfield.

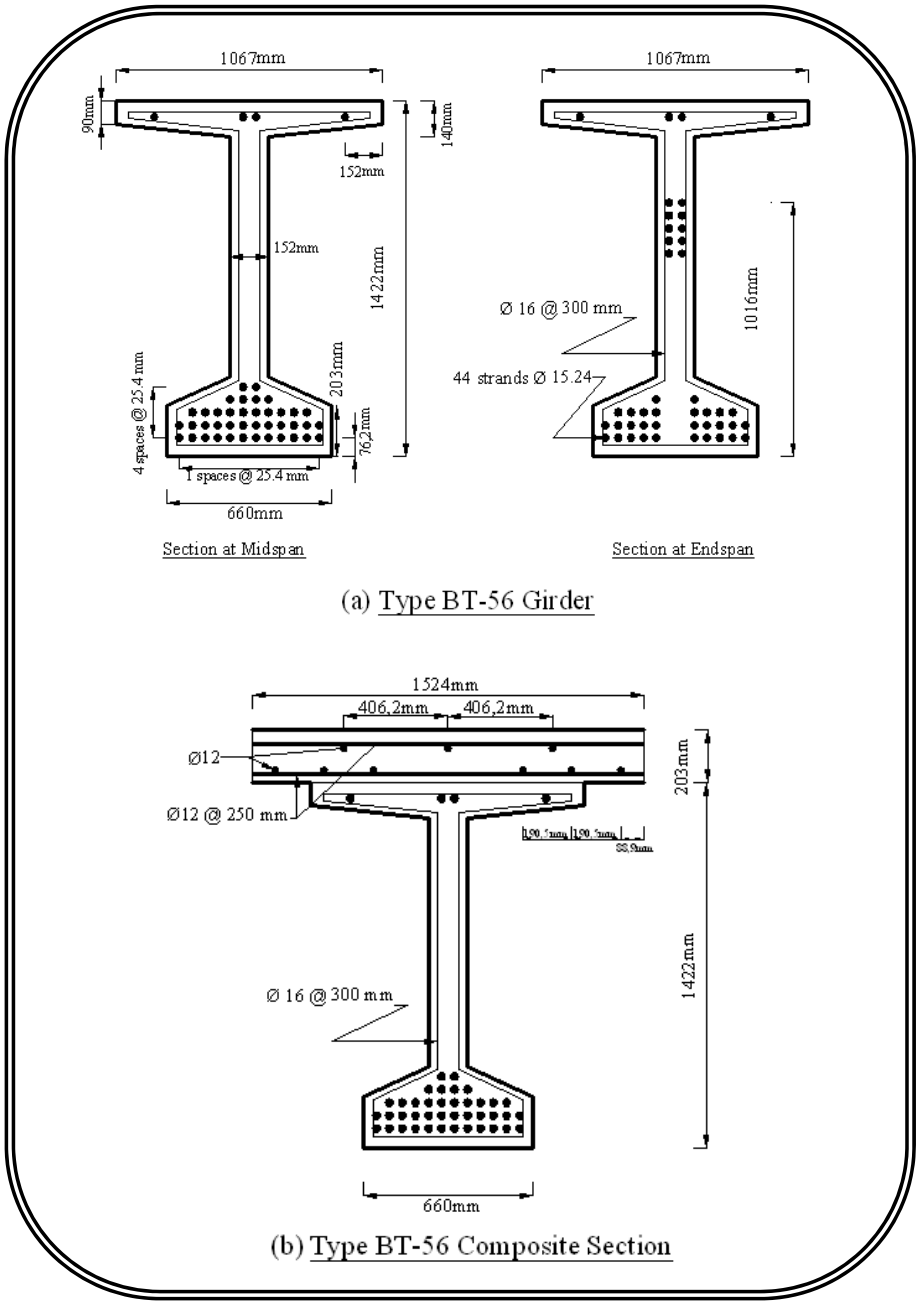

Figure (5.17) Cross section and reinforcement details of the prestressed girder type (BT-56)

Table (5.9) Materials properties of prestressed girder type (BT-56)

Properties of concrete girder		Properties of (15.24^{mm}) prestressing strands	
Modulus of Elasticity, E (GPa)	33.329	Modulus of Elasticity, E (GPa)	204.65
Compressive strength, f_c' (MPa)	104.4	Ultimate strength, f_{pu} (MPa)	1827.5
Tensile strength, f_t (MPa)	6.335	Tangent Modulus, (MPa)	2743.8
Poisson's ratio, v	0.18	Poisson's ratio, v	0.3
Density, γ (kN\m^3)	24	Prestressing Force (kN)	198.8256
		Total Prestress Losses (kN)	39
Properties of concrete deck		Properties of steel reinforcement	
Modulus of Elasticity, E (GPa)	24.173	Modulus of Elasticity, E (GPa)	200
Compressive strength, f_c' (MPa)	45.87	Yield stress, f_y (MPa)	510.59
Tensile strength, f_t	4.199	Tangent Modulus, (MPa)	2541.3
Poisson's ratio, v	0.18	Poisson's ratio, v	0.3
Density, γ (kN\m^3)	24		

5.5.2 Finite Element Idealization

In this example, the finite element model is similar to that used model in previous examples where the brick element (SOLID65) with embedded model of steel (ordinary and prestress) reinforcement within brick element used to represent the prestressed concrete girder, see ***Figure (5.18)***. An equivalent pressure model is used to represent the prestressing force in the present analysis.

Table (5.10) A multilinear stress-strain that used in analysis of the girder (BT-56)

Concrete Girder		Concrete Deck	
Strain	Stress (MPa)	Strain	Stress (MPa)
0.000994	31.32	0.00057	13.778
0.00156	52.2	0.00065	15.67
0.00219	73.08	0.00093	23.24
0.00282	93.96	0.001	31.44
0.00313	104.4	0.0015	37.65
0.00626	208.8	0.0021	40.82
		0.0028	41.26
		0.003235	45.87

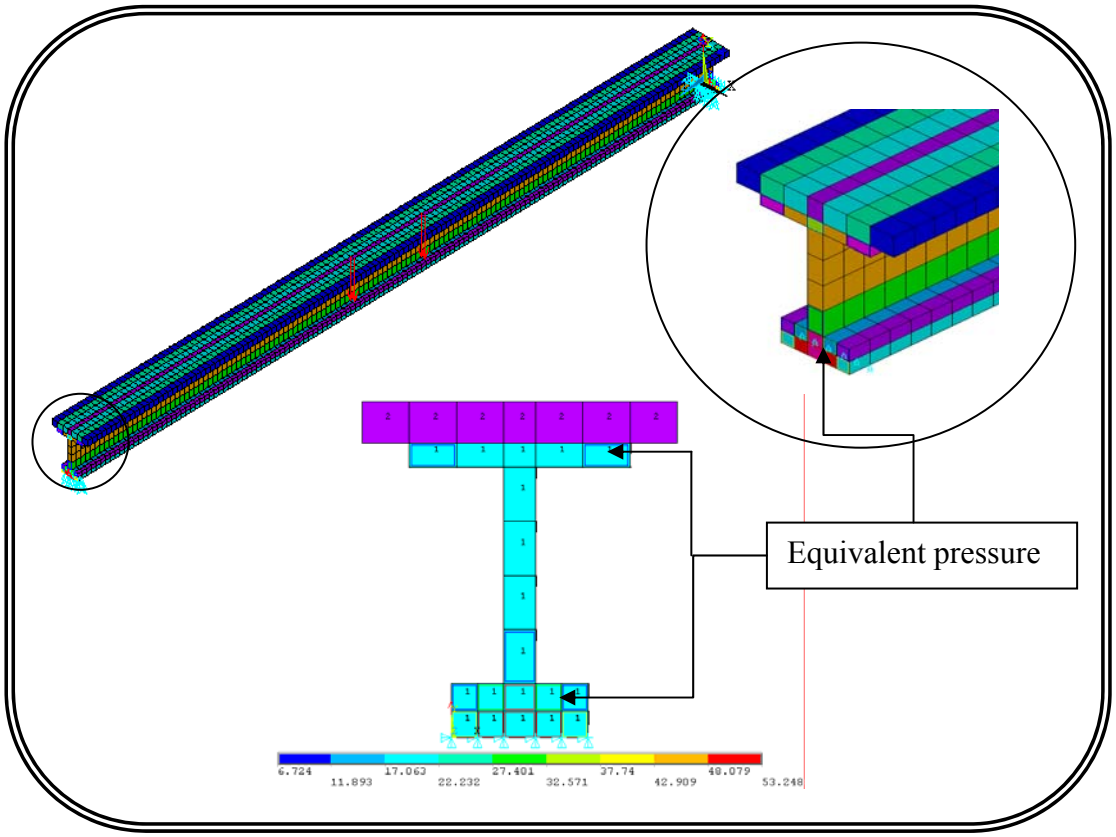

Figure (5.18) Finite element idealization of the prestressed girder type (BT-56) in ANSYS

In ANSYS, three cases of the mesh size are considered, as shown in ***Figure (5.19)***, to represent the prestressed concrete girder type (BT-56) to choose the best mesh size in finite element method for this example and to get a good convergence for the experimental data. These cases are represented as the following:

Case (a): total number of elements =2856

Case (b): total number of elements =3536

Case (c): total number of elements =9248

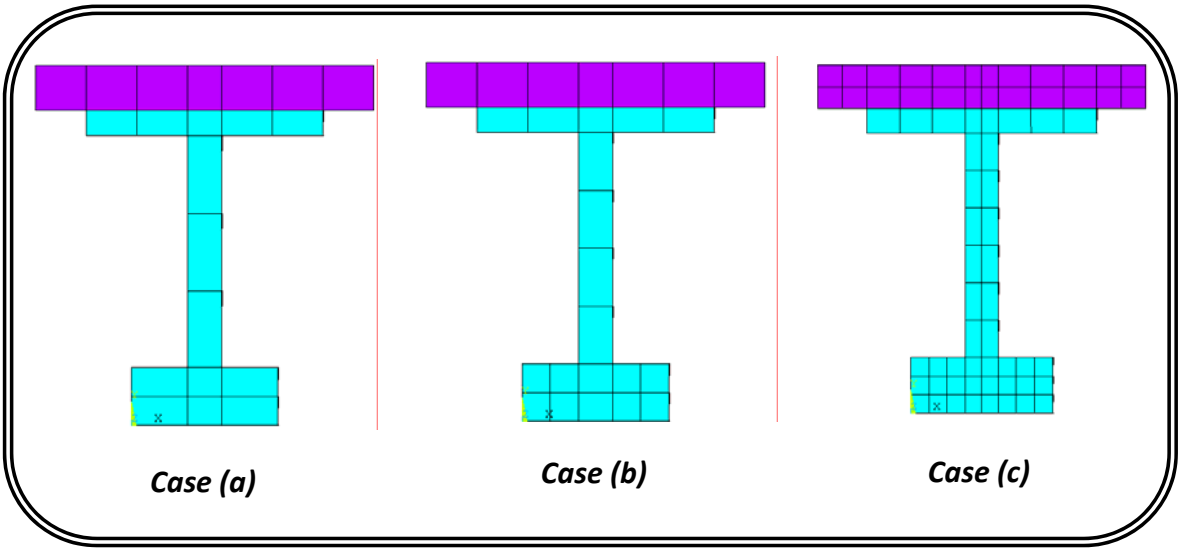

Figure (5.19) Mesh size details of the prestressed girder type (IV)

5.5.3 Checking The Adopted Model

Similar to the previous example (girder IV), many stages for the cases of mesh size which adopted to represent the prestressed concrete girder type (BT-56) are checked with experimental data to choose the best mesh, where the cambering of mid-span of the girder (BT-56) for these stages are found and compared with experimental results and as shown in ***Table (5.11)***.

Table (5.11) Cambering of mid-span prestressed girder (BT-56) in various stages

Stages	Experimental (mm)	Mesh a (mm)	Mesh b (mm)	Mesh c (mm)
Girder without deck	71.4	61.932	67.336	68.362
Girder with deck Initial	63	53.91	59.108	61.203
Girder with deck Final	60	47.1	56.559	57.221

Figure (5.20a) below shows the comparison between the experimental data and the cases of mesh size for the prestressed girder type (BT-56) under flexural load to choose the best mesh size for the girder to adopted in other analysis where the flexural test that considered in the present example is the same as the test setup that done in the previous example, (review ***Figure (5.15)***).

From these results it can be seen that the mesh (b and c) are the best cases. The difference between these cases is very small and also the number of element for case (c) is nearly three times the number of element for case (b) so that the mesh (b) has been used in the other analysis for the prestressed concrete girder type (BT-56), see ***Figure (5.20b)***.

Part Three: General Behavior

From the two parts above, the effect of dynamic moving load on the prestressed concrete girder has been considered where a moving force (P) is moved on the girder from one end to the other end with a constant velocity (V) by using ANSYS.

Where (P) equivalent to the resultant of half weight of HS15-44 in example (2) because of ultimate load of Wolanski beam, and in the other examples (3 and 4), (P) is equivalent to the resultant of half weight of HS20-44.

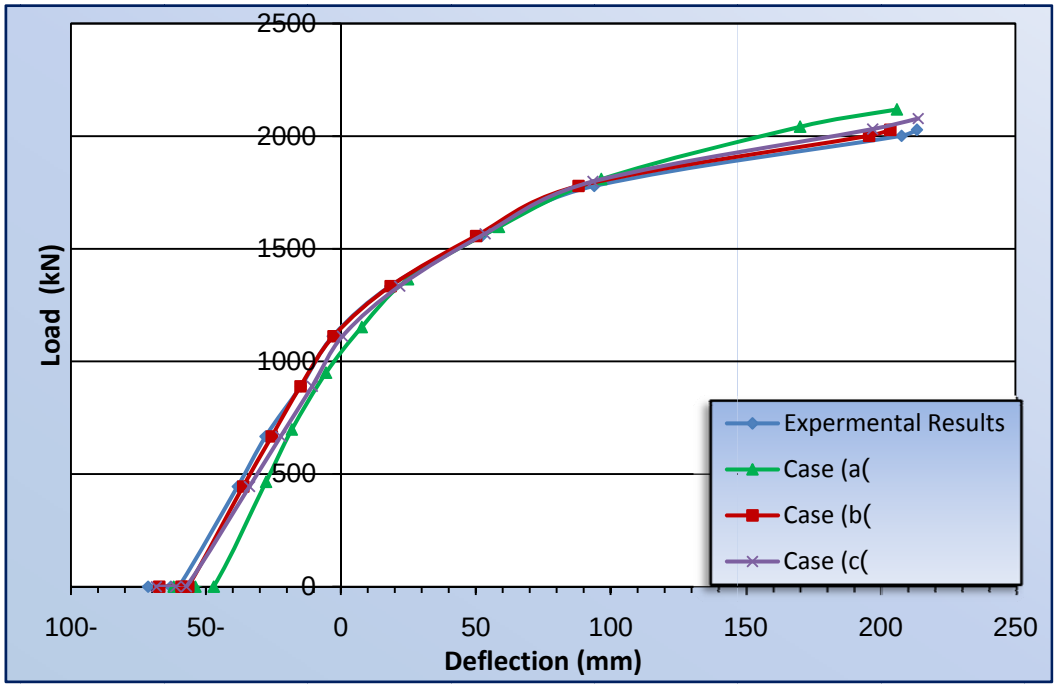

(a) Effect the number of elements on the girder

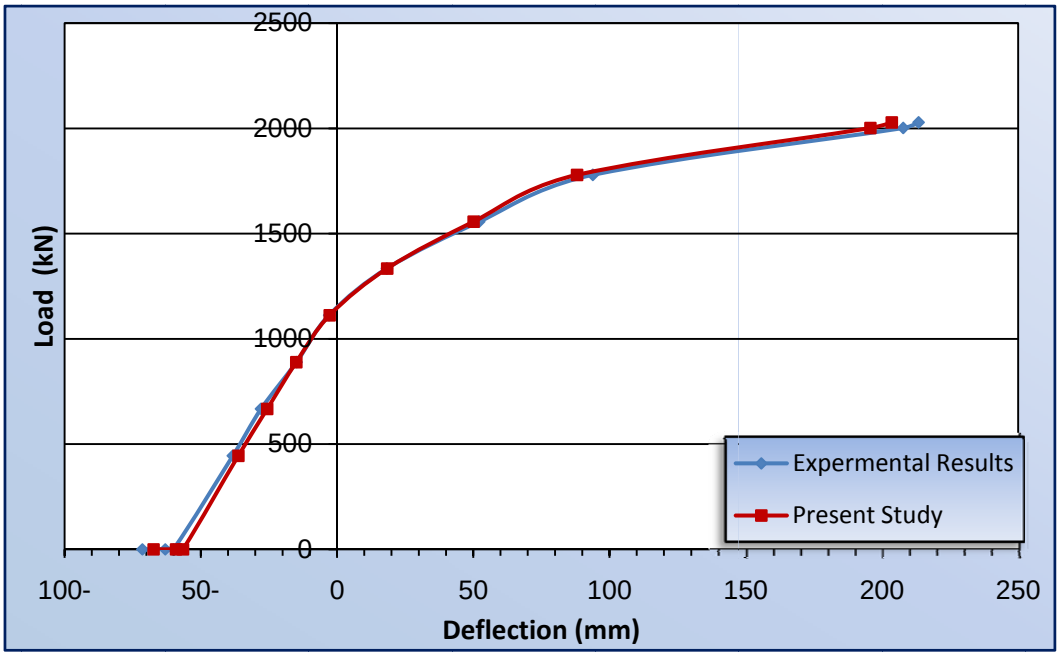

(b) The used model of the girder (case (b))

Figure (5.20) Load-deflection curve of mid-span prestressed girder (BT-56)

5.6 Dynamic Response of Prestressed Concrete Girder under Moving Load

In ANSYS, a transient analysis is used to move the force (P) from left end to the right end at a constant velocity where the same procedure that used in example (1) is used to represent the moving load to investigate the dynamic response of prestressed concrete girders under moving load.

Table (5.12) shows the number of time steps to simulate the moving force from the left end to the right end and time steps size (Δt) that used in the transient analysis for every girder that used in this investigation where (Δt) represent the required time to move force (P) from one node to the next node, ***review Figure (4.5) in the previous chapter***, and (Δt) is calculated according to ***equation (5.1)***. Several velocity values for the moving load are considered.

Table (5.12) No. of time steps and time steps size (Δt) that used in the transient analysis

Girder Type	No. of Time Steps	Time Steps Size (Δt) sec		
		60 km/h	80 km/h	120 km/h
Wolanski Beam (Example 2)	14	0.02025	15.1875×10^{-3}	10.125×10^{-3}
Type (IV) (Example 3)	17	0.096	0.072	0.048
Type (BT-56) (Example 4)	17	0.096	0.072	0.048

Note: *upward deflection is positive for the dynamic analysis only.*

5.6.1 Effect of Velocities

Vehicle velocity plays an important parameter in the dynamic behavior of the bridge so that the dynamic response of prestressed concrete girder under variuos velosities (60,80 and 120)km/h are adopted in this study, and the found results of the above examples (2, 3 and 4) are shown in ***Figures (5.21),(5.22)*** and ***(5.23)*** respectively.

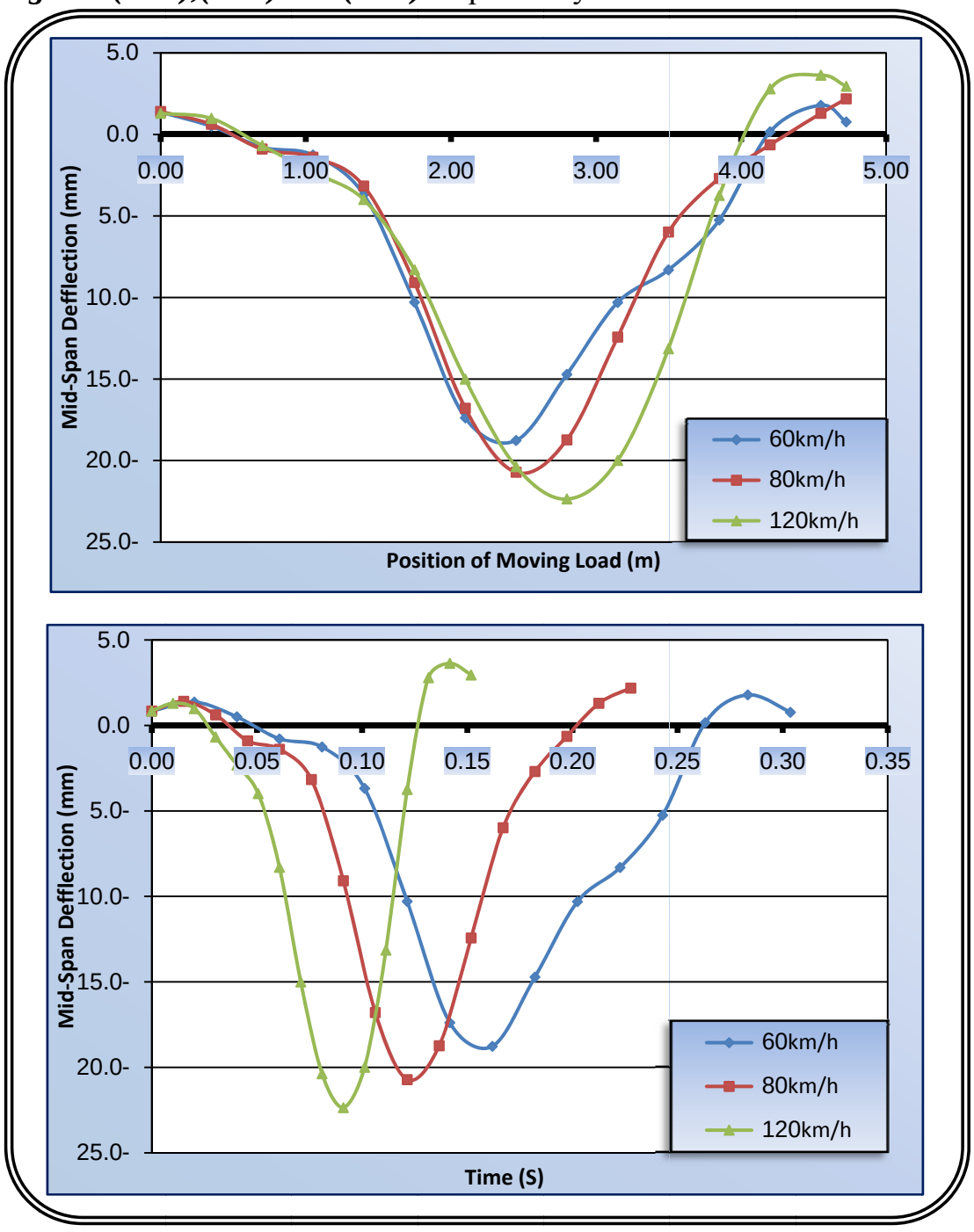

Figure (5.21) Mid-span deflection of prestressed Wolanski beam under various velocities

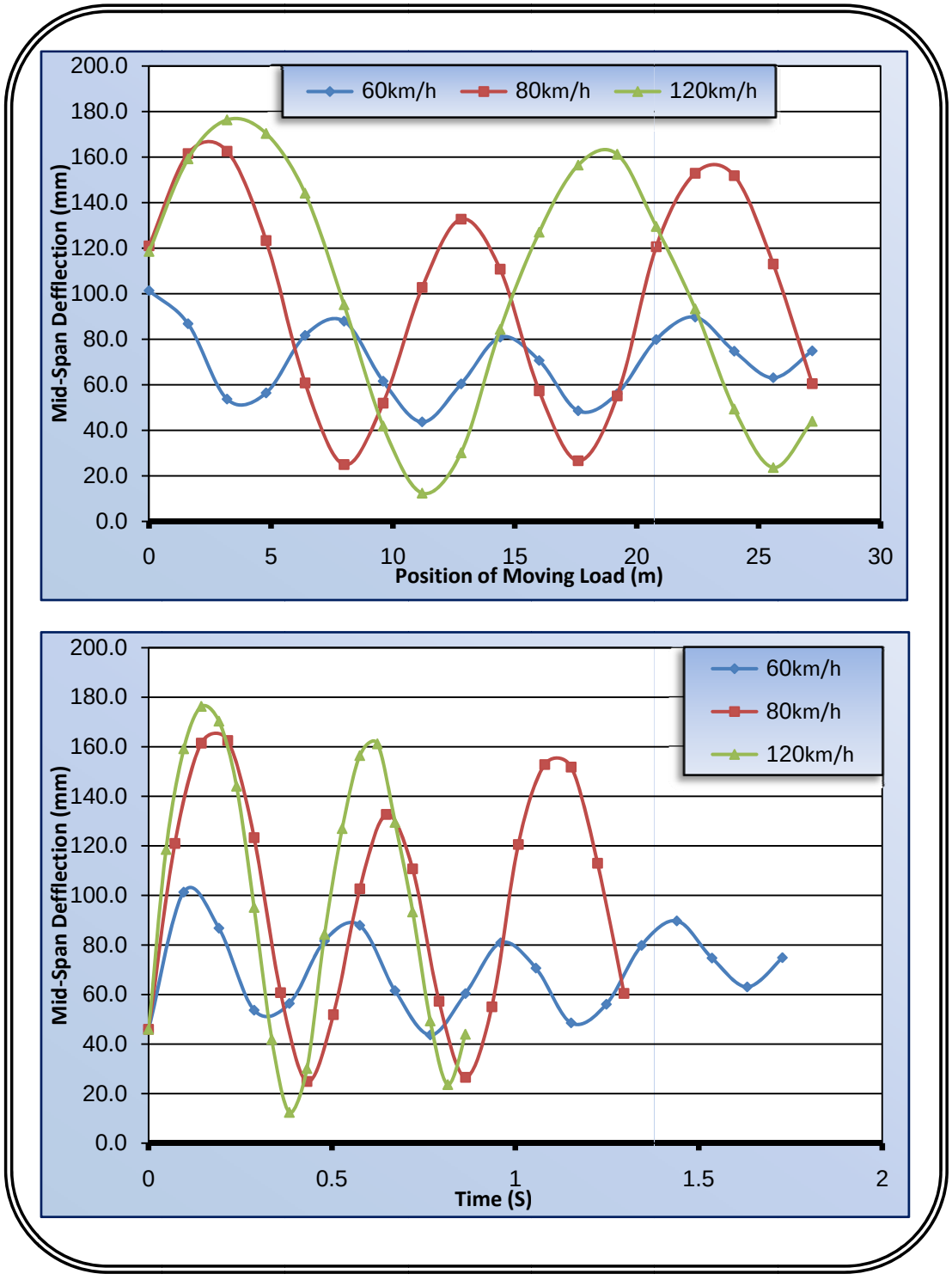

Figure (5.22) Mid-span deflection of girder (IV) under various velocities

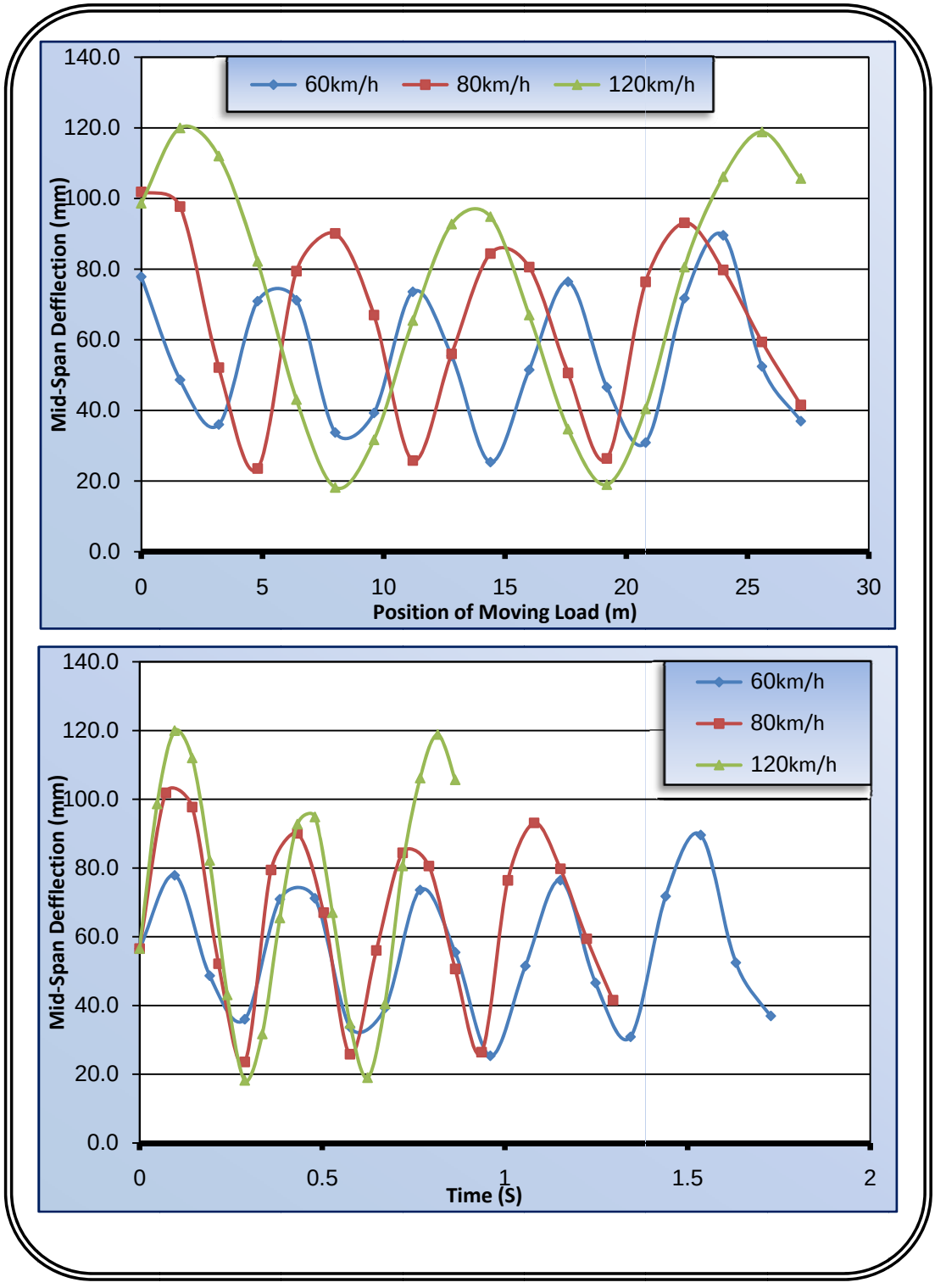

Figure (5.23) Mid-span deflection of girder (BT-56) under various velocities

The results of ***Figures (5.21),(5.22)*** and ***(5.23)*** show that the dynamic response of the prestressed concrete girders increase directly by increasing vehicle velocity this is due to the effect of weight ratio so as to

the span length of the girder, which has a much greater influence for higher velocity than for low velocity and the effect of prestressing force can be observed clearly in ***Figures (5.22)*** and ***(5.23)*** above where the mid-span deflection of the prestressed concrete girders remains frequence in a positive (upward).

The natural frequency and the period of frequency of prestressed concrete girder are remained approximatly a constant for every velocity where the natural frequency and the period of frequency are represented as the following [57]:-

$$f = \frac{1}{T} \quad \text{..... (5.2)}$$

$$\omega = 2\pi . f \quad \text{..... (5.3)}$$

Where: f = the cyclic frequency (hertz).

T = the period of frequency (sec), see ***Figure (5.24)***.

ω = the natural frequency (rad).

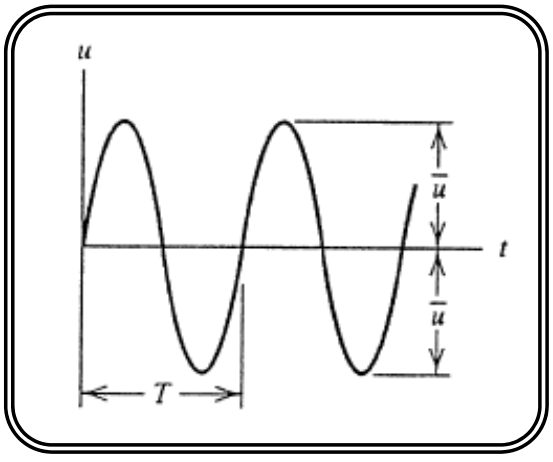

Figure (5.24) General details of natural frequency [57]

From equations (5.2) and (5.3) it can be seen clearly the increasing of natural frequency of girders with increasing load velocity, see ***Table (5.13)***, which depends on stiffness matrix and mass matrix of the prestressed girder because the natural frequency ($\omega \propto \sqrt{\frac{k}{m}}$).

Table (5.13) Effect of increasing vehicle velocity on the natural frequency

Girder Type	Natural Frequency ω (rad)		
	60 km/h	80 km/h	120 km/h
Wolanski Beam (Example 2)	14.681	19.297	28.534
Type (IV) (Example 3)	12.577	12.731	13.823
Type (BT-56) (Example 4)	17.167	17.849	18.451

In the present study, the velosity (120 km/h) will be adopted to study the effect of varios parameters on the prestressed concrete girders because it is a critical velosity.

5.6.2 Effect No. of Axles in Representation Moving Load

Every vehicle contains at least four axles, and for more realistic it is important to study the effect of No. of axles in representation of moving load where the distance between the front and rear axles is taken in this investigation according to Standard AASHTO truck (HS).

The variable distance between the rear axles of HS20-44 is taken as 4.25m to get the maximum response, and this investigation is applied only in the example (3 and 4) because of ,in example (2), the span is equal to 4.725m and the distance between the axles in HS15-44 - which used in its analysis for its load capacity - is equal to 4.25m.

The three axles are moved from left end to the right end at velosity (120 km/h) and their results are compared with the results of the moving resultant of the three forces, as shown in ***Figures (5.25)***, and ***(5.26)***.

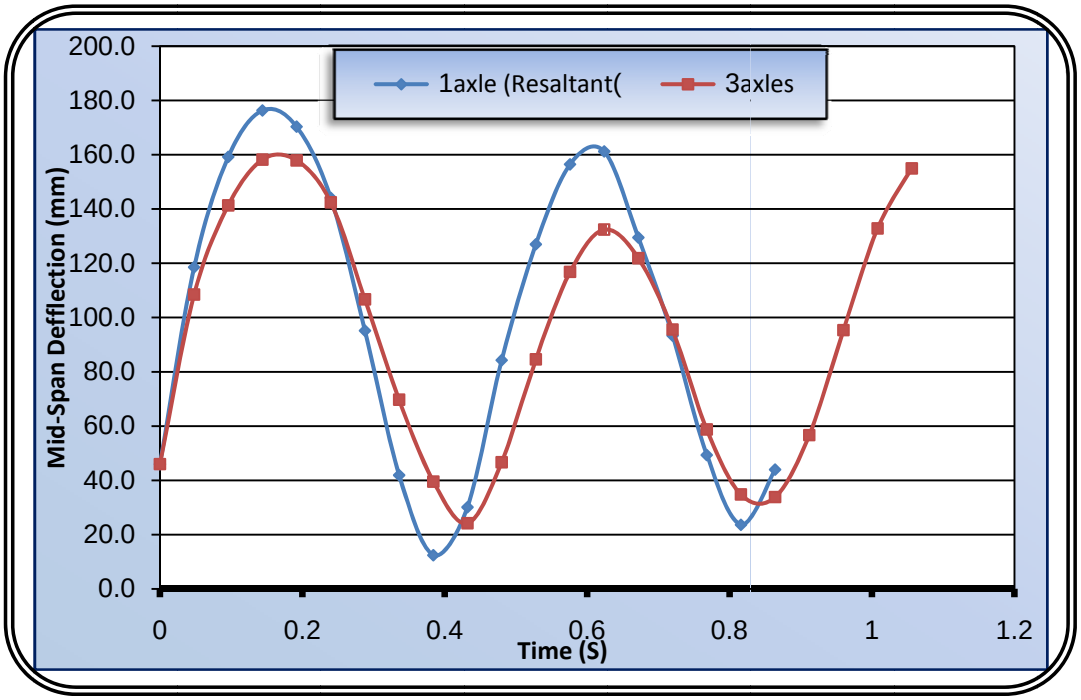

Figure (5.25) Mid-span deflection of prestressed girder (IV) under various No. of axles (V=120km/h)

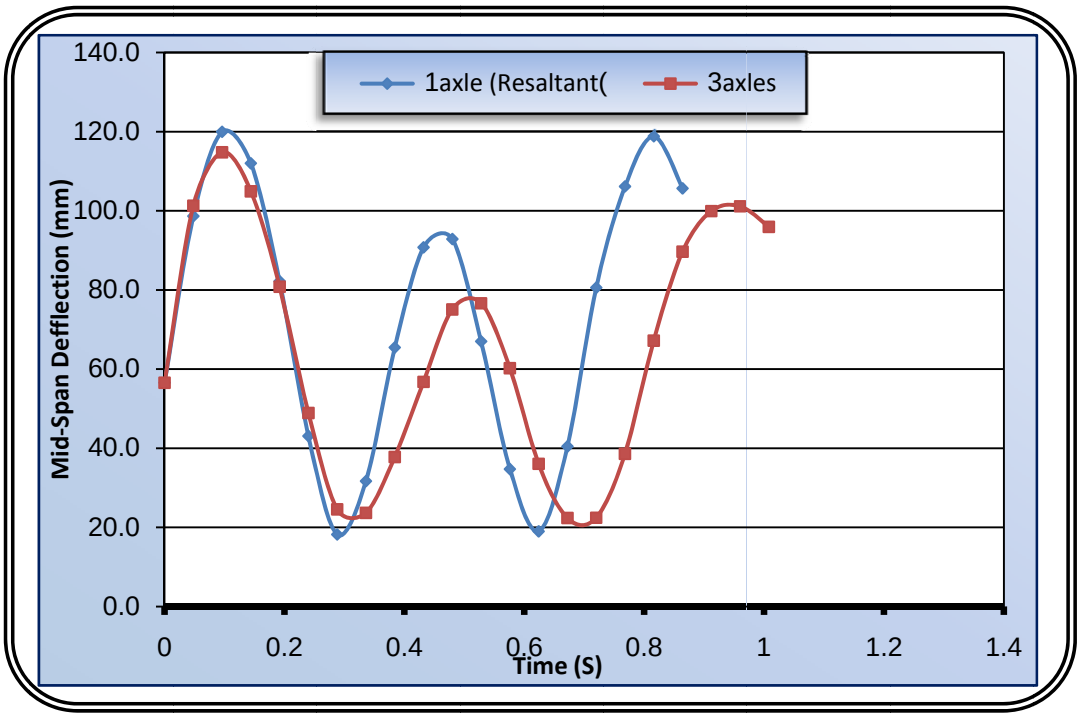

Figure (5.26) Mid-span deflection of prestressed girder (BT-56) under various No. of axles (V=120km/h)

Figurs (5.25) and ***(5.26)*** show that the use of the resultant force of the vehicle axles in the representation of the moving load gives a maximum dynamic response larger than the three axles representation at a disparate ratio where in girder IV (3.4%), and in girder BT (20%) this is due to the difference of a mount of prestressing force and the flexural rigidity of each girder. Also the natural frequency of the prestressed girder varies with change the representation of the vehicle where the natural frequency of the multi (three) forces smaller than the resultant of these forces, see ***Table (5.14)***.

Table (5.14) Effect of vehicle representation on the natural frequency

Girder Type	Natural Frequency ω (rad)	
	One Axle (Resultant)	Three Axles
Type (IV) (Example 3)	13.823	13.122
Type (BT-56) (Example 4)	18.451	15.812

From above table, the multi (three) forces give a dynamic response smaller than the resultant of these forces so that it can be used a resultant force in dynamic analysis of the girder under moving load for more safely and easly.

5.6.3 Effect No. of Passing Vehicles

Some times a family of trucks are passing on the bridge sequencely so that this case is critical and it is very important to analyze this case on the bridges to show the behavior of prestressed concrete girder under various number of passing vehicles. Three cases are studied in the present study

by using HS20-44 truck and the length of the truck is tacken in account. One, two and three trucks are moved from the left end to the right end and the results of these analyses are shown in ***Figurs (5.27)*** and ***(5.28)***.

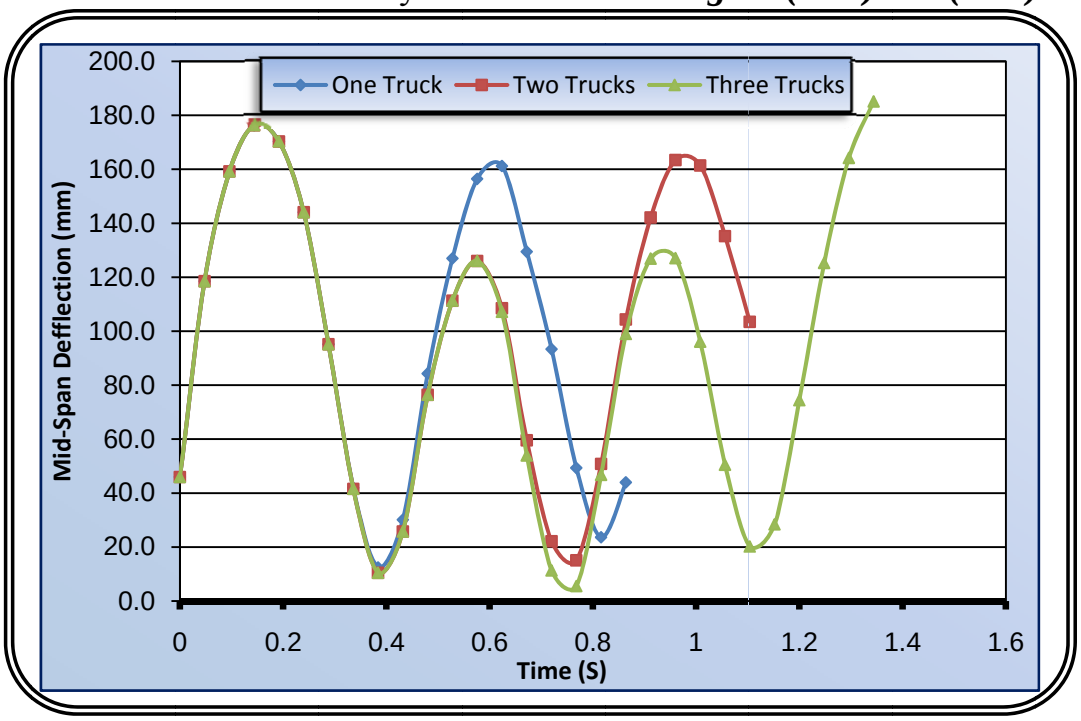

Figure (5.27) Time histories of mid-span under various No. of trucks passing on girder (IV) (V=120km/h)

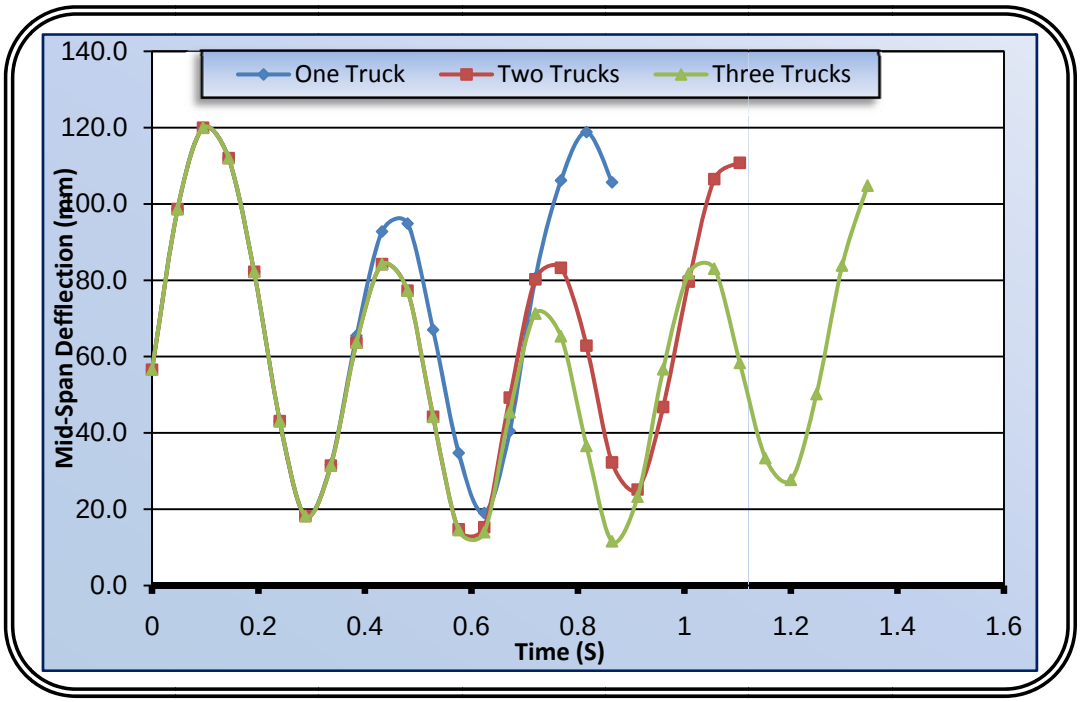

Figure (5.28) Time histories of mid-span under various No. of trucks passing on girder (BT-56) (V=120km/h)

From these analysis, the maximum deflection is getting by moving three trucks sequencely as expected. Generally, the maximum deflection of the prestressed concrete girder increases with increasing number of passing vehicle where the maximum deflection at passing two and three trucks is larger than one passing truck by (1.5) and (4) times respectivly for girder (IV) while by (1.3) and (1.65) times respectively for girder (BT) and the three passing trucks is larger than two passing trucks by (2.72) times for girder (IV) while (1.3)times for girder (BT) this is due to the defference of prestressing force amount.

The time period (*T*) of the prestressed girder decreases with the increaseing number of passing trucks because of the next truck will be as a damper to the dynamic response of the previous truck, see ***Figures (5.27)*** and ***(5.28)***, so that the natural frequency of the prestressed concrete girder increases with increasing the number of passing vehicle, see ***Table (5.15)***.

Table (5.15) Effect of No. of passing vehicles on the natural frequency

Girder Type	Natural Frequency ω (rad)		
	One Truck	Two Trucks	Three Trucks
Type (IV) (Example 3)	13.823	15.598	16.184
Type (BT-56) (Example 4)	18.451	19.407	20.344

5.6.4 Effect of Cross Section

The cross section and flexural rigidity are important factors in geometrical properties which are effect on the response of the girder, so that three cases of cross section are considered in this study to show the

behavior of the rectangular prestressed concrete girder under dynamic response of the moving load. These cases represented by:-

1- The same weight (area) with rearranged the strands.

2- The same stiffness (moment of inertia) with rearranged the strands.

3- The same stiffness (moment of inertia) with the same arranged of the strands.

Figures (5.29) and ***(5.30)*** show the dimensions and strands arrangement of the equivalent rectangular section of the prestressed concrete girders (IV and BT) for the three cases above. These cases are used to investigate the best section that can be used as a replaced to I-section for more easily construct and more economic.

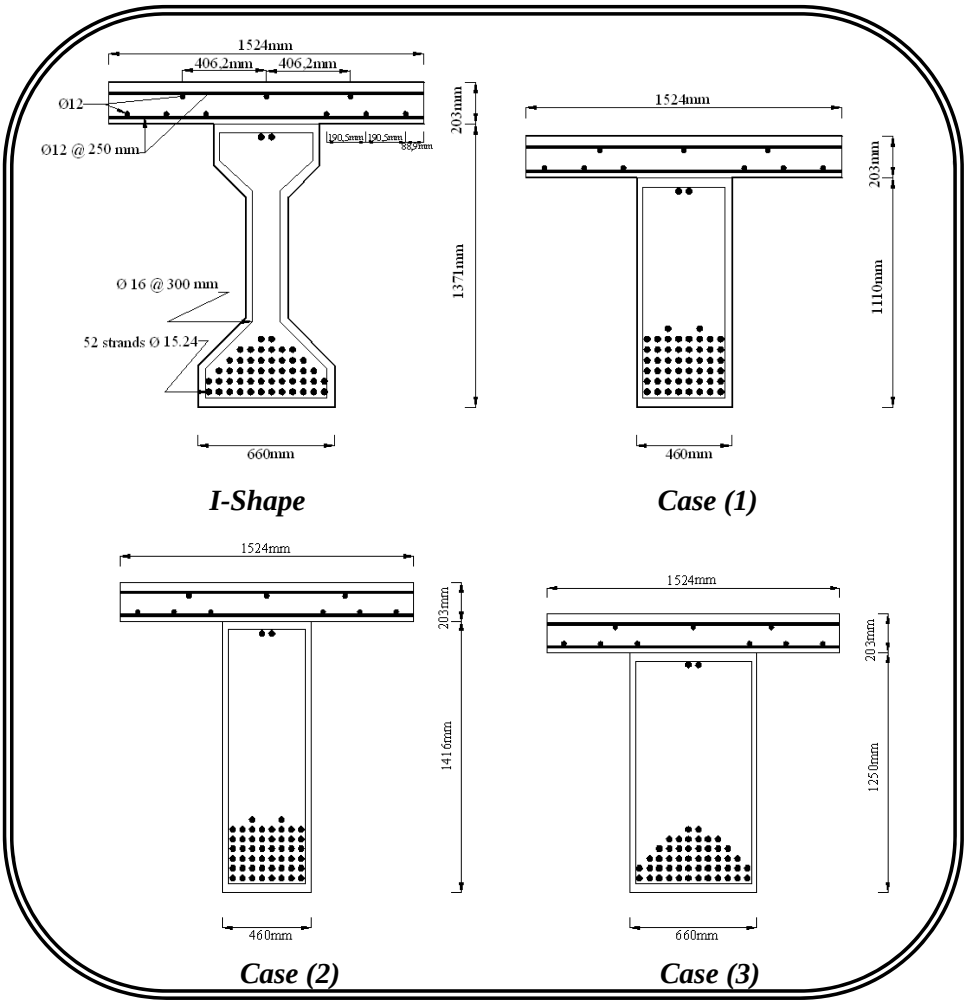

Figure (5.29) Cases of the equivalent rectangular section of prestressed concrete girder (IV)

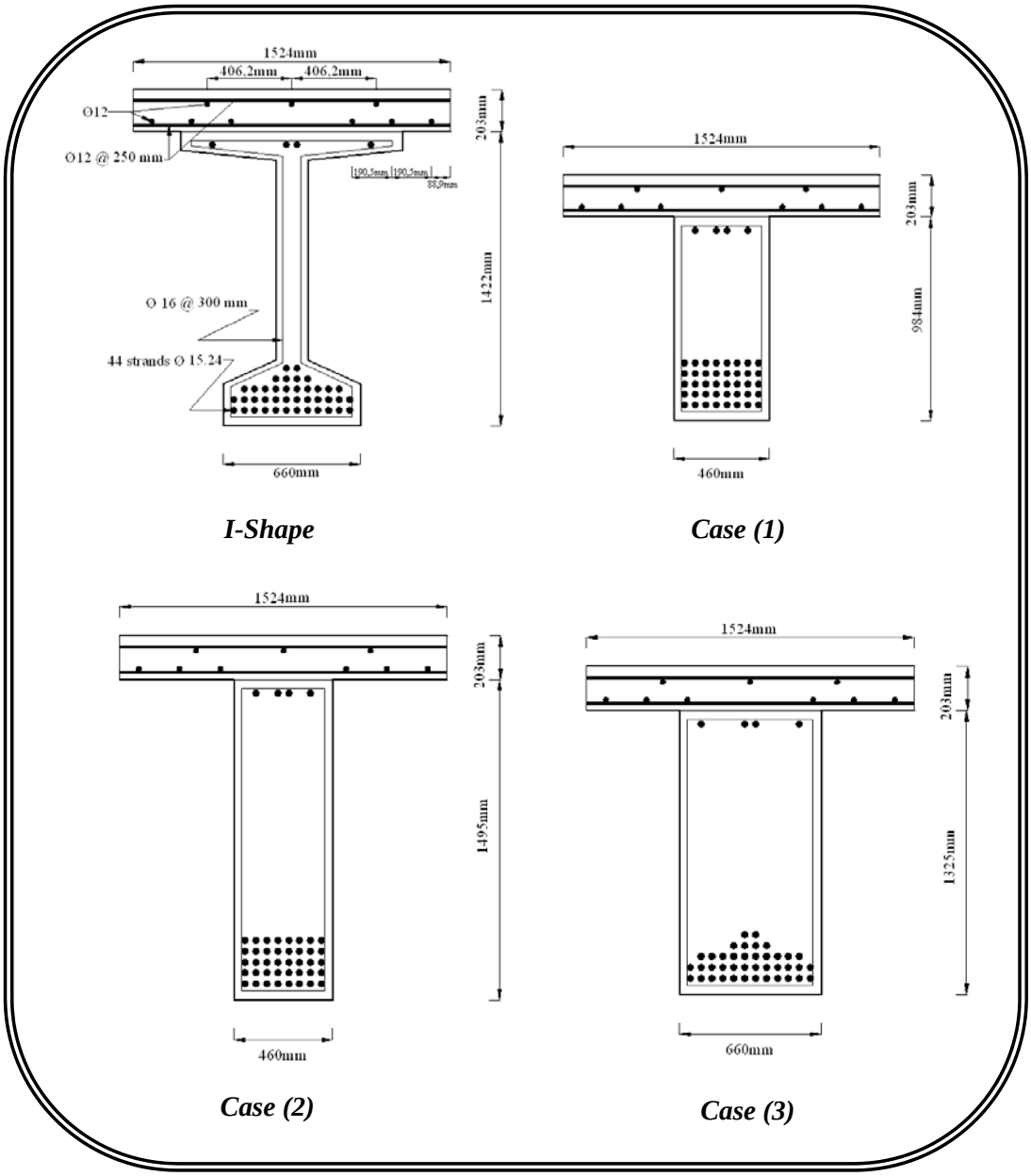

Figure (5.30) Cases of the equivalent rectangular section of prestressed concrete girder type (BT-56)

In analysis these cases for the prestressed girders (IV and BT) under dynamic moving load and compared the results, as shown in ***Figures (5.31)*** and ***(5.32)***, it can be seen clearly that the case (1) which depending on the same weight has less strength from the other cases because of smallest flexural rigidity where the control of deflection is the flexural rigidity that depends on the girder depth. While the cases (2 and 3) which

depending on the moment of inertia of the girders get an acceptable dynamic response with a very good convergance in deflection as compared with (I section) of the same girder.

The natural frequency of the rectangular section is less than the (I shape) this is due to the increasing in the weight of the girder where the relation between the natural frequancy and the mass is ($\omega \propto \sqrt{\frac{k}{m}}$), see ***Table (5.16)***.

Finally when comparing the last cases (2 and 3) it can be seen that a good convergence between them and the difference in their dynamic response is due to the effect of prestressing force and it is arrangement.

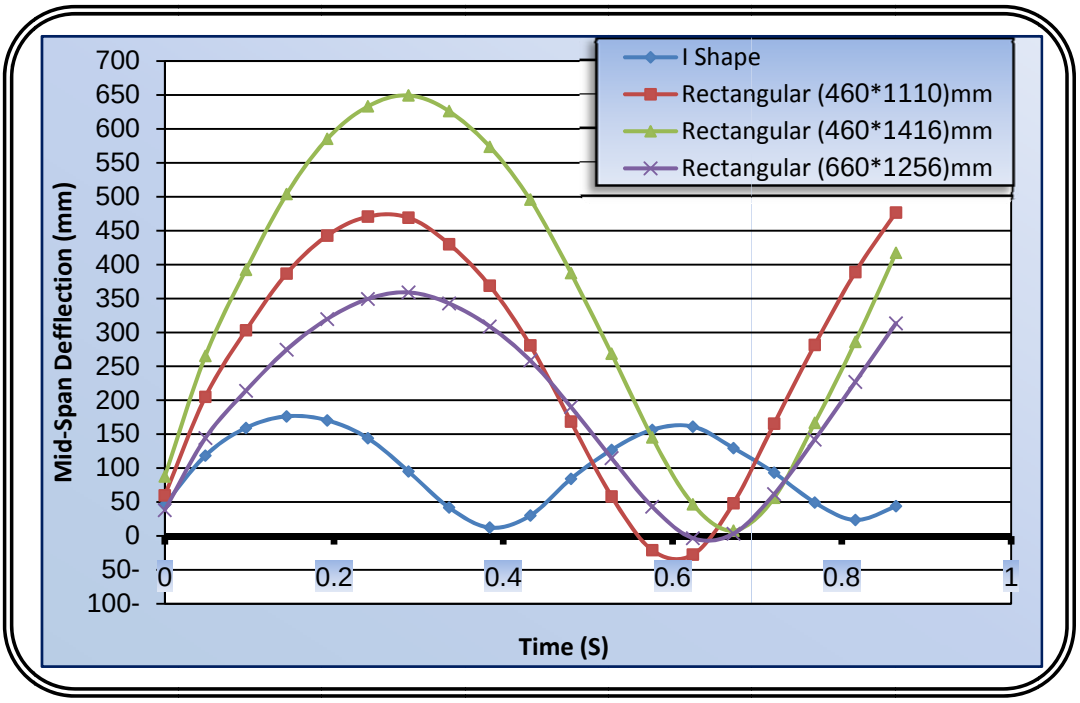

Figure (5.31) Time history of mid-span deflection of girder (IV) with various cross sections

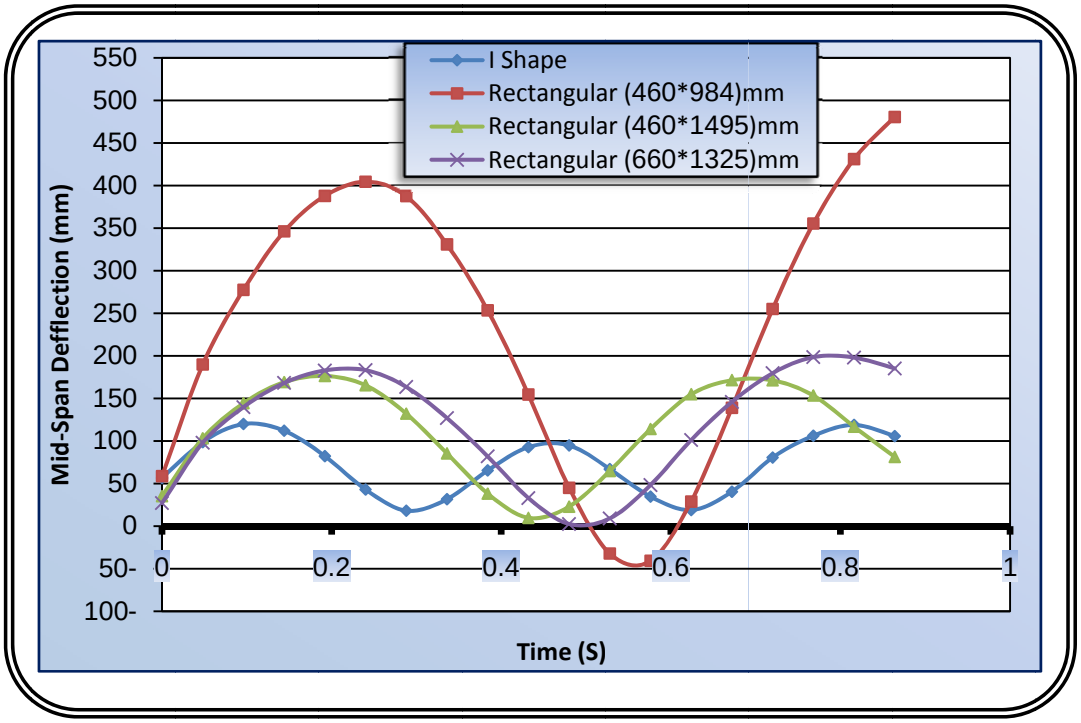

Figure (5.32) Time history of mid-span deflection of girder (BT) with various cross sections

Table (5.16) Effect cross section of prestressed girders on the natural frequency

Girder Type	Natural Frequency ω (rad)			
	I section	Rectangular Case (1)	Rectangular Case (2)	Rectangular Case (3)
Type (IV) (Example 3)	13.823	9.279	8.524	8.796
Type (BT-56) (Example 4)	18.451	9.861	12.936	11.277

Chapter Six

Conclusions and Recommendations

6.1 Conclusions:

From the results obtained from analyzing the prestressed concrete girders under moving loads, it can be concluded that:-

1. The representation of prestressing force as equivalent external force seems an efficient model in representing the prestressed concrete in finite element method where very good agreement is obtained through comparing the analytical results with the experimental results.
2. When the natural frequency is the control design of the prestressed concrete girder, the rectangular cross section seems the best section from the I-shape having the same flexural rigidity with the same strands arrangement and the I-shape is the best when the deflection is the control design.
3. Amount of prestressing force, strands arrangement are important factors governing the natural frequency and period of prestressed concrete girder.
4. The natural frequency of the rectangular section is less than the (I shape); this is due to increasing in the weight of the girder.
5. The dynamic response of prestressed concrete girder increases with increasing the velocity of moving load at an unequal ratio so as to the natural frequency.
6. Increasing the vehicle velocity, i.e., decreasing the required time for vehicle to pass a specific point will decrease the period (T) and increase the natural frequency.

7. The increasing number of passing vehicles increases the dynamic response where the maximum deflection for two and three passing trucks is larger than one passing truck.
8. The period of prestressed concrete girder decreases with increasing the number of passing vehicles while the natural frequency will increase.
9. When more than one vehicle passing on the prestressed concrete girder the next vehicle plays as a frequency damper for the upper peak to the previous one with a maximum response (deflection) for the lower peak of the natural frequency curve.
10. The resultant force of the vehicle axles in representation of the moving load gives a maximum dynamic response which is larger than the three axles representation at an unequal ratio where in AASHTO type (IV) girder (3.4%), and in modified PCI (BT-56) girder (20%) this is due to the difference of a mount of prestressing force.

6.2 Recommendations for Further Studies:

1. The dynamic response of prestressed multi-girder concrete bridge under moving load and studying the effect of deck continuity.
2. Geometrical nonlinear analysis of prestressed concrete girder under dynamic moving load.
3. Moving mass analysis of prestressed concrete girder.
4. Vehicle idealization model passing on prestressed concrete girder.
5. Effect of magnitude prestressing force on the natural frequency of prestressed concrete girder.
6. The dynamic response of prestressed concrete girder with opening under moving load.

List of Contents